

Sub-Poissonian processes in quantum optics

Luiz Davidovich

Instituto de Física, Universidade Federal do Rio de Janeiro, 21945-970 Rio de Janeiro, Rio de Janeiro, Brazil

The author reviews methods for generating sub-Poissonian light and related concepts. This light has energy fluctuations reduced below the level which corresponds to a classical Poissonian process (shot-noise level). After an introduction to the concept of nonclassical light, an overview is given of the main methods of quantum-noise reduction. Sub-Poissonian processes are exemplified in different areas of optics, ranging from single-atom resonance fluorescence to nonlinear optics, laser physics, and cavity quantum electrodynamics. Emphasis is placed on the conceptual foundations, and on developments in laser theory that lead to the possibility, already demonstrated experimentally, of linewidth narrowing and sub-Poissonian light generation in lasers and masers. The sources of quantum noise in these devices are analyzed, and four noise-suppression methods are discussed in detail: regularization of the pumping, suppression of spontaneous-emission noise, nonadiabatic evolution of the atomic variables, and twin-beam generation.

CONTENTS

I. Introduction	127
II. Nonclassical Light	129
A. Standard quantum limits	129
B. Squeezed states	130
C. Quasiprobabilities	131
D. Number-phase squeezing	132
E. Relation between quadrature and number squeezing	132
F. Photon antibunching	134
G. Measurement of quadrature squeezing	135
H. Effect of dissipation	136
I. Applications of sub-Poissonian light	136
III. Experiments	136
A. Parametric processes	137
B. Second-harmonic generation	138
C. Resonant atomic fluorescence	138
D. Optical bistability	138
E. Lasers and masers	139
F. Twin-photon beams	140
G. Quantum nondemolition measurements	141
IV. Sources of Quantum Noise in Lasers	141
A. Excitation model	141
B. Contribution of dissipation	143
C. Steady state	143
D. Photon-number variance	144
1. Lasers	144
2. Micromasers	145
E. Production of sub-Poissonian atomic beams by micromasers	146
V. Quantum Theory: The Generalized Master Equation	146
A. Derivation of the master equation	146
B. Results for Poissonian and regular pumping	147
C. Application to the micromaser	148
1. Poissonian-pumped micromaser	148
2. Trapping states	148
3. Regularly pumped micromaser	150
VI. Langevin Approach and Atomic Dynamic Effects	150
A. Heisenberg-Langevin equations	151
1. Langevin forces for the field	152
2. Atomic Langevin forces	153
3. Macroscopic operators	153

4. Equivalent c -number equations	155
B. Semiclassical theory	157
1. Adiabatic elimination and rate equations	157
2. Steady state	157
C. Dynamics of fluctuations	158
D. Photon-number variance	160
E. Phase diffusion	161
F. Laser linewidth	161
G. Spectra of the output field	162
1. Quadrature spectra	163
2. Quantum-noise compression	164
VII. Generation of Fock States Through Quantum Nondemolition Measurements	165
VIII. Twin-Photon Processes	166
A. Twin-beam effects in two-photon oscillators	167
B. Noise spectrum of the output field	168
IX. Conclusions and Outlook	169
Acknowledgments	170
References	170

I. INTRODUCTION

"I am incessantly busy with the question of radiation... This quantum question is so uncommonly important and difficult that it should concern everyone." (Letter from Einstein to Laub, 1908)

This century has witnessed a revolutionary change in the concept of light. This revolution began at the very dawn of the century, with the work of Planck (1900a, 1900b), and was further developed by the contributions of Einstein (1905, 1906, 1909a, 1909b, 1917), Compton (1923), Dirac (1927), and Bohr (1928), among others. It led to the concept of the dual or complementary nature of light: depending on the experimental setup, either the corpuscle or the wave character would manifest itself.

This duality was well illustrated by a relation put forward by Einstein (1909a, 1909b), for the energy fluctuation ϵ of blackbody radiation in a frequency interval between ν and $\nu + d\nu$, inside a volume V , and for a spectral density $\rho(\nu, T)$ (energy per unit volume and unit frequency interval):

$$\langle \epsilon^2(\nu, T) \rangle = \left(h\nu\rho + \frac{c^3}{8\pi\nu^2} \rho^2 \right) V d\nu. \quad (1.1)$$

Einstein observed that this relation, derived from Planck's law, is incompatible with the classical wave theory of light. In fact, the classical theory, which leads to the Rayleigh-Jeans law for the spectral density, would yield only the second term on the right-hand side of the above equation, which could thus be referred to as the "wave term." The first term, the other hand, is characteristic of independently moving pointlike quanta with energy $h\nu$ (Einstein, 1909a). Indeed, this term, commonly called "shot noise," is the sole contribution to the variance of a flux of independent particles with random arrival times (for example, raindrops falling on a roof—in which case, $\langle \epsilon^2 \rangle$ would refer to the variance in the number of raindrops hitting the roof during a fixed time interval). Therefore, Eq. (1.1) displays both the particle and the wave aspects of radiation.

For a long time only thermal sources were available, and Planck's distribution was considered the cornerstone of the statistical description of light. This situation changed drastically with the invention of the first laser in 1960 (Maiman, 1960), which brought about a second revolution in the concept of light. Lasers work in a situation far from thermal equilibrium, and generate radiation with a statistical distribution markedly different from Planck's formula. In fact, well above the oscillation threshold, the statistics of the emitted light approaches that of an ensemble of independent particles, so that only the shot-noise term is present in Eq. (1.1), corresponding to a Poissonian distribution for the number of photons. The statistical distinction between laser and thermal light was experimentally demonstrated in 1965 (Arecchi, 1965).

The new source of light motivated an important theoretical effort, aimed at establishing a general framework for the description of states of radiation. Glauber (1963b, 1963c) and Sudarshan (1963) introduced phase-space distributions, which allowed averages of normal-ordered products of field operators to be computed as quasiclassical integrals of the corresponding c -number functions. This result is especially important in view of the fact, established by Glauber (1963a, 1963b, 1963c, 1965), that photodetection rates can be expressed in terms of quantum averages of normal-ordered products of field operators (*optical coherence functions*), for photodetectors based on photon absorption. For the special case of thermal light, the phase-space distribution was derived by Glauber (1963c), while Sudarshan (1963) proposed a general expression for the weight function in terms of a series of derivatives of delta functions of arbitrarily high orders, thus demonstrating in principle the possibility of expressing quantum-mechanical photo-counting rates as quasiclassical statistical averages, for any state of the field. This formal correspondence between the quantum-mechanical and classical statistical descriptions of optical coherence functions is the essence of the optical equivalence theorem (Sudarshan, 1963; Klauder *et al.*, 1965; Mehta and Sudarshan, 1965). These

developments led to a generalization of Eq. (1.1) for any kind of radiation. The photon-number variance can be written (by reexpressing it in terms of normal-ordered products of field operators and then using the optical equivalence theorem) as

$$\langle \Delta n^2 \rangle = \langle (n - \langle n \rangle)^2 \rangle = \langle n \rangle + \int d\{\alpha_{\vec{k},s}\} P(\{\alpha_{\vec{k},s}\}) (\Delta U)^2, \quad (1.2)$$

where $\alpha_{\vec{k},s}$ is the complex amplitude of the field for the mode with wave vector \vec{k} and polarization s , the symbol $d\{\alpha_{\vec{k},s}\}$ stands for the phase-space volume element $\prod_{\vec{k},s} d^2\alpha_{\vec{k},s}$, and $U \equiv \sum_{\vec{k},s} |\alpha_{\vec{k},s}|^2$ is the c number corresponding to the total photon number operator \hat{n} . The first term on the right-hand side of this equation corresponds to the particlelike term in Eq. (1.1). The second term, associated with departure from the Poisson law, can be interpreted as a quasiclassical variance, the phase-space Glauber-Sudarshan distribution $P(\{\alpha_{\vec{k},s}\})$ playing the role of a probability measure. More importantly, it was realized that $P(\{\alpha_{\vec{k},s}\})$ may become highly singular and negative. This forbids an interpretation like Einstein's, that the second term on the right-hand side of Eq. (1.2) is associated with a classical wave contribution. When this term is negative, the photon-number variance is smaller than the average number of photons, corresponding to a *sub-Poissonian distribution*.

States of the electromagnetic field for which $P(\{\alpha_{\vec{k},s}\})$ is highly singular [more singular than a tempered distribution—note that for a delta function one would get from Eq. (1.2) a Poissonlike result] or negative are called "nonclassical states." Of course this definition is quite arbitrary, since in principle any state of the electromagnetic field exhibits a quantum character, associated with the discreteness of the photon-number distribution. Historically, the definition was motivated by the comparison between Eqs. (1.1) and (1.2), and, more generally, by the optical equivalence theorem. The production of nonclassical states opened up a new field of research, motivated both by the new and subtle conceptual problems involved, requiring a deeper understanding of the nature of light and of its interactions with matter, and by the possibility, noted above, of obtaining light beams with fluctuations below the shot-noise level.

In fact, nonclassical behavior of light appears already at the single-atom level, as predicted by Carmichael and Walls (1976a, 1976b), Cohen-Tannoudji (1977), and Kimble and Mandel (1976), who established that light produced in single-atom resonant fluorescence would display the phenomenon of *antibunching*. This effect is associated with two-photon correlation measurements: the probability of detecting the second photon decreases as the time delay between the two measurements goes to zero, due to the fact that the atom that emitted the first photon must be re-excited before emitting the second one. This is opposite to the behavior of photons in thermal beams, where intensity fluctuations lead to photon bunching. Antibunching is closely related to sub-Poissonian behavior, though not equivalent to it (the re-

lation between these two properties will be discussed in Sec. II.F). The first experimental demonstration of antibunching in atomic resonant fluorescence was achieved in 1977, by Kimble, Dagenais, and Mandel (Kimble *et al.*, 1977) while the sub-Poissonian behavior of the resulting radiation was verified by Short and Mandel (1983).

Many other experiments have been carried out since, dealing not only with photon-number fluctuations, but also with noise in the quadrature components of the field. Analogous to the position and momentum of a harmonic oscillator, these components cannot be measured simultaneously, and their dispersions are related through a Heisenberg inequality. Nonlinear interactions between the electromagnetic field and atomic media may lead to the compression of noise in one of the components, at the expense of increasing the fluctuations in the other. The first experimental demonstration was due to Slusher *et al.* (1985). Several applications have been envisaged for radiation with reduced quantum fluctuations, in optical communications (Takahashi, 1965; Yuen, 1976) and precision measurements (Caves, 1981).

This research has also led to developments in laser theory, adding new insights and interesting refinements to the original results of the 1960's (for which, see Lax, 1966a, 1966b; Gordon, 1967; Scully and Lamb, 1967; Lax and Louisell, 1969; Haken, 1970). Up to 1987, laser light could still be described in classical terms (i.e., by a positive-definite probability distribution in phase space). Below threshold, one had essentially a thermal lamp, while above threshold the photon-number statistical distribution would change from super-Poissonian ($\langle \Delta n^2 \rangle > \langle n \rangle$), as the laser started oscillating, to Poissonian, high above threshold. In 1987, however Machida, Yamamoto, and Itaya demonstrated generation of sub-Poissonian light by a semiconductor laser (Machida *et al.*, 1987). The key point was the control of pumping noise, which had masked the quantum character of laser light in previous experiments. A correct understanding of the sources of quantum noise in lasers, starting with the pioneer work of Golubev and Sokolov (1984), was essential for these new developments. Generation of sub-Poissonian radiation in the microwave region has also been demonstrated in masers operating in the microscopic regime (Rempe *et al.*, 1990), even without control of pumping noise. The inhibition of intensity fluctuations in this case is due to a stabilization mechanism stemming from a negative differential gain, which is related to the suppression of spontaneous-emission noise.

Another quantum-mechanical twist came with the discovery of twin-photon beams, which are generated in certain crystals on pumping by a light beam. The two photons are emitted simultaneously, the sum of their frequencies being equal to the frequency of the pump. The same process occurs in two-photon lasers and masers. The fact that they are emitted simultaneously implies that their fluctuations are highly correlated. In the non-degenerate case, in which the two photons differ in frequency, polarization, or propagation direction, it is possible therefore to obtain fluctuations below shot noise in

the difference of intensities. A noise reduction factor of 86% below the classical level was achieved by Mertz *et al.* (1991). Furthermore, the fluctuations in one of the beams can be counteracted by monitoring the behavior of the other beam. This active-control technique has been demonstrated in several labs.

One can see that the attitude expressed by Einstein in the quotation that began this section (cited by Pais, 1982) is still justified today. In recent years, several review papers have been devoted to the production and applications of nonclassical light (Walls, 1983; Loudon and Knight, 1987; Teich and Saleh, 1989; Reynaud, 1990; Yamamoto *et al.*, 1990; Fabre, 1992; Kimble, 1992; Reynaud *et al.*, 1992; see also the special issues *Journal of the Optical Society of America B* **4**, 1987; *Journal of Modern Optics* **34**, 1987; and *Applied Physics B* **55**, 1992).

This paper reviews recent work on the generation of sub-Poissonian light, with emphasis on the basic concepts involved. Several methods are discussed, but particular attention is given to active devices (lasers and masers). This distribution of emphasis is dictated by the fact that the production of nonclassical states by passive systems has already been extensively covered by previous reviews, and possible applications of this kind of radiation have also been discussed in detail (see, for instance, Yamamoto *et al.*, 1990). This does not seem to be the case, however, for lasers and masers. In fact, detailed studies of the possibilities of nonclassical light generation in these devices have led to generalizations of laser theory, on the fundamental side, and to hopes of possible application as bright sources of low-noise radiation.

In Sec. II, some of the basic notions related to nonclassical states of light are reviewed, with a discussion of the connections between several useful concepts, including squeezing, sub-Poissonian behavior, and antibunching. Some applications are also discussed, but a review of the main experimental achievements is left to Sec. III. In Sec. IV, a general analysis is provided of the sources of quantum noise in lasers and masers, with emphasis on the physical principles involved. The following two sections are devoted to the presentation and discussion of the quantum theory of these devices. Section V presents the derivation of a generalized master equation for the corresponding field density matrix. Section VI introduces the Langevin approach, which allows a detailed treatment of the atomic dynamics and its effects on quantum-noise reduction. Section VII discusses the possibility of generating dispersion-free photon-number states using quantum non-demolition measurements. Section VIII discusses some general results on two-photon devices. Section IX contains conclusions and a tentative outlook.

II. NONCLASSICAL LIGHT

A. Standard quantum limits

Quantum mechanics imposes fundamental limits on electromagnetic field measurements. Let us consider the

electric field operator corresponding to a mode of the electromagnetic field in a cavity with volume V , with angular frequency ω , at time t (assumed for simplicity to be linearly polarized):

$$\hat{E}(t) = \frac{E_0}{2}(\hat{a}e^{-i\omega t} + \hat{a}^\dagger e^{i\omega t}), \quad (2.1)$$

where $E_0 = (h\omega/V)^{1/2}$ is the one-photon field, \hat{a} and \hat{a}^\dagger are the photon annihilation and creation operators, with $[\hat{a}, \hat{a}^\dagger] = 1$, and the hats identify operators. The electric field can be rewritten as

$$\hat{E}(t) = E_0(\hat{X}\cos\omega t + \hat{Y}\sin\omega t), \quad (2.2)$$

where \hat{X} and \hat{Y} are the *quadrature component* operators, given by

$$\hat{X} = \frac{1}{2}(\hat{a} + \hat{a}^\dagger), \quad \hat{Y} = -i\frac{1}{2}(\hat{a} - \hat{a}^\dagger), \quad (2.3)$$

so that

$$[\hat{X}, \hat{Y}] = \frac{i}{2}. \quad (2.4)$$

The quadratures \hat{X} and \hat{Y} correspond to the position and momentum operators of an harmonic oscillator, as can be seen from their definitions (2.3).

From (2.4) it follows that the product of the dispersions in the measurements of the two quadratures \hat{X} and \hat{Y} satisfies a Heisenberg inequality:

$$\Delta X \Delta Y \geq \frac{1}{4}, \quad (2.5)$$

where $\Delta X = (\langle \Delta X^2 \rangle)^{1/2}$.

For *coherent states* (Glauber, 1963b, 1965; Sudarshan, 1963; Klauder and Skagerstam, 1987), the above relation is satisfied as an equality, and the two dispersions are identical: $\Delta X = \Delta Y = 1/2$. A coherent state of the field corresponds to a displaced harmonic-oscillator ground state, and can be obtained from the vacuum state (ground state of the harmonic oscillator) by applying to it a displacement operator:

$$|\alpha\rangle = D(\alpha)|0\rangle = \exp(\alpha\hat{a}^\dagger - \alpha^*\hat{a})|0\rangle, \quad (2.6)$$

where $\alpha = |\alpha|\exp(i\phi)$ is a complex number, corresponding to the phasor representation of the electromagnetic field in an Argand diagram. The state $|\alpha\rangle$ is an eigenstate of the annihilation operator \hat{a} :

$$\hat{a}|\alpha\rangle = \alpha|\alpha\rangle, \quad (2.7)$$

and, as shown by Glauber (1965), it is the state of the field generated by a classical current. The expansion of $|\alpha\rangle$ in terms of Fock states of the field (eigenstates of the number operator $\hat{n} = \hat{a}^\dagger\hat{a}$) is given by

$$|\alpha\rangle = e^{-|\alpha|^2/2} \sum_{n=0}^{\infty} \frac{\alpha^n}{\sqrt{n!}} |n\rangle, \quad (2.8)$$

corresponding to a Poisson distribution of the photon number:

$$\begin{aligned} p(n) &= |\langle n|\alpha\rangle|^2 = \exp(-|\alpha|^2) \frac{|\alpha|^{2n}}{n!} \\ &= \exp(-\langle n \rangle) \frac{\langle n \rangle^n}{n!}. \end{aligned} \quad (2.9)$$

For this distribution, one has $\langle (\Delta n)^2 \rangle = \langle n \rangle$.

Using Eq. (2.8), it is easy to derive the completeness relation

$$\frac{1}{\pi} \int d^2\alpha |\alpha\rangle\langle\alpha| = 1, \quad (2.10)$$

as well as the relation

$$|\langle\alpha|\alpha'\rangle|^2 = \exp(-|\alpha - \alpha'|^2), \quad (2.11)$$

so that coherent states do not form an orthonormal set, implying that Eq. (2.10) is actually an overcompleteness relation.

B. Squeezed states

Applications in communication or precision measurements require only one of the quadratures of the field. It is thus possible to circumvent the quantum limitation expressed by the Heisenberg inequality by reducing the fluctuation in one of the quadratures below that of a coherent state, at the expense of increasing the noise in the other quadrature, preventing the Heisenberg inequality from being violated. We call such states *squeezed states* (Stoler, 1970, 1971; Yuen, 1975, 1976). Frequently this name is reserved for the states with a product of dispersions saturating the Heisenberg relation. One should note, however, that for the applications mentioned above, this characteristic is not essential, the main requirement being the reduction of quantum fluctuations in the quadrature to be used for transmission of a signal or for a precision measurement.

A special class of squeezed states of the minimum-uncertainty type may be obtained by applying to the vacuum state the unitary transformation (Caves, 1981)

$$U(\xi) = \exp[(\xi^*\hat{a}^2 - \xi\hat{a}^{\dagger 2})/2], \quad (2.12)$$

where $\xi = re^{i\theta}$ is an arbitrary complex number. It is easy to show that this transformation amounts to compressing and stretching the two rotated quadratures \hat{X}' and \hat{Y}' , defined by

$$\hat{X}' + i\hat{Y}' = (\hat{X} + i\hat{Y})e^{-i\theta/2}. \quad (2.13)$$

Indeed,

$$\begin{aligned} U^\dagger(\xi)\hat{X}'U(\xi) &= \hat{X}'e^{-r}, \\ U^\dagger(\xi)\hat{Y}'U(\xi) &= \hat{Y}'e^r, \end{aligned} \quad (2.14)$$

so that the variances become, in the state $|\xi\rangle = U(\xi)|0\rangle$,

$$\langle\xi|\Delta X'^2|\xi\rangle = \frac{1}{4}e^{-2r}, \quad (2.15a)$$

and

$$\langle \xi | \Delta Y'^2 | \xi \rangle = \frac{1}{4} e^{2r}. \quad (2.15b)$$

The above transformation has therefore the effect of producing a squeezed state with noise below that of a coherent state in a quadrature making an angle $\theta/2$ with respect to the phase-space axes, as shown in Fig. 1. The parameter r is the *squeezing factor*, and the state $|\xi\rangle$ is called *squeezed vacuum*, even though its average photon number is different from zero. Indeed,

$$\langle \xi | \hat{a}^\dagger \hat{a} | \xi \rangle = \sinh^2 r. \quad (2.16)$$

A more general class of states can be obtained by first squeezing the vacuum, and then displacing it (Caves, 1981):

$$|\alpha, \xi\rangle = D(\alpha) U(\xi) |0\rangle. \quad (2.17)$$

Equations (2.15) remain valid for these states. The average photon number is now given by

$$\langle \alpha, \xi | \hat{a}^\dagger \hat{a} | \alpha, \xi \rangle = |\alpha|^2 + \sinh^2 r. \quad (2.18)$$

Coherent squeezed states may also be defined by first displacing the vacuum state, then squeezing it (Yuen, 1976). The final results are equivalent, so long as the squeezing and displacement parameters are translated properly.

C. Quasiprobabilities

A convenient way of representing the states of the field is through quasiprobability distributions. They allow one to write down quantum expectation values of operators as integrals of the corresponding classical quantities weighted by the distribution function corresponding to the state. These representations depend on the chosen order of the operators in the quantum averages, since in the c -number integral this order is irrelevant. Thus, for normal ordering (annihilation operators to the right, creation operators to the left), one has, for a one-mode field:

$$\langle (\hat{a}^\dagger)^m \hat{a}^n \rangle = \text{Tr}[\rho (\hat{a}^\dagger)^m \hat{a}^n] = \int (\alpha^*)^m \alpha^n P(\alpha) d^2 \alpha, \quad (2.19)$$

where $P(\alpha)$ is the *Glauber-Sudarshan representation* (Glauber, 1963b; Sudarshan, 1963). This distribution is very useful from the computational point of view, since it reduces quantum averages to quasiclassical integrals. However, it suffers from pathological behavior, especially when squeezed states are considered. For a coherent state, $\rho = |\alpha_0\rangle\langle\alpha_0|$, so that $\text{Tr}[\rho (\hat{a}^\dagger)^m (\hat{a})^n] = (\alpha_0^*)^m \alpha_0^n$, which corresponds to $P(\alpha) = \delta^{(2)}(\alpha - \alpha_0)$ in the above integral. Thus, the normal-ordering representation of a coherent state may be taken as a delta function (due to the overcompleteness of the coherent states, this representation is not unique). For squeezed states, $P(\alpha)$ becomes negative, thus justifying the designation “nonclassical” for these states. This may be seen by the following explicit calculation:

$$\begin{aligned} \langle \Delta X^2 \rangle &= \frac{1}{4} \langle (\hat{a} + \hat{a}^\dagger)^2 - \langle \hat{a} + \hat{a}^\dagger \rangle^2 \rangle \\ &= \frac{1}{4} [\langle \hat{a}^2 + \hat{a}^{\dagger 2} + 2\hat{a}^\dagger \hat{a} + 1 \rangle - \langle \hat{a} + \hat{a}^\dagger \rangle^2] \\ &= \frac{1}{4} \left\{ 1 + \int d^2 \alpha P(\alpha) [(\alpha + \alpha^*)^2 - \langle \alpha + \alpha^* \rangle^2] \right\}, \end{aligned} \quad (2.20)$$

which shows that $\langle \Delta X^2 \rangle < \frac{1}{4}$ only if $P(\alpha)$ is not positive definite. The constant contribution $\frac{1}{4}$ on the right-hand side of the above expression comes from the commutator of \hat{a} and \hat{a}^\dagger in the process of normal-ordering the original expression. It is thus a manifestation of the quantum character of the field (“shot noise”). Equation (2.20) may be written in a more compact form in the following way:

$$\langle \Delta X^2 \rangle = \frac{1}{4} + \langle : \Delta X^2 : \rangle, \quad (2.21)$$

where the double dots indicate the normal form of the operator.

For antinormal ordering, one has the *Q representation*, which can be obtained immediately by inserting Eq. (2.10) into the corresponding quantum-mechanical average:

$$\langle \hat{a}^m (\hat{a}^\dagger)^n \rangle = \frac{1}{\pi} \int d^2 \alpha \langle \alpha | \rho | \alpha \rangle \alpha^m (\alpha^*)^n, \quad (2.22)$$

so that

$$Q(\alpha) = \frac{1}{\pi} \langle \alpha | \rho | \alpha \rangle. \quad (2.23)$$

It is clear that this representation is always positive, since ρ is a positive-definite operator. Also, $|Q(\alpha)| \leq 1/\pi$. For a coherent state $|\alpha_0\rangle$, one gets from Eqs. (2.11) and (2.23) that $Q(\alpha) = (1/\pi) \exp(-|\alpha - \alpha_0|^2)$, i.e., $Q(\alpha)$ is a Gaussian in phase space. The section of this Gaussian with radius $\frac{1}{2}$ may be used to represent the coherent state in phase space, the radius corresponding to the dispersion in the measurements of the quadratures of the field. Analogously, the squeezed states $|\alpha, \xi\rangle$ may be represented in phase space by ellipses. This is displayed in Fig. 1, which also exhibits the effect of the transformation (2.12) on the vacuum state. Note that, in terms of the Q representation, the equation equivalent to Eq. (2.20) is

$$\begin{aligned} \langle \Delta X^2 \rangle &= \frac{1}{4} [\langle \hat{a}^2 + \hat{a}^{\dagger 2} + 2\hat{a}^\dagger \hat{a} - 1 \rangle - \langle \hat{a} + \hat{a}^\dagger \rangle^2] \\ &= \frac{1}{4} \left\{ -1 + \int d^2 \alpha Q(\alpha) [(\alpha + \alpha^*)^2 - \langle \alpha + \alpha^* \rangle^2] \right\}, \end{aligned} \quad (2.24)$$

and therefore squeezing now implies that the integral on the right-hand side must be smaller than 2 (it is necessarily larger than 1, since $\langle \Delta X^2 \rangle > 0$).

Symmetrical ordering of the operators leads to the *Wigner representation* $W(\alpha)$ (Wigner, 1932; Hillery *et al.*, 1984). This can be shown to be always nonsingular (although it may still attain negative values). Moreover, for the squeezed states $|\alpha, \xi\rangle$, it is always positive. Note that the equation equivalent to Eq. (2.20) is now

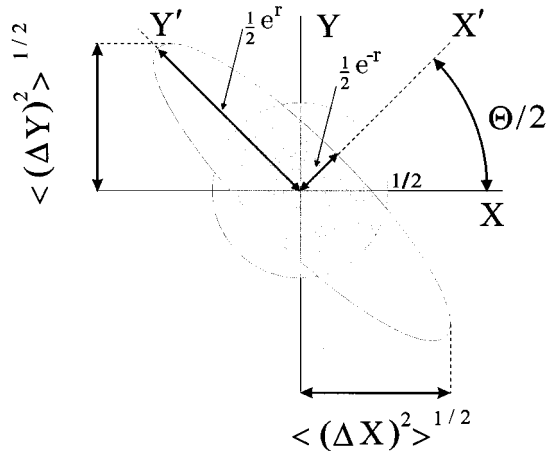


FIG. 1. Vacuum state and squeezed vacuum. The squeezed state is obtained from the vacuum state by applying the transformation (2.12).

$$\begin{aligned} \langle \Delta X^2 \rangle &= \frac{1}{4} [\langle \hat{a}^2 + \hat{a}^{\dagger 2} + \hat{a} \hat{a}^\dagger + \hat{a}^\dagger \hat{a} \rangle - \langle \hat{a} + \hat{a}^\dagger \rangle^2] \\ &= \frac{1}{4} \int d^2 \alpha W(\alpha) [(\alpha + \alpha^*)^2 - \langle \alpha + \alpha^* \rangle^2]. \end{aligned} \quad (2.25)$$

Therefore, for the Wigner representation the dispersion is given directly by the c -number integral; there is no shot-noise term. Of course, the final result should be independent of the representation.

Still other representations have been defined. Thus, a generalization of the Glauber-Sudarshan representation was proposed by Drummond and Gardiner (1980): the *positive- P representation* is a function of two complex variables satisfying

$$\langle (a^\dagger)^m a^n \rangle = \int d^2 \alpha d^2 \beta P(\alpha, \beta) (\beta^*)^m \alpha^n. \quad (2.26)$$

It is always positive and nonsingular, at the expense, however, of doubling the number of variables in phase space.

D. Number-phase squeezing

A related, though not equivalent, class of quantum-noise-compressed states are the *number-phase squeezed states*. The precise definition of these states requires the introduction of an operator corresponding to the phase of an electromagnetic field, which is an old problem in physics, first attempted by Dirac (1927). This question was analyzed in detail by Susskind and Glogower (1964). A Hermitian phase operator was introduced by Pegg and Barnett (1988, 1989). For a coherent state $|\alpha\rangle$, with $|\alpha| \gg 1$, its average value coincides with the phase of α , while its variance is given by $\langle \Delta \phi^2 \rangle = 1/4 \langle n \rangle$ (Barnett and Pegg, 1989). Note that the same value for the dispersion would be obtained from a phase-space picture, in the limit of large average photon number, as shown in Fig. 2. Since, for a coherent state, the photon-number variance is given by $\langle (\Delta n)^2 \rangle = \langle n \rangle$, we have $\langle \Delta n^2 \rangle \langle \Delta \phi^2 \rangle = 1/4$, which represents the stan-

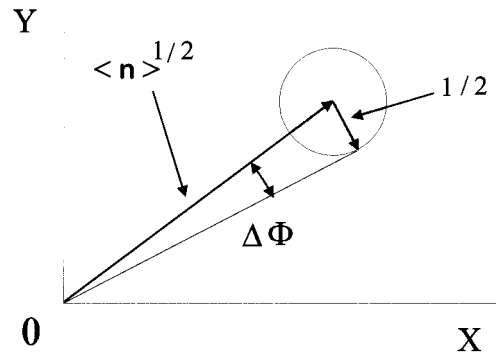


FIG. 2. Phase uncertainty for a coherent state $|\alpha\rangle$.

dard quantum limit in this case. Squeezing in photon number or in phase is obtained when the respective dispersions get smaller than those for a coherent state. The corresponding states are also “nonclassical,” in the same sense as for quadrature-squeezed states. In fact, for the photon-number variance, one has

$$\langle \Delta n^2 \rangle = \langle n \rangle + \langle (\hat{a}^\dagger \hat{a}^\dagger \hat{a} \hat{a} - \langle \hat{a}^\dagger \hat{a} \rangle^2) \rangle, \quad (2.27)$$

or, using the Glauber-Sudarshan representation,

$$\langle \Delta n^2 \rangle = \langle n \rangle + \int d^2 \alpha P(\alpha) (|\alpha|^2 - \langle |\alpha|^2 \rangle)^2. \quad (2.28)$$

This is the equation displayed in the introductory section—Eq. (1.2)—specialized to the one-mode case. As discussed before, $\langle \Delta n^2 \rangle < \langle n \rangle$ only if $P(\alpha)$ is not positive definite. For a classical field, Eq. (2.28) exhibits explicitly the dual nature of light: the first contribution on the right-hand side is a corpusclelike contribution (shot noise), while the remaining term is characteristic of wave fluctuations. However, while for a thermal or a coherent field this separation is clear cut, this is not so for a squeezed state, since the integral in this case becomes negative, and therefore also reflects the quantum nature of the state.

E. Relation between quadrature and number squeezing

Quadrature squeezing and photon-number quenching are not equivalent: squeezed states may have super-Poissonian photon statistics, and sub-Poissonian states are not necessarily squeezed.

Indeed, for the Fock state $|n\rangle$, which has zero variance in photon number, one has

$$\langle \Delta X^2 \rangle = \langle \Delta Y^2 \rangle = \frac{1}{4} (2n+1) \geq \frac{1}{4}. \quad (2.29)$$

On the other hand, the photon-number variance for the squeezed states $|\alpha, \xi\rangle$ given by Eq. (2.17) is

$$\langle \Delta n^2 \rangle = |\alpha \cosh r - \alpha^* e^{i\theta} \sinh r|^2 + 2 \cosh^2 r \sinh^2 r. \quad (2.30)$$

Setting $\alpha = |\alpha| e^{i\phi}$, then for $\theta = 2\phi + \pi$, one has

$$\langle \Delta n^2 \rangle = |\alpha|^2 e^{2r} + 2 \sinh^2 r \cosh^2 r. \quad (2.31)$$

This corresponds to a squeezing that is $\pi/2$ out of phase with the complex field amplitude (*phase-squeezed state*),

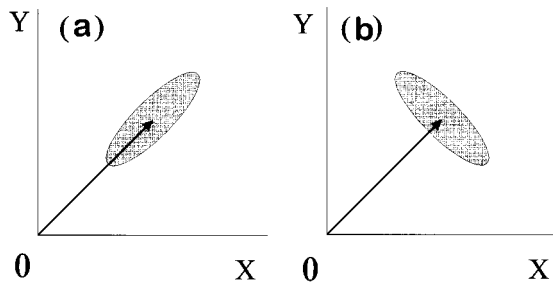


FIG. 3. (a) Phase-squeezed state. (b) Amplitude-squeezed state.

as shown in Fig. 3(a). In this situation, the state has increased amplitude fluctuations compared to a coherent state, and the photon-number statistics is super-Poissonian.

On the other hand, for $\theta = 2\phi$, one finds

$$\langle \Delta n^2 \rangle = |\alpha|^2 e^{-2r} + 2 \sinh^2 r \cosh^2 r. \quad (2.32)$$

The squeezing is now in phase with the complex amplitude, and the corresponding state is called an *amplitude-squeezed state*—see Fig. 3(b). The first term on the right-hand side represents the contribution of the squeezed amplitude, while the second term is associated with the photon-number fluctuations in the corresponding squeezed-vacuum state. For sufficiently large average photon numbers, that is, for $|\alpha|^2 \gg 2e^{2r} \sinh^2 r \cosh^2 r$, the first term dominates over the second, and one gets an amplitude-squeezed state with sub-Poissonian photon distribution. For $r \approx 1$, so that the dispersion in the amplitude is reduced by a factor $e^{-1} \approx 0.37$, this corresponds to $|\alpha|^2 \gg 50$. Under these conditions, one has also $\langle n \rangle \approx |\alpha|^2$, so that, using Eq. (2.15), one may write

$$\langle \Delta n^2 \rangle \approx |\alpha|^2 e^{-2r} = 4 \langle n \rangle \langle \Delta X'^2 \rangle, \quad (2.33)$$

which exhibits a simple relation between the dispersion in the photon number and the dispersion in the amplitude quadrature. Note that for $r=1$, one gets $\Delta n^2 \approx 0.14 \langle n \rangle$, already a highly sub-Poissonian state. The relation (2.33) corresponds to the classical relation between intensity and amplitude fluctuations, valid for small fluctuations:

$$I = \mathcal{A}^2 \Rightarrow \delta I \approx 2 \mathcal{A} \delta \mathcal{A} \Rightarrow (\delta I)^2 \approx 4 \mathcal{A}^2 (\delta \mathcal{A})^2. \quad (2.34)$$

One should note, however, that Eq. (2.33) refers to dispersions of operators. In particular, writing as in Eq. (2.21) $\langle \Delta X'^2 \rangle = \frac{1}{4} + \langle : \Delta X'^2 : \rangle$, one may write Eq. (2.33) as

$$\langle \Delta n^2 \rangle \approx \langle n \rangle + 4 \langle n \rangle \langle : \Delta X'^2 : \rangle. \quad (2.35)$$

On the other hand, for a fixed value of the average number of photons, and as the squeezing factor r increases from zero, one gets first a sub-Poissonian distribution and then, for sufficiently large r , a super-Poissonian distribution. The latter occurs when $\langle \Delta n^2 \rangle > \langle n \rangle$, or $|\alpha|^2 e^{-2r} + 2 \sinh^2 r \cosh^2 r > |\alpha|^2 + \sinh^2 r$. For $|\alpha|^2 \gg 1$, this relation will be satisfied by r such that $\cosh^2 r \gg 1$ and $\sinh^2 r \cosh^2 r \approx e^{4r}/16$, so that the inequality

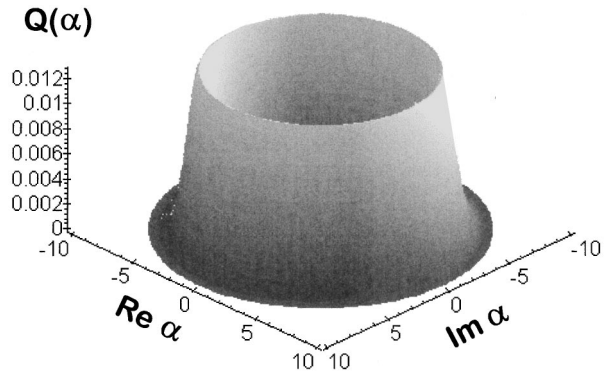


FIG. 4. Q representation of a laser field highly above threshold. The average number of photons is taken as 50 for illustration purposes.

becomes $\frac{1}{8} e^{4r} > 8 |\alpha|^2$, or $r > \frac{1}{4} \ln(8 |\alpha|^2)$. For $|\alpha|^2 = 1000$, this yields $r > 2.25$, corresponding to amplitude squeezing by a factor $e^{-r} \approx 0.11$. The minimum dispersion in photon number is obtained by minimizing Eq. (2.32). For $r > 1$, one may approximate as before $\sinh^2 r \cosh^2 r \approx \frac{1}{16} e^{4r}$, getting then the minimum value of Eq. (2.32) for $r = \frac{1}{6} \ln(4 |\alpha|^2)$, corresponding to $\langle \Delta n^2 \rangle_{\min} \approx 0.94 |\alpha|^2 \approx (\langle n \rangle)^{2/3}$. The fact that the photon-number distribution becomes super-Poissonian as the squeezing increases can be heuristically understood from Fig. 3(b): as the uncertainty ellipse becomes more compressed, the range of intensities (squares of the distances to the origin) associated to the points within it becomes larger and larger, resulting in a wider photon-number distribution.

The relation (2.33), or equivalently (2.35), is actually a very useful one, since it allows the computation of the photon-number variance, which involves a fourth-order correlation of field variables, in terms of the amplitude quadrature variance, which involves second-order correlations. We have demonstrated that this relation holds, under some conditions, for the squeezed states $|\alpha, \xi\rangle$. Its range of validity is much wider, however. It can be applied, for instance, to a laser far above threshold. The corresponding photon-number distribution can then be shown to be very approximately Poissonian, but the phase distribution is completely random, so that the associated Q representation looks like a “volcano ring,” as shown in Fig. 4. Note that, contrary to what happens to the amplitude-squeezed state displayed in Fig. 3(b), the region around the peak of the distribution remains equidistant from the origin, and the applicability of the relation (2.33) in this case follows from the fact that the amplitude fluctuations go to zero as the laser intensity increases, as will be shown in Sec. V.

Fourth-order correlations of field variables offer a more detailed description of the statistical behavior of the field, and unveil further nonclassical properties. One such is the phenomenon of antibunching, which we review next.

F. Photon antibunching

Intensity-correlation experiments have provided powerful tools in astronomy, since they allow the determination of the angular diameter of distant stars (see, for instance, Mandel and Wolf, 1965; Nussenzveig, 1974). The first experiment was conducted by Hanbury-Brown and Twiss (1956). The measured quantity is the joint probability of counting a photon at t and another at $t + \tau$. This probability is, according to Glauber (1963a), proportional to the normal-ordered correlation function

$$G^{(2)}(\tau) = \langle \hat{n}(t) \hat{n}(t + \tau) \rangle, \quad (2.36)$$

where the double dots indicate normal ordering, and $\hat{n}(t)$ is the photon-number operator at time t . The fact that $G^{(2)}$ does not depend on t is characteristic of a stationary process. The second-order degree of coherence is defined as

$$g^{(2)}(\tau) = \frac{G^{(2)}(\tau)}{|\langle n \rangle|^2}. \quad (2.37)$$

This quantity describes whether the photons in the beam tend to group together or stay apart. If $g^{(2)}(\tau) = 1$, the probability of joint detection coincides with the probability of independent detection. This should be the case when $\tau \rightarrow \infty$, since in this case the memory of the first photodetection dies out. If $g^{(2)}(\tau) < g^{(2)}(0)$, the probability of detecting the second photon decreases with the time delay, indicating a *bunching* of photons. If on the other hand $g^{(2)}(\tau) > g^{(2)}(0)$, the probability of detecting the second photon increases with the time delay, which is characteristic of photon *antibunching*.

For a single-mode field (not necessarily monochromatic), one has

$$g^{(2)}(0) = \frac{\langle a^\dagger a^\dagger a a \rangle}{(\langle a^\dagger a \rangle)^2}. \quad (2.38)$$

If this mode is in a coherent state, we have $g^{(2)}(0) = 1$. On the other hand, for a Fock state $|n\rangle$, with $n \geq 2$, one has

$$g^{(2)}(0) = 1 - \frac{1}{n}, \quad (2.39)$$

while for $n=0$ or $n=1$, one finds trivially that $g^{(2)}(0) = 0$.

More generally, if the state of the field is described by the Glauber-Sudarshan distribution $P(\{\alpha_{\vec{k},s}\})$, it follows from Eqs. (2.36) and (2.37) that

$$\begin{aligned} g^{(2)}(0) &= \frac{\int d\{\alpha_{\vec{k},s}\} P(\{\alpha_{\vec{k},s}\}) (\sum_{\vec{k},s} |\alpha_{\vec{k},s}|^2)^2}{(\sum_{\vec{k},s} |\alpha_{\vec{k},s}|^2)^2} \\ &= 1 + \frac{\int P(\{\alpha_{\vec{k},s}\}) [\sum_{\vec{k},s} (|\alpha_{\vec{k},s}|^2 - \langle |\alpha_{\vec{k},s}|^2 \rangle)]^2}{(\sum_{\vec{k},s} |\alpha_{\vec{k},s}|^2)^2}. \end{aligned} \quad (2.40)$$

This equation establishes that, for classical fields, with $P(\{\alpha_{\vec{k},s}\}) \geq 0$, one should have $g^{(2)}(0) \geq 1$. It follows also, by applying the Schwarz inequality to the classical correlation function corresponding to Eq. (2.36), that

one should always have $g^{(2)}(\tau) \leq g^{(2)}(0)$, so that classical fields are never antibunched (Loudon, 1980, 1983). Therefore, the two properties $g^{(2)}(0) < 1$ and $g^{(2)}(\tau) > g^{(2)}(0)$ are characteristic of nonclassical light [an instance of the first property is provided by Eq. (2.39)]. Since $g^{(2)}(\tau) \rightarrow 1$ when $\tau \rightarrow \infty$, the property $g^{(2)}(0) < 1$ always implies that there is antibunching for some range of values of τ [unless $g^{(2)}(\tau)$ is independent of τ].

The relation between antibunching and sub-Poissonian statistics is a subtle one (Mandel, 1986; Zou and Mandel, 1990). In fact, from Eq. (2.38), one can show the following relation between the second-order degree of coherence and the photon-number variance, for a single-mode field:

$$g^{(2)}(0) = 1 + \frac{\langle \Delta n^2 \rangle - \langle n \rangle}{\langle n \rangle^2}. \quad (2.41)$$

Therefore, in this case sub-Poissonian statistics implies $g^{(2)}(0) < 1$, which, unless $g^{(2)}(\tau)$ does not depend on τ , implies antibunching for some range of τ . On the other hand, one cannot say in general that antibunching leads to sub-Poissonian statistics, since $g^{(2)}(\tau) > g^{(2)}(0)$ does not necessarily imply $g^{(2)}(0) < 1$. In fact, for a stationary field the variance of the number of photons measured by a photodetector during a counting interval T can be expressed in terms of $g^{(2)}(\tau)$ in the following way (Zou and Mandel, 1990):

$$\langle \Delta n^2 \rangle - \langle n \rangle = \frac{\langle n \rangle^2}{T} \int_{-T}^{+T} d\tau (T - |\tau|) [g^{(2)}(\tau) - 1]. \quad (2.42)$$

If $g^{(2)}(\tau) < 1$ for all τ , the field will exhibit sub-Poissonian statistics. One could have, however, $g^{(2)}(\tau) > g^{(2)}(0)$, while still having super-Poissonian statistics for some time interval. Furthermore, for a single monochromatic mode, $g^{(2)}(\tau)$ does not depend on τ , and coincides with the value for $\tau=0$. In this case, $g^{(2)}(0) < 1$ does not imply antibunching for any counting interval, since neither short or long time intervals between photons are favored.

An example of a field that is sub-Poissonian and bunched may be constructed using two modes with parallel \vec{k} and the same polarization s , but different frequencies ω_1 and ω_2 (Zou and Mandel, 1990). Placing an equal number $n/2$ of photons in each mode, one finds

$$g^{(2)}(\tau) = 1 - \frac{1}{n} + \frac{1}{2} \cos[(\omega_1 - \omega_2)\tau], \quad (2.43)$$

so that, using Eq. (2.42),

$$\langle \Delta n^2 \rangle - \langle n \rangle = \langle n \rangle^2 \left\{ \frac{1}{2} \left[\frac{\sin(\omega_1 - \omega_2)T/2}{(\omega_1 - \omega_2)T/2} \right]^2 - \frac{1}{n} \right\}. \quad (2.44)$$

It follows that for certain time intervals, for example $T = 2\pi/|\omega_1 - \omega_2|$, the photon-counting statistics are sub-Poissonian. On the other hand, the slope of $g^{(2)}(\tau)$ is negative for $\tau=0$, so that the photons exhibit short-time bunching.

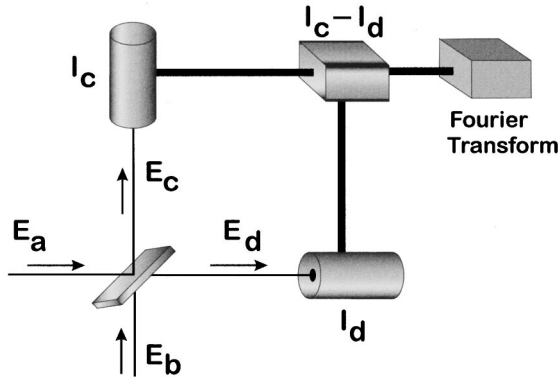


FIG. 5. Method of homodyne detection.

Bunching occurs in a thermal field; this property is used in stellar interferometry to find the angular diameter of stars. On the other hand, antibunching was predicted for the fluorescence of a single atom subjected to a resonant laser field (Carmichael and Walls, 1976a, 1976b; Kimble and Mandel, 1976; Cohen-Tannoudji, 1977). As mentioned in the Introduction, the physical origin of this phenomenon is the dead time between the emission of a photon by an atom undergoing de-excitation and the subsequent emission of a second photon by the same atom, which requires its reexcitation.

G. Measurement of quadrature squeezing

Several methods have been proposed to measure quadratures of the electromagnetic field (for a review, see Loudon and Knight, 1987). The general idea is to mix the signal to be detected with an intense coherent signal, called *local oscillator*, before detection (Yuen and Shapiro, 1980; Caves, 1981; Yuen and Chan, 1983; Schumaker, 1984).

The discussion here is restricted to the method of *balanced homodyne detection*, sketched in Fig. 5. The field to be measured (complex amplitude E_a) is sent on a beam splitter, together with a coherent field (complex amplitude E_b) with the same frequency. One then measures the difference of intensity of the two beams emerging from the beam splitter (complex amplitudes E_c and E_d). The detection is said to be balanced when the mirror transmits 50% of the incident light.

Let r and t be the reflection and transmission coefficients of the mirror, respectively. One has then

$$E_c = rE_a - tE_b, \quad (2.45a)$$

$$E_d = tE_a + rE_b, \quad (2.45b)$$

or, in matrix form,

$$\begin{pmatrix} E_c \\ E_d \end{pmatrix} = \begin{pmatrix} r & -t \\ t & r \end{pmatrix} \begin{pmatrix} E_a \\ E_b \end{pmatrix}. \quad (2.46)$$

Energy conservation (assuming that losses are negligible) implies that

$$|E_c|^2 + |E_d|^2 = |E_a|^2 + |E_b|^2. \quad (2.47)$$

From Eqs. (2.46) and (2.47), one finds

$$|r|^2 + |t|^2 = 1, \quad (2.48a)$$

$$r^*t - rt^* = 0. \quad (2.48b)$$

If one takes r real and equal to $\sqrt{\eta}$, it follows from Eq. (2.48) that $t = \pm(1-\eta)^{1/2}$. Choosing the positive sign, one has then

$$\begin{pmatrix} E_c \\ E_d \end{pmatrix} = \begin{pmatrix} \sqrt{\eta} & -\sqrt{1-\eta} \\ \sqrt{1-\eta} & \sqrt{\eta} \end{pmatrix} \begin{pmatrix} E_a \\ E_b \end{pmatrix}. \quad (2.49)$$

Normalizing the intensity to the photon number, and introducing the annihilation operators through

$$E_a \rightarrow \hat{a}, \quad E_b \rightarrow \hat{b},$$

$$E_c \rightarrow \hat{c}, \quad E_d \rightarrow \hat{d},$$

one gets, from Eq. (2.49),

$$\hat{c} = \sqrt{\eta}\hat{a} - \sqrt{1-\eta}\hat{b}, \quad (2.50a)$$

$$\hat{d} = \sqrt{1-\eta}\hat{a} + \sqrt{\eta}\hat{b}. \quad (2.50b)$$

For balanced detection, $\eta = 1/2$, so that

$$\hat{c} = \frac{1}{\sqrt{2}}(\hat{a} - \hat{b}),$$

$$\hat{d} = \frac{1}{\sqrt{2}}(\hat{a} + \hat{b}).$$

Note that the conditions (2.48) imply that the transformation between the field operators corresponding to Eq. (2.46) is unitary (this is the requirement for operators that corresponds to energy conservation for the classical fields).

The difference between the intensities of the fields E_d and E_c is given then by

$$I = \hat{d}^\dagger \hat{d} - \hat{c}^\dagger \hat{c} = \hat{a}^\dagger \hat{b} + \hat{b}^\dagger \hat{a}. \quad (2.51)$$

Assuming that the field E_b can be described classically (as would be the case for a coherent state with large average photon number), one replaces \hat{b} by $\beta = B e^{-i(\omega t + \theta)}$, so that Eq. (2.51) becomes

$$I = B[\hat{a} e^{i(\omega t + \theta)} + \hat{a}^\dagger e^{-i(\omega t + \theta)}]. \quad (2.52)$$

Since $\hat{a} = \hat{a}_0 e^{-i\omega t}$, one gets finally

$$I = B(\hat{a}_0 e^{i\theta} + \hat{a}_0^\dagger e^{-i\theta}). \quad (2.53)$$

This equation shows that the difference in intensity, measured by the method of homodyne detection, is directly proportional to the quadrature $\hat{X}(\theta)$ of the field E_a , defined by

$$\hat{X}(\theta) = \frac{1}{\sqrt{2}}(\hat{a}_0 e^{i\theta} + \hat{a}_0^\dagger e^{-i\theta}). \quad (2.54)$$

Therefore, by detecting the difference in intensity as the phase of the local oscillator E_b is changed, one can measure an arbitrary quadrature of the field E_a . In actual experiments, the phase of the local oscillator is adjusted to yield the maximum possible quadrature squeezing.

The shot-noise level is determined by blocking the signal field, so only the local oscillator field reaches the detector. The results of the measurements are spectrally analyzed, allowing determination of the amount of squeezing as a function of the frequency.

H. Effect of dissipation

Dissipation can be simulated by the beam splitter in Fig. 5, if one assumes that the field E_b is in the vacuum state. Indeed, in this case, the field E_c contains the two outcomes of a dissipation process: an intensity-reduced contribution from the signal field E_a , and an admixture of Poisson noise, associated with the vacuum field E_b . From Eq. (2.50a), one has

$$\langle \Delta c^2 \rangle = \eta \langle \Delta a^2 \rangle + (1 - \eta) \langle \Delta b^2 \rangle, \quad (2.55)$$

so that, since $\langle \Delta b^2 \rangle = 1/4$,

$$\langle \Delta c^2 \rangle - \frac{1}{4} = \eta \left(\langle \Delta a^2 \rangle - \frac{1}{4} \right). \quad (2.56)$$

Therefore, the smaller η is (simulating a stronger dissipation process), the closer the variance of \hat{c} will be to the shot-noise level: dissipation spoils squeezing, and \hat{c} will be less squeezed than \hat{a} .

I. Applications of sub-Poissonian light

Applications of squeezed light have been extensively discussed in the literature (Yamamoto *et al.*, 1990; Reynaud, 1990; Walls and Milburn, 1994). For this reason, only a brief summary will be presented here, restricted to some of the most important applications envisaged for sub-Poissonian light.

One of the main possible applications of sub-Poissonian beams of light is in communication (see, for instance, Yamamoto *et al.*, 1990), where one wants to use signals with the lowest possible intensity, and the least possible-noise. Since dissipation strongly affects quantum-noise compression, one usually envisages short-distance communications with low losses, for instance through optical fibers in a local network. A communication system based on photon counting would involve on and off pulses (intensity modulation). An error rate of 10^{-9} is considered to be the maximum tolerable. This error arises because, for a given pulse, there is a photon-number distribution that allows for a finite probability of having 0 photons. Indeed, for the Poissonian distribution (2.9), one has $p(0) = \exp(-\langle n \rangle)$, so that $p(0) < 10^{-9}$ implies that the average number of photons in the pulse should be larger than 21. If in addition one assumes that on and off pulses are sent with equal probabilities, one finds that the average number of photons should be larger than 10.5. This number is very close to the best sensitivity obtained for photon communication, of the order of 50 photons per pulse (Levine and Bethea, 1984). Sub-Poissonian pulses would allow reduction of the minimum average photon number, while still keeping the bit error smaller than 10^{-9} .

A cavity containing a Fock state of the field was proposed by Braginsky and Vorontsov (1974) as an ex-

tremely sensitive sensor for small vibrations, which could be used in the detection of gravitational waves. Their idea was to couple such a cavity to a massive bar, and measure the change in the number of photons due to conversion of vibration phonons. The fact that the photon number in the cavity is dispersion-free allows the detection of very small changes in the photon number, which is essential for the detection of the very weak forces associated with gravitational waves (Caves *et al.*, 1980).

Several proposals have been made to increase the maximum sensitivity of interferometric detectors of gravitational radiation by using squeezed light (Caves, 1980; Unruh, 1983; Bondurant and Shapiro, 1984; Jaekel and Reynaud, 1990; Pace *et al.*, 1993).

The detection of gravitational waves is but one example of the extremely precise measurements made possible by the utilization of squeezed light. Extensive discussion can be found in the literature on methods for measuring very small phase shifts in Mach-Zender interferometers (Grangier *et al.*, 1987; Xiao *et al.*, 1987), on the application of squeezed light to increase the sensitivity of gyroscopes (Ezekiel *et al.*, 1978; Dorschner *et al.*, 1980; Chow *et al.*, 1985), and on spectroscopy with resolution below the natural linewidth (Gardiner, 1986; Gardiner *et al.*, 1987; Parkins and Gardiner, 1988; Polzik *et al.*, 1992). Noise decrease in interference measurements through the use of sub-Poissonian laser radiation was discussed by Kolobov and Sokolov (1986).

Photon-number noise can also be reduced in the difference of twin-photon beams, generated by nonlinear processes that result in the simultaneous emission of two photons. The intensity fluctuations in the two beams are highly correlated. This can be used for instance in very precise measurements of absorption, by letting one of the beams cross the resonant sample, and analyzing the low-noise difference in intensities.

III. EXPERIMENTS

In recent years, several experiments have demonstrated the production of nonclassical light. In spite of the large multiplicity of methods and media, one can recognize four main classes of processes: (i) processes in which the atomic medium is essentially passive, playing the role of a nonlinear refraction index—this is the case of parametric processes and second-harmonic generation; (ii) processes in which atoms play an active role, through their coherence and exchange of energy with the field—this is the case in resonant atomic fluorescence, optical bistability, and sub-Poissonian lasers and masers; (iii) processes in which there is simultaneous emission of two nondegenerate photons, leading to reduced quantum noise in the difference of intensities—both parametric devices and two-photon lasers can be used for this purpose; and (iv) processes in which quantum-noise reduction results from information obtained through measurements—this is the case for active-control techniques, in which the measurements are used to counteract the fluctuations of the light beam,

and for state-vector projection obtained by continuous monitoring of the system, for instance through quantum nondemolition measurements. In the following, the main experimental achievements are summarized. They are grouped according to the techniques and media involved.

A. Parametric processes

Most of the experiments leading to the production of squeezed states are based on parametric processes, originating from nonlinear optical devices. The process of parametric amplification is well known from the swing example: the modulation of the length of a swing with a frequency twice its oscillation frequency leads to amplification of one of the quadrature components, and exponential damping of the other. In nonlinear devices, it is the index of refraction that is modulated by a pump field, in such a way that one of the quadrature components of the signal field is amplified, and the other is damped, thus generating a squeezed state.

That a nonlinear medium is essential for obtaining squeezing can be seen from Eq. (2.12). Indeed, the squeezing operator can be interpreted as corresponding to a time-evolution operator, generated by a Hamiltonian quadratic in the field operators (Yuen, 1975, 1976):

$$H = \frac{\hbar}{2} (\eta^* \hat{a}^2 + \eta \hat{a}^{\dagger 2}), \quad (3.1)$$

with ξ in Eq. (2.12) related to η through $\xi = i\eta t$. This Hamiltonian describes the creation or annihilation of pairs of identical photons. The pump field is described by a c number, and its amplitude E_p is incorporated into the coupling constant. If $\eta = \chi^{(2)} E_p$, where $\chi^{(n)}$ is the n th-order susceptibility, one has a *degenerate parametric down-conversion* or *degenerate three-wave mixing*: in this case, the frequency of the pump field is twice that of the signal field. If on the other hand $\eta = \chi^{(3)} E_p^2$, one has *degenerate four-wave mixing* and the frequency of the pump field is equal to that of the signal field. While in the first case one photon of the pump field generates two photons of the signal field (hence the name “three-wave mixing”), in the second case one needs two photons of the pump field in order to produce two photons of the signal field (thus yielding a four-wave mixing). Of course, dissipation must also be taken into account.

More generally, one can have the two photons of the signal field belonging to modes differing in propagation direction, polarization or frequency, leading to the corresponding nondegenerate processes. If ω_s and ω_i are the frequencies of the two modes (conventionally termed signal and idler beams), and ω_p is the frequency of the pump field, one has $\omega_p = \omega_s + \omega_i$ for three-wave mixing, and $2\omega_p = \omega_s + \omega_i$ for four-wave mixing. The two processes are illustrated in Fig. 6. Conservation of photon momentum requires that $\vec{k}_p = \vec{k}_s + \vec{k}_i$ for three-wave mixing and $2\vec{k}_p = \vec{k}_s + \vec{k}_i$ for four-wave mixing (*phase-matching* conditions). This is a limiting factor in the first case, since then the frequency of the pump field is quite

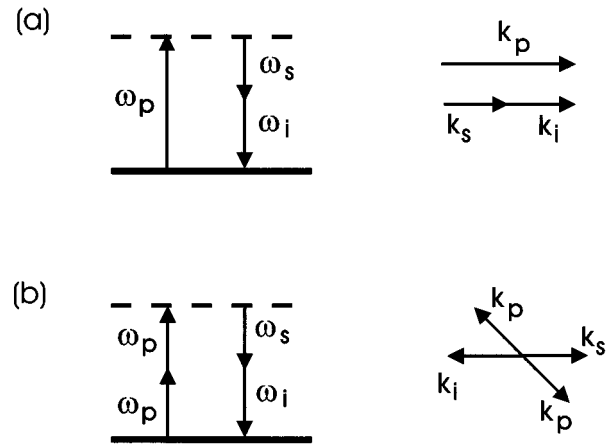


FIG. 6. Three- and four-wave mixing in the parametric amplifier. (a) Three-wave mixing. (b) Four-wave mixing.

different from the frequency of the signal and idler waves, implying quite different values for the nonlinear index of refraction, so that the relation $\omega_p = \omega_s + \omega_i$ does not imply conservation of momenta for aligned beams: proper nonlinear crystals and frequencies must be chosen to satisfy the phase-matching condition. This condition is easier to satisfy in the four-wave-mixing case, since then ω_p is close to ω_s and ω_i : it suffices to choose an appropriate angle between the three signals [see Fig. 6(b)]. The nonlinearity can be enhanced by making the process resonant, so that the pump field induces a transition between two atomic levels. This has, however, the disadvantage of leading to population of the excited level, which may decay spontaneously, thus generating noise which spoils squeezing. One should look therefore for a compromising detuning: small enough to enhance the wave-mixing process, but not so small as to produce too much spontaneous-emission noise.

Since the second- and third-order susceptibilities are very small, the medium is usually placed inside a high- Q cavity, causing the system to oscillate, thus enhancing the nonlinear coupling. In this case, one has an *optical parametric oscillator*. The squeezing effect is more pronounced close to the oscillation threshold, where the fluctuations of the amplified component diverge. Due to conservation of phase-space volume for the Hamiltonian process governed by Eq. (3.1), this implies compression of the fluctuations associated to the other quadrature component. The validity of this argument depends of course on the absence of loss for the two quadratures, either through dissipation or through nonlinear frequency conversion. Large squeezing of the transmitted-signal mode was predicted in the degenerate optical parametric oscillator near the oscillation threshold (Yurke, 1984; Collett and Gardiner, 1984; Collett and Walls, 1985).

Measurements of squeezing usually employ the technique of homodyne detection, spectrally analyzing the intensity difference between the signal and the local oscillator field (see Sec. II.G.). One searches for squeezing as a function of frequency, the desirable feature being a

large reduction of quantum noise in a wide frequency band. The first experimental observation of squeezing was made by Slusher *et al.* (1985), using resonant four-wave mixing in a sodium atomic beam, the interaction taking place inside an optical cavity. They observed amplitude squeezing 16% below the shot-noise level. This result was strongly affected by the spontaneous-emission noise mentioned above.

A nonresonant four-wave-mixing experiment was performed by Shelby *et al.* (1986) in a single-mode silica fiber, cooled to 1.4 K to suppress the phonon-scattering noise. They observed squeezing of 17% below shot noise. In this case, squeezing is spoiled by fluctuations in the index of refraction due to Brillouin scattering (Shelby *et al.*, 1985).

Four-wave mixing squeezing without an optical cavity was observed by Maeda *et al.* (1986), using a dense sodium medium.

Three-wave mixing has allowed better results. Wu *et al.* (1986, 1988) measured quadrature amplitude squeezing of 63% (-4 dB) below the shot-noise level, with a balanced homodyne detection of the nearly degenerate transmitted-signal beam. The nonlinear medium was a MgO: LiNbO₃ crystal, placed inside a high- Q optical cavity, and pumped by the frequency-doubled output of a 1.06 μm Nd:YAG laser. Correcting the result for the detection-circuit quantum efficiency and the cavity internal loss, it was possible to show that the noise level of the cavity field was 90% (-10 dB) below shot-noise level. In spite of the more difficult situation with respect to phase matching, as mentioned before, the process of three-wave mixing has two advantages over the four-wave-mixing method: first, the lower-order nonlinearity allows significant signal levels in a nonresonant situation, thus eliminating spontaneous emission noise; and second, since $\omega_p = \omega_s + \omega_i$, the pumping frequency is quite different from the signal frequencies, which allows easy elimination of noise associated with the pump field.

B. Second-harmonic generation

Second-harmonic generation may be considered as inverse to parametric downconversion: the pump field with frequency ω_p generates a field with frequency $2\omega_p$. Again, maximum squeezing is obtained near the oscillation threshold for the field with frequency $2\omega_p$, due to critical fluctuations in one of the quadrature components. Amplitude squeezing was demonstrated by Pereira *et al.* (1989) and by Sizman *et al.* (1990). Both groups used a crystal of MgO: LiNbO₃. While the first group placed the crystal in an optical cavity, the second used a monolithic crystal with dielectric mirror coatings on the end faces of the crystal. They obtained squeezing of 13% and 40% below shot noise, respectively.

C. Resonant atomic fluorescence

It should be stressed that the Hamiltonian (3.1), as well as the analogous one for the nondegenerate process, replaces the atomic medium by a nonlinear suscep-

tibility. This procedure disregards the effects of atomic dynamics. It can be justified if the relaxation constants of the nonlinear system are large compared to the cavity decay rate. In this case, the atomic transients die out very fast, and the atomic variables follow the field adiabatically (an example of adiabatic elimination of atomic variables will be discussed in Sec. VI.B.1.). This is the situation for many of the experiments performed so far. There are, however, some important exceptions, one of which corresponds in fact to the first experimental demonstration of nonclassical radiation: the generation of sub-Poissonian and antibunched light by an atom that interacts with a resonant laser beam. As discussed in Sec. II.F, antibunching in this case results from the fact that, after emitting a photon, an atom has to be re-excited before it emits a second photon, implying that the probability of joint detection of two photons increases as the time interval between detections increases from zero (vanishing probability) to a time of order the lifetime of the transition. Experimental demonstration of antibunching was achieved by Kimble *et al.* (1977, 1978), with a low-density beam of sodium atoms crossing a laser beam (see also Dagenais and Mandel, 1978). The fluctuation in the number of atoms in the interaction region did not, however, allow demonstration of the sub-Poissonian character of the radiation [the experiment established a positive slope for $g^{(2)}(\tau)$ around $\tau=0$]. On the other hand, Short and Mandel (1983) measured the number of photons emitted in a short time interval in the process of resonance fluorescence, for a very weak beam of sodium atoms (average distance between atoms equal to 1 cm), and showed that the corresponding probability distribution was sub-Poissonian. More recently, Diedrich and Walther (1987) measured $g^{(2)}(\tau)$ for the fluorescence of a single atomic ion trapped in a Paul radio-frequency trap, establishing both the antibunched and the sub-Poissonian character of the emitted light.

D. Optical bistability

Another example of the important role that may be played by atomic dynamics is squeezed-state generation in the phenomenon of optical bistability, which occurs when a nonlinear medium is placed inside an optical cavity subjected to an injected field (for a review, see Lugiato, 1984). Under some conditions, two values of the output intensity can be obtained for the same intensity of the injected signal, the actual values depending on the history of the system. The Hamiltonian that describes the interaction between the atoms and the cavity mode is

$$H_I = g(\hat{R}_- \hat{a}^\dagger + \hat{R}_+ \hat{a}), \quad (3.2)$$

where \hat{R}_+ and \hat{R}_- are collective raising and lowering operators, respectively, corresponding to a system of N two-level atoms interacting with the field mode. An injected coherent field may be simulated by adding to the above Hamiltonian the term $g'(\lambda^* a + \lambda a^\dagger)$, where λ is the complex amplitude of the injected field, and g' is proportional to the transmission coefficient of the input

port (semitransparent mirror). It was shown by Carmichael (1986) that a low- Q cavity can produce better squeezing than a high- Q cavity, for absorptive optical bistability (resonant case). Under these conditions, the atomic variables cannot be eliminated adiabatically, and full consideration must be given to atomic dynamics. Generalization of these results to include the dispersive case was carried out by Castelli *et al.* (1988) and by Reid (1988), confirming that the high- Q cavity was less favorable for squeezing. The relevant experiments, conducted by Raizen *et al.* (1987) and Orozco *et al.* (1987), correspond to a situation in which the collective Rabi frequency $g\sqrt{N}$, which is the frequency of the coherent exchange of energy between atoms and field, is much larger than the atomic and field decay constants. Under these conditions, consideration of atomic dynamics is strictly necessary, in order to account for the coherent exchange of excitation. The observed amplitude squeezing was 30% below shot noise, when measured by balanced homodyne detection at the collective Rabi frequency, and close to the bistability threshold (where the phase quadrature undergoes critical fluctuations).

E. Lasers and masers

Atomic dynamics must also be considered in several possible domains of operation of lasers and masers. One case is lasers operating in the bad-cavity limit (field relaxation much faster than atomic relaxation), which occurs for instance for near-infrared noble-gas lasers and many far-infrared lasers. Atomic dynamics may then lead to sub-Poissonian statistics. This will be discussed in detail in Sec. VI. Careful consideration of atomic dynamics is also important for the description of micromasers, microlasers, and correlated-emission lasers (see below).

Two-photon lasers have been considered as squeezed-state generators since Yuen's proposal of the effective Hamiltonian (3.1) as a generator of squeezing (Yuen, 1975, 1976). It was soon realized, however, that in lasers and masers the spontaneous-emission noise associated with an inverted system ends up destroying any possibility of obtaining squeezed light at steady state (Lugiato and Strini, 1982; Reid and Walls, 1983); so that only transient squeezing is possible (Davidovich *et al.*, 1987). This is the reason why parametric amplifiers have been preferred as generators of squeezed light: in these systems the atoms are far from saturation and there is no population inversion, so spontaneous emission noise is negligible, especially when the fields are off resonance with respect to the atomic transitions.

For these reasons, lasers and masers have been disregarded for a long time as generators of light with reduced quantum noise; however, three noteworthy exceptions should be mentioned.

(i) If the active atoms are pumped into an appropriate superposition of the lasing levels, quenching of spontaneous-emission noise may occur, thus leading to the simultaneous presence of squeezing and gain in a resonant process. The corresponding devices are called

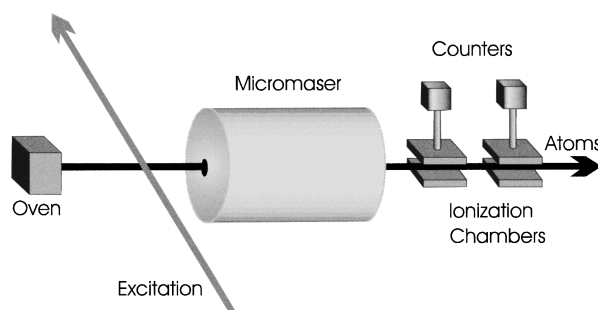


FIG. 7. Micromaser experiment. An atomic beam is excited to a Rydberg level, then injected into a superconducting cavity having a field mode resonant with the transition between the atomic excited state and a lower level. The first ionization chamber ionizes atoms that exit the cavity in the upper state, while the second chamber ionizes atoms in the lower resonant state, allowing measurement of the probability of atoms leaving the cavity in the upper or the lower state.

“correlated-emission lasers” (Scully, 1985; Scully and Zubairy, 1987; Schleich and Scully, 1988; Scully, Wódkiewicz, Zubairy, Bergou, Lu, and Meyer ter Vehn, 1988; Benkert, Scully, and Orszag, 1990; Bergou *et al.*, 1990; Dutra and Davidovich, 1994). While correlated-emission lasers based on single-photon transitions give rise to amplitude squeezing (Benkert, Scully, and Orszag, 1990), correlated-emission two-photon lasers may produce phase squeezing (Scully, Wódkiewicz, Zubairy, Bergou, Lu, and Meyer ter Vehn, 1988; Bergou *et al.*, 1990; Dutra and Davidovich, 1994). The fluctuations of the excitation process, which affect the relative phase between the two lasing states, may, however, spoil the squeezing in these devices. This explains why there has been only one experimental confirmation so far (Winters *et al.*, 1990). On the other hand, this process is closely related to the injection into a laser of the output signal of another laser. This method has also been shown to produce amplitude squeezing (Agarwal *et al.*, 1991; Fontenelle and Davidovich, 1995).

(ii) Spontaneous emission can also be controlled by sending highly excited atoms (Rydberg atoms) into high- Q cavities, so that the atomic transit time is smaller than its decay time. This is the case for *micromasers*, devices in which a beam of Rydberg atoms, typically highly excited rubidium or cesium (having principal quantum numbers around 50), crosses a high- Q superconducting cavity that is in resonance with a transition between the initial state and another Rydberg level (the frequencies are in the microwave range). Due to the large atomic dipole moments and the low dissipation in the cavity, it is possible to reach oscillation with a very low beam intensity, such that at most one atom in the average is in the cavity at a time. Successful operation has been obtained both for one-photon transitions between neighboring Rydberg levels (Meschede *et al.*, 1985; Rempe *et al.*, 1987), and for two-photon transitions between levels with the same parity (Brune *et al.*, 1987). The radiation from such a device is sub-Poissonian for an extended range of parameters, as demonstrated

experimentally by Rempe *et al.* (1990). The field produced is, however, extremely weak, and cannot be measured directly. Information about the field is gathered by detecting the atoms that exit the cavity, and measuring the probability that they are in the upper or lower resonant level. A typical experiment is sketched in Fig. 7. Recently, laser oscillation with less than one atom, on the average, in an optical resonator was demonstrated by An *et al.* (1994), thus extending the previous results to the optical regime. Furthermore, the field can be measured directly in this case. A detailed discussion will be presented in Sec. IV.D.2.

(iii) Sub-Poissonian light can also be obtained from lasers excited by a low-noise source. In usual lasers, the pumping of the atoms to the excited state (either by injecting excited atoms into a cavity, as in dye lasers, or by exciting the atoms in the laser cavity through light or collisions) can be very well approximated by a Poissonian distribution for the number of atoms excited during a given time. Most theoretical work on lasers assumes either implicitly or explicitly this type of distribution. The pioneer work on lasers pumped in a regular way (i.e., having equal numbers of atoms pumped in equal time intervals) was due to Golubev and Sokolov (1984). Experimental work demonstrating a reduction of amplitude fluctuations due to the regularization of the pumping of a light source was first presented by Teich and Saleh (1985). They observed sub-Poissonian light coming from a mercury-vapor lamp pumped by a space-charge-limited electron beam. The space-charge effect, which is the accumulation of electric charge between the cathode and the anode of a discharge lamp, was well known in thermionic tubes: due to the distributed charge accumulated in space, the charges repel each other and arrive in the anode in a regular way. Tapster *et al.* (1987) observed sub-Poissonian light coming from a light-emitting diode driven by a constant-current source, and S. Machida *et al.* (1987) observed sub-Poissonian light emitted by semiconductor lasers (both $0.85\ \mu\text{m}$ GaAs and $1.5\ \mu\text{m}$ InGaAsP lasers were used) excited by a regularized electric current (see also Machida and Yamamoto, 1988, 1989). In these experiments, noise reduction from 9% to 19% was obtained over a frequency range from near dc to 1.1 GHz, corresponding to an amplitude squeezing of 32% (-1.7 dB). The main limitation came from the measurement system, due to optical feedback and a limited light-collection efficiency. These problems were solved by using a direct “face-to-face” coupling of the laser and the detector, which were both located inside a cryostat at liquid-helium temperature (Richardson *et al.*, 1991). In this way, 85% noise reduction was obtained. Sub-Poissonian behavior from commercial semiconductor lasers, working at room temperature, can be obtained if one succeeds in eliminating spurious modes, so they operate in a monomode regime. This has been accomplished either through injection locking (Inoue *et al.*, 1993), optical feedback from a grating (Freeman *et al.*, 1993; Wang *et al.*, 1993), or active stabilization of the laser temperature (Kitching *et al.*, 1994). Much theoretical and experimental work has

been published, both on semiconductor (Yamamoto, Machida, and Nilsson, 1986; Yamamoto and Machida, 1987; Kennedy and Walls, 1989; Richardson and Shelby, 1990; Lai *et al.*, 1991) and atomic lasers and masers (Katanayev and Troshin, 1987; Bergou *et al.*, 1989a, 1989b; Haake *et al.*, 1989, 1990; Marte and Zoller, 1990; Benkert, Scully, Bergou, Davidovich, Hillery, and Orszag, 1990; Guerra *et al.*, 1991; Zhu *et al.*, 1991, 1992; Davidovich *et al.*, 1992; Kolobov *et al.*, 1993). The best quantum-noise reduction is achieved when the lifetime of the lower lasing state is much smaller than that of the upper state: this precludes reexcitation through reabsorption of radiation by the lower level, and decreases spontaneous-emission noise. This problem will be discussed in detail in Sec. VI. An alternative approach is to build a laser operating with a closed system of states, so the same atoms undergo many cycles of pumping and stimulated emission, producing a dynamic pump-noise suppression, which results in antibunching of laser photons (Ralph and Savage, 1991; Ritsch *et al.*, 1991; Ritsch *et al.*, 1992).

F. Twin-photon beams

For nondegenerate oscillators, an interesting option for reducing quantum noise is to subtract the intensities of the twin-photon beams. The underlying nonclassical property is the simultaneous creation of “twin” signal and idler photons by parametric downconversion or any other two-photon-generating technique. In a lossless cavity, the intracavity field would thus increase in such a way that the numbers of signal and idler photons would be exactly equal (zero fluctuation). Since cavity dissipation is a random process acting independently on each mode, at steady state the field inside any real lossy cavity has nonzero fluctuations in the intensity difference. However, if all the removed photons are detected (as will be the case for ideal detectors provided dissipation in the cavity and in the mirrors is negligible), the lossless zero-noise photon configuration is, after a time interval much larger than the cavity decay time, exactly reproduced at the photodetectors, resulting in a noiseless difference between the photocurrents for the signal and idler beams. In the frequency domain, this means that the noise spectrum vanishes at zero frequency, and that quantum-noise reduction is expected for frequencies smaller than the cavity bandwidth.

Parametric processes are involved in all the experiments realized so far. The simultaneity in the emission of the two photons was established experimentally by Burnham and Weinberg (1970) and Friberg *et al.* (1984). It was shown by Reynaud (1987) and Reynaud *et al.* (1987), that in the parametric downconversion the fluctuations in the intensity difference are reduced well below the classical level. Since then, this technique has been studied both theoretically (Lane *et al.*, 1988; Björk and Yamamoto, 1988; Fabre *et al.*, 1989) and experimentally (Heidman *et al.*, 1987; Debuisschert *et al.*, 1989; Nabors and Shelby, 1990). A reduction of 30% was obtained by Heidmann *et al.* (1987) at a frequency of 8

MHz. They used a type II potassium triphosphate crystal placed inside an optical cavity, working above oscillation threshold. In this situation, the crystal emits two cross-polarized twin photons with approximately the same frequency. The photon beams are separated by polarizing beam splitters, and absorbed by two photodetectors. The resulting currents are subtracted and spectrally analyzed. Using the same technique, Debuisschert *et al.* (1989) reported noise reduction of 70% below shot-noise level. A noise-reduction factor of 86% below the classical level was achieved by Mertz *et al.* (1991). Squeezed-vacuum generation using twin beams in single-pass experiments (no cavity) have the advantage that the squeezing bandwidth is not limited by the cavity bandwidth. The lower efficiency due to the absence of a cavity is compensated for by using higher-intensity pulsed light. A quadrature squeezing of 75% was demonstrated by Kim and Kumar (1994).

Many applications of twin beams have been developed. One example is the generation of sub-Poissonian light using active-control techniques: the quantum noise of the signal beam can be suppressed by counteracting its fluctuations with the measurement result for the idler beam (Walker and Jakeman, 1985; Haus and Iamamoto 1986; Jakeman and Jefferson, 1986; Machida and Yamamoto, 1986; Stoler and Yurke, 1986; Yamamoto, Imoto, and Machida, 1986; Yuen, 1986; Rarity, Tapster, and Jakeman, 1987; Shapiro *et al.*, 1987; Björk and Yamamoto, 1988; Teich and Saleh, 1988; Mertz *et al.*, 1990; Kim and Kumar, 1991, 1992). Another application is the enhancement of the sensitivity of absorption and polarization-rotation measurements (Snyder *et al.*, 1990; Tapster *et al.*, 1991).

G. Quantum nondemolition measurements

It is possible to generate sub-Poissonian states of the field in a cavity by means of quantum nondemolition (QND) measurements. These measurements, by definition, leave the quantity being measured unaltered, both in the present and in the future (Braginsky *et al.*, 1977; Unruh, 1978; Caves *et al.*, 1980; Imoto *et al.*, 1985). QND measurements of the photon number in a cavity would allow the detection of very small classical forces acting on the cavity walls, which would occur if these cavities were used as sensors of oscillations of bar-type gravitational-wave detectors.

QND methods are generally based on dispersive and nonlinear effects. One may, for instance, send a light beam through a dispersive medium with a nonlinear index of refraction (Kerr cell). As long as absorption is kept negligible, the intensity of the beam does not change. Only its phase changes, but this change does not affect the intensity. On the other hand, the change in the index of refraction, and therefore the intensity of the beam, can be determined by measuring the dephasing of another beam sent through the same medium (Yamamoto *et al.*, 1986). This possibility was demonstrated experimentally by Levenson *et al.* (1986) and LaPorta *et al.* (1989). This measurement can be used to reduce quan-

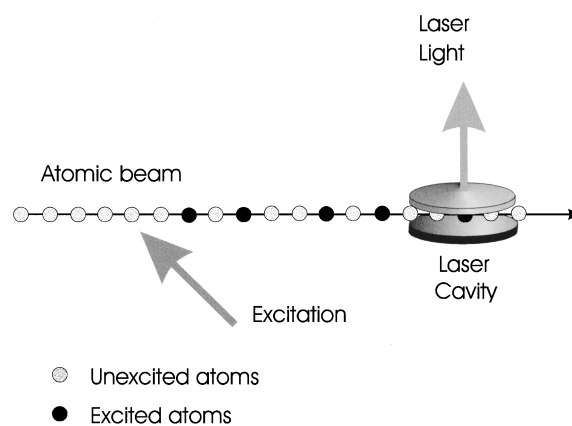


FIG. 8. Model of laser pumping.

tum fluctuations in the original beam through the technique of active stabilization (Yamamoto *et al.*, 1987; Caves, 1987), similar to the one used for twin-photon beams: the intensity fluctuations of the beam are counteracted according to the result of the nondemolition measurement.

A subtle way of using QND measurements to build sub-Poissonian states of the field is through the gradual increase of quantum-mechanical knowledge about the state of the field, acquired by a continuous QND measurement (Brune *et al.*, 1990; Brune *et al.*, 1992). This method, which can actually produce a Fock state of the field in a cavity, will be discussed in detail in Sec. VII.

IV. SOURCES OF QUANTUM NOISE IN LASERS

Well above threshold, the photon-number distribution in a laser is approximately Poissonian, with a dispersion equal to the square root of the number of photons. This noise has three sources: (i) random fluctuations in the pumping process, which puts the lasing atoms into the excited state, (ii) spontaneous emission, which randomly provokes transitions of excited atoms to other states, thus “stealing” photons from the lasing mode, (iii) cavity dissipation, associated both to losses in the cavity and to the random process by which photons are transmitted through the output coupling mirror.

This section develops a heuristic model that clearly exhibits the role of these three sources, and is an extension of the analysis presented by Bergou *et al.* (1989a, 1989b).

A. Excitation model

Let us assume that a dense flux of regularly spaced atoms goes through an excitation region, just before going into the laser cavity (Fig. 8). It is not necessary to worry at this moment about how such a beam could be produced. In the excitation region, the atoms are excited to an upper level, such that one of the cavity modes is resonant with a downward transition to a lower level. Let R be the number of atoms per unit time in the incoming beam, and $K = R\tau$ the number of atoms that

reach the excitation region during the time interval τ . If p is the probability for an atom to get excited, then the probability $\mathcal{P}(k, K)$ that k atoms get excited during the time τ is given by

$$\mathcal{P}(k, K) = \binom{K}{k} p^k (1-p)^{K-k}. \quad (4.1)$$

The average number of excited atoms and the corresponding variance are easily obtained from Eq. (4.1):

$$\bar{k} = \sum_{k=0}^K k \mathcal{P}(k, K) = pK = r\tau, \quad (4.2)$$

and

$$\overline{\Delta k^2} = \overline{k^2} - \bar{k}^2 = (1-p)pK = (1-p)\bar{k}, \quad (4.3)$$

where $r = pR$ is the number of atoms per unit time in the outgoing atomic beam. One should note that $\overline{\Delta k^2} = 0$ when $p = 1$, as expected (all the atoms are excited, so the outgoing beam is also regular), while the result for a Poissonian distribution is obtained when $p \rightarrow 0$ and $R \rightarrow \infty$, so that r remains finite. Indeed, in this limit, the binomial distribution turns into a Poissonian distribution:

$$\begin{aligned} \lim_{p \rightarrow 0} \mathcal{P}(k, K = r\tau/p) &= \lim_{\substack{p \rightarrow 0 \\ K = r\tau/p}} \frac{K!}{k!(K-k)!} p^k (1-p)^{K-k} \\ &= \lim_{p \rightarrow 0} \frac{(pK)^k}{k!} e^{-pK} = \frac{\bar{k}^k}{k!} e^{-\bar{k}}. \end{aligned} \quad (4.4)$$

As a matter of fact, one may now even forget about the excitation model and think about Eq. (4.1) as just a convenient way of parameterizing the statistical distribution of the excited atoms that are brought into interaction with the cavity field (either by direct injection into the cavity or by being excited inside the cavity from some lower-lying state). This parameterization allows one to go continuously from the regular to the Poissonian case.

After crossing the pumping region, the atoms go on into the resonant cavity (Fig. 8). Let $P(n)$ be the probability that an excited atom emits a photon into the lasing mode, when there are n photons in the cavity. We assume that the time scale over which the field distribution is changing is much larger than either τ or the flight time of the atoms through the cavity, so that $P(n)$ can be taken to be constant over time τ . If k atoms reach the cavity during this time interval, then the probability that they release \tilde{n} photons in the cavity is given by

$$\mathcal{A}(\tilde{n}|k) = \binom{k}{\tilde{n}} P(n)^{\tilde{n}} [1 - P(n)]^{k-\tilde{n}}. \quad (4.5)$$

The quantity $\mathcal{A}(\tilde{n}|k)$ is actually a conditional probability, i.e., it is the probability of adding \tilde{n} photons to the cavity in time τ , provided the number of excited atoms during this time interval is equal to k . The total probability that \tilde{n} photons are added to cavity in time τ is then

$$\mathcal{A}(\tilde{n}, \tau) = \sum_{k=0}^K \mathcal{A}(\tilde{n}|k) \mathcal{P}(k, K), \quad (4.6)$$

with $\mathcal{P}(k, K)$ given by Eq. (4.1). Therefore, in order to calculate the average of a function of \tilde{n} , say $f(\tilde{n})$, one can first calculate the conditional average using Eq. (4.5), and then average the result over the k distribution:

$$\langle f(\tilde{n}) \rangle = \sum_{k=0}^K \left[\sum_{\tilde{n}=0}^k f(\tilde{n}) \mathcal{A}(\tilde{n}|k) \right] \mathcal{P}(k, K). \quad (4.7)$$

One finds therefore

$$\langle \tilde{n} \rangle = P(n) \bar{k} \quad (4.8)$$

and

$$\langle (\tilde{n})^2 \rangle = [P(n) - P(n)^2] \bar{k} + P(n)^2 \bar{k}^2, \quad (4.9)$$

where the bar indicates the average over the k distribution. Since \tilde{n} is the number of photons emitted into the cavity during the time interval τ , we have $\tilde{n} = n(t + \tau) - n(t)$, where $n(t)$ is the total number of photons inside the cavity at time t . Taking into account also the results (4.2) and (4.3), one finds

$$\langle [n(t + \tau) - n(t)] \rangle = rP(n)\tau, \quad (4.10)$$

and

$$\langle [n(t + \tau) - n(t)]^2 \rangle = (1 - pP)rP\tau + r^2P^2\tau^2. \quad (4.11)$$

The quantities on the left-hand side of Eqs. (4.10) and (4.11) are the *conditional* or *transition moments*, of order one and two, respectively, of the random process associated to the photon-number dynamics. In the theory of random processes (Van Kampen, 1981), the conditional moments are used to define the coefficients in the Kramer-Moyal expansion of the conditional probability. Let $\mathcal{P}(n, t|n_0, t_0)$ be the conditional probability that there are n photons in the cavity at the instant t , if at t_0 there were n_0 photons. Let us assume that the average number of photons is much larger than one, and let us approximate the photon-number distribution by a continuous one. The Kramer-Moyal expansion in this case is (Van Kampen, 1981)

$$\frac{\partial}{\partial t} P(n, t|n_0, t_0) = \sum_{\ell=1}^{\infty} \left(-\frac{\partial}{\partial n} \right)^{\ell} [D_{\ell}(n) P(n, t|n_0, t_0)], \quad (4.12)$$

the coefficients $D_{\ell}(n)$ being given by

$$D_{\ell}(n) = \lim_{\tau \rightarrow 0} \frac{1}{\tau^{\ell}} \int dn' (n' - n)^{\ell} \mathcal{A}(n', t + \tau, |n, t). \quad (4.13)$$

Assuming that the distribution is peaked around a photon number much greater than 1, and is sufficiently smooth and sharp, it is often possible to neglect in the above expansion the derivatives of order higher than two. One gets then the Fokker-Planck equation (Van Kampen, 1981; Risken, 1984):

$$\begin{aligned} \frac{\partial}{\partial t} \mathcal{P}(n, t|n_0, t_0) &= -\frac{\partial}{\partial n} [D_1(n) \mathcal{P}(n, t|n_0, t_0)] \\ &+ \frac{\partial^2}{\partial n^2} [D_2(n) \mathcal{P}(n, t|n_0, t_0)], \end{aligned} \quad (4.14)$$

where D_1 is the *drift coefficient* and D_2 is the *diffusion coefficient*.

From this equation, it is easy to show that

$$\frac{d}{dt}\langle n \rangle = \int dn D_1(n) \mathcal{P}(n, t | n_0, t_0) = \langle D_1(n) \rangle, \quad (4.15)$$

and

$$\frac{d}{dt}[\langle n^2 \rangle - \langle n \rangle^2] = 2\langle D_2(n) \rangle + 2[\langle (n - \langle n \rangle) D_1(n) \rangle]. \quad (4.16)$$

In these equations, the average now refers not only to the atomic distribution, but also to the photon distribution inside the cavity. Equation (4.16), relating the diffusion and the drift coefficients, is an example of an *Einstein relation* (Sargent, 1974; Van Kampen *et al.*, 1981). In particular, if the drift coefficient vanishes and the diffusion coefficient is constant, one gets from Eq. (4.16) that $\langle \Delta n^2 \rangle = \langle n^2 \rangle - \langle n \rangle^2 = 2D_2 t$, the characteristic solution of the diffusion equation.

From Eqs. (4.10), (4.11), and (4.13), one obtains the drift and diffusion coefficients for the photon-number random process:

$$D_1(n) = \lim_{\tau \rightarrow 0} \frac{\langle n(t+\tau) - n(t) \rangle}{\tau} = rP(n), \quad (4.17)$$

and

$$D_2(n) = \lim_{\tau \rightarrow 0} \frac{\langle [n(t+\tau) - n(t)]^2 \rangle}{2\tau} = \frac{1}{2}[1 - pP(n)]rP(n). \quad (4.18)$$

It is clear from Eq. (4.18) that regularization of the pumping helps to reduce the diffusion coefficient. Note also that if the deexcitation probability for each atom in the cavity is small ($P \ll 1$), the pumping statistics becomes irrelevant.

B. Contribution of dissipation

In order to have a steady state, dissipation must be included. For low temperatures, so that thermal photons may be neglected, it may be modeled by a master equation of the form

$$\frac{d}{dt}p(n) = -\gamma n p(n) + \gamma(n+1)p(n+1), \quad (4.19)$$

where $p(n)$ is the probability of finding n photons in the cavity, and γ is the photon decay rate. Equation (4.19) states that photons are lost from the n -photon level at a rate given by γn , and fed to this level from the $n+1$ level at a rate $\gamma(n+1)$.

From this equation, one finds

$$\frac{d\langle n \rangle}{dt} = -\gamma \langle n \rangle, \quad (4.20)$$

and

$$\frac{d}{dt}\langle \Delta n^2 \rangle = -2\gamma \langle \Delta n^2 \rangle + \gamma \langle n \rangle. \quad (4.21)$$

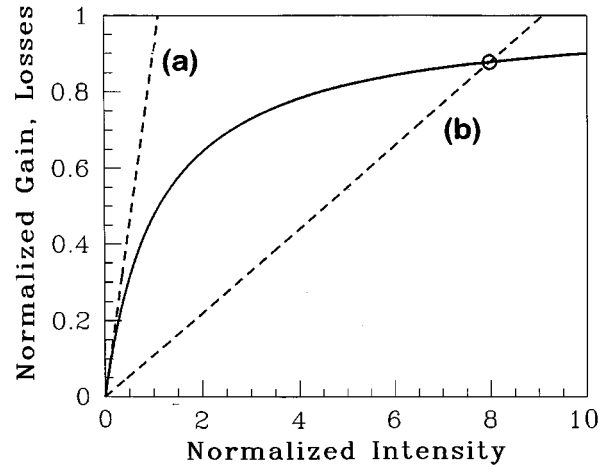


FIG. 9. Gain (solid line) and loss (dashed lines) for a laser, as functions of the normalized intensity I/I_S , where I_S is the saturation intensity. The two loss curves correspond to (a) below threshold, and (b) above threshold. The steady-state photon number is given by the intersection of the two curves. The open circle indicates that the steady state is stable. The origin ($n=0$) is stable below threshold, and unstable above threshold.

Adding up these contributions to Eqs. (4.15) and (4.16), and replacing at the same time D_1 and D_2 by the expressions (4.17) and (4.18), one has

$$\frac{d\langle n \rangle}{dt} = r\langle P(n) \rangle - \gamma \langle n \rangle, \quad (4.22)$$

and

$$\begin{aligned} \frac{d}{dt}\langle \Delta n^2 \rangle = & 2r\langle P(n)(n - \langle n \rangle) \rangle + r\langle P(n)[1 - pP(n)] \rangle \\ & - 2\gamma \langle \Delta n^2 \rangle + \gamma \langle n \rangle. \end{aligned} \quad (4.23)$$

Equation (4.22) is the usual gain-loss equation for lasers or masers. The first term on the right-hand side represents gain, associated with deexcitation of pumped atoms, while the second term represents for loss (including that from transmission of the field through the coupling mirror). If the photon distribution is sufficiently sharp, one may set $\langle P(n) \rangle \approx P(\langle n \rangle)$, and Eq. (4.22) becomes an equation of motion for the average number of photons, which corresponds to a semiclassical limit of the theory:

$$\frac{d\langle n \rangle}{dt} = rP(\langle n \rangle) - \gamma \langle n \rangle. \quad (4.24)$$

C. Steady state

Steady-state operation corresponds to $d\langle n \rangle/dt = 0$, so that Eq. (4.24) yields for the average photon number n_0 ,

$$rP(n_0) = \gamma n_0. \quad (4.25)$$

The solutions of this equation correspond graphically to the intersections of the gain curve with the loss curve. For a typical laser, this graphical solution is displayed in Fig. 9, both for above- and below-threshold operation. The gain curve in this case exhibits the saturation behavior typical of lasers: as the average intensity increases, the absorption processes between the two lasing levels become comparable to the stimulated-emission processes, so P ceases to increase. The asymptotic value attained by P depends on the ratio of lifetimes of the two working levels. Thus, in the limit when the lifetime τ_a of the upper level is much larger than the lifetime τ_b of the lower level, each active atom returns to the ground state only from the lower level, and therefore gives up all its relative excitation to the lasing mode. In this case, P tends to one when the intensity increases. For equal lifetimes, each atom returns to the ground state half the time from the upper state, and half from the lower state. One has then $P \rightarrow \frac{1}{2}$ when $n_0 \rightarrow \infty$. In general, if Γ_a and Γ_b are the decay rates of the upper and lower level, respectively, the probability that the lasing mode is fed, at saturation, is given by the relative probability that the atom is in the upper lasing level, that is $\tau_a/(\tau_a + \tau_b) = \Gamma_b/(\Gamma_a + \Gamma_b)$.

In order that the steady-state solution be stable, the slope of the gain curve must be smaller than that of the loss curve at the intersection point. In this case, a small increase in the number of photons around n_0 will make loss larger than gain, driving the number of photons back to n_0 . On the other hand, a small decrease will make gain larger than the loss, so again n will go back to n_0 . The stability condition is thus

$$r \frac{dP(\langle n \rangle)}{d\langle n \rangle} \Big|_{\langle n \rangle = n_0} < \gamma. \quad (4.26)$$

D. Photon-number variance

Let us now go back to Eq. (4.23). For steady-state operation, one has $d\langle \Delta n^2 \rangle / dt = 0$, so that

$$\langle \Delta n^2 \rangle_0 = (r/\gamma) \langle P(n)(n - \langle n \rangle) \rangle + \frac{1}{2}(r/\gamma) \langle P(n)[1 - pP(n)] \rangle + \frac{1}{2}n_0. \quad (4.27)$$

This expression allows one to pinpoint the several contributions to laser noise. The third term on the right-hand side stems from dissipation, which is thus seen to contribute half of the usual Poisson noise. The second term is associated with the gain mechanism. It contains the effect of randomness in the pumping and in the spontaneous-emission process. Note that if the photon-conversion efficiency is maximal, i.e., $P(n) = 1$, and $p = 1$, i.e., pumping is regular, then this term is equal to zero. This is easy to understand physically: for complete conversion of the atomic excitation into photons, the photon statistics of the gain process just mirrors the pumping of the atoms into the excited state. Finally, the first term on the right-hand side of Eq. (4.27) depends on the correlation between $P(n)$ and the photon-number fluctuations $n - \langle n \rangle$. This term may actually help

to decrease the dispersion $\langle \Delta n^2 \rangle$, as long as there is an anticorrelation between $P(n)$ and $n - \langle n \rangle$, that is, if $P(n)$ decreases when $n - \langle n \rangle > 0$, and increases when $n - \langle n \rangle < 0$. This is referred to as *negative differential gain* around $n = \langle n \rangle$; the gain process then provides a stabilization mechanism for the photon-number fluctuations.

Further insight into the expression (4.27) may be obtained by expanding $P(n)$ around $P(n_0)$, and keeping only the terms proportional to the first power of the first derivative of $P(n)$. Note that, for a photon distribution sharply peaked around $n_0 \gg 1$, each derivative of $P(n)$ will bring in a new power of $1/n_0$. Since the relevant fluctuations should be of order $\sqrt{n_0}$, this means that each new term in this expansion will bring in a new power of $1/\sqrt{n_0}$. This implies that, in lowest order in this quantity, only the derivative coming from the first term on the right-hand side of Eq. (4.27) should be considered. One has then

$$\langle \Delta n^2 \rangle_0 = (r/\gamma) P'(n_0) \langle \Delta n^2 \rangle_0 + \frac{1}{2}(r/\gamma) P(n_0) [1 - pP(n_0)] + \frac{1}{2}n_0, \quad (4.28)$$

where

$$P'(n_0) \equiv \left. \frac{dP(n)}{dn} \right|_{n=n_0}. \quad (4.29)$$

Using now Eq. (4.25), one finds

$$\langle \Delta n^2 \rangle_0 = (r/\gamma) P'(n_0) \langle \Delta n^2 \rangle_0 + \frac{1}{2}n_0 [1 - pP(n_0)] + \frac{1}{2}n_0, \quad (4.30)$$

which allows one to write, for the variance,

$$\langle \Delta n^2 \rangle_0 = \frac{n_0 [1 - pP(n_0)/2]}{1 - (r/\gamma) P'(n_0)}. \quad (4.31)$$

This equation allows one to predict interesting noise-reduction properties for lasers and micromasers.

1. Lasers

For a laser well above threshold, $P'(n_0) \rightarrow 0$, so the contribution of the first term on the right-hand side of Eq. (4.30) vanishes. If furthermore the pumping is Poissonian ($p = 0$), then the contributions of gain and loss [second and third terms on the right-hand side of Eq. (4.30)] are both equal to $n_0/2$, and their sum yields the usual Poissonian result for the variance: $\langle \Delta n^2 \rangle_0 = n_0$. For more regular pumping, and using the saturation limit for the atomic deexcitation probability, one has

$$\langle \Delta n^2 \rangle_0 = n_0 \left(1 - \frac{\Gamma_b}{\Gamma_a + \Gamma_b} \frac{p}{2} \right). \quad (4.32)$$

This equation shows that, for $\Gamma_b \gg \Gamma_a$, one can get a 50% reduction in the variance. This result was obtained for the first time by Golubev and Sokolov (1984). Its origin should be clear from the above discussion: it represents the complete elimination of gain noise, due to the fact that each pumped atom gives up its excitation to the lasing mode, and therefore just reproduces the noiseless character of the pumping. The remaining contribution is due to loss (including the random subtrac-

tion of photons from the cavity by the output coupling mirror). Note that the derivative contribution in the denominator of Eq. (4.31) is a correction to this result that takes into account the variation of $P(n)$ with n , and stems from the first term on the right-hand side of Eq. (4.27). Since $P'(n) > 0$ for a laser (see Fig. 9), this variation will act to increase the variance. Therefore, from this point of view, the super-Poissonian character of laser radiation above threshold may be interpreted as due to the corresponding positive differential gain, which amplifies photon-number fluctuations.

Of course, a system with negative differential gain could produce sub-Poissonian radiation even if the pumping is Poissonian. Such is the case for the micromaser, which is considered in the following.

2. Micromasers

Besides presenting a wealth of interesting effects related to their quantum nature, micromasers offer a powerful testing ground for basic models in quantum optics, like the Jaynes-Cummings model (Jaynes and Cummings, 1963). This has motivated a large number of theoretical papers (Filipowicz *et al.*, 1986a, 1986b; Krause *et al.*, 1986; Davidovich *et al.*, 1987; Meystre *et al.*, 1988) since the first experimental demonstration by Meschede *et al.* (1985).

Since in these devices the lifetime of the atoms is larger than their transit times, the gain function is given by the oscillatory transition probability of one atom in the presence of a single-mode field. The oscillation frequency (Rabi frequency) is proportional to the atom-field coupling constant and to the field amplitude, which is proportional to the square root of the number of photons. The corresponding semiclassical equation of motion for the average number of photons is then

$$\frac{d\langle n \rangle}{dt} = r \sin^2(gt_{\text{int}}\sqrt{\langle n \rangle}) - \gamma\langle n \rangle, \quad (4.33)$$

where g is the atom-field coupling constant and t_{int} is the interaction time between the atom and the field mode (assumed here for simplicity to have a constant spatial profile). The argument of the sine is half the Rabi angle developed by each atom as it crosses the cavity (a Rabi angle equal to π means that the atom has undergone a transition from the upper to the lower state). The steady states correspond to the solutions of the equation

$$\sin^2(\theta_{\text{int}}\sqrt{n_0/n_{\text{ex}}}) = n_0/n_{\text{ex}}, \quad (4.34)$$

where $n_{\text{ex}} = r/\gamma$ is the number of excited atoms that come into the cavity during the damping time $t_{\text{cav}} = 1/\gamma$ and $\theta_{\text{int}} = g\sqrt{n_{\text{ex}}}t_{\text{in}}$ is half the Rabi angle developed by each atom when there are n_{ex} photons in the cavity. A large value of θ_{int} indicates that each atom undergoes many emissions and reabsorptions as it crosses the cavity.

The graphical solutions of Eq. (4.34) are exhibited in Fig. 10. The oscillation threshold occurs when the slope of the gain curve coincides with the slope of the loss curve at the origin. From Eq. (4.34) it is easy to see that

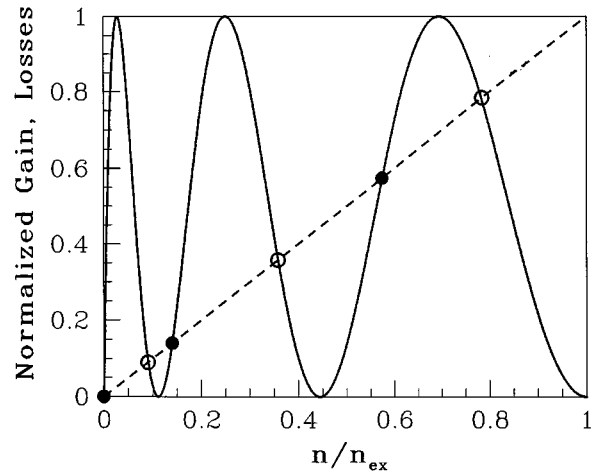


FIG. 10. Graphical solution for steady states of the micromaser, for $\theta_{\text{int}} = 3\pi$. Normalized gain (solid curve) and normalized loss (dashed curve) are plotted as functions of the normalized number of photons n/n_{ex} . Stable and unstable states are indicated by open and closed circles, respectively.

this happens when $\theta_{\text{int}} = 1$. Figure 10 displays two interesting differences with respect to the laser case. First, one may now get many stable steady states, indicated by open circles in Fig. 10 (as before, the solutions are stable if and only if the slope of the gain curve is smaller than the slope of the loss curve at the intersection point). Second, the intersections occur at regions of negative differential gain. This opens up the possibility of producing sub-Poissonian radiation even with Poissonian pumping, which was experimentally verified by Rempe *et al.* (1990). The sub-Poissonian behavior will occur whenever the photon distribution is concentrated around one of the steady-state solutions of the semiclassical equations, and will be interspersed by super-Poissonian peaks, which correspond to two or more steady-state solutions occurring with approximately equal probabilities. For large values of θ_{int} , an interesting effect occurs: as mentioned before, each atom undergoes then many cycles of emission and reabsorption of photons, so that a large number of micromaser photons is emitted by the same atom. This leads to an antibunching of the radiation, as in the single-atom resonance fluorescence phenomenon discussed in Sec. II.F, which remains true even in the super-Poissonian region (Quang, 1992). The micromaser offers thus a nice example of the distinction between antibunching and sub-Poissonian statistics.

From Eq. (4.33), one can get the corresponding equation of motion for a laser (with equal lifetimes for the upper and lower states): it suffices to integrate the gain term over t_{int} , with the weight function $\tau^{-1}\exp(-t_{\text{int}}/\tau)$, where τ is the lifetime of the lasing levels. This weight function simulates the exponential decay of the excited atom, and yields the same result as would a more realistic approach that included lower levels to which the two lasing levels would decay (Sargent, Scully, and Lamb, 1974). If τ is much smaller than the

atomic transit time, this integration can be taken to infinity, leading to

$$\frac{d\langle n \rangle}{dt} = \frac{r}{2} \frac{\langle n \rangle / n_S}{1 + \langle n \rangle / n_S} - \gamma \langle n \rangle, \quad (4.35)$$

where $n_S = (4g^2\tau^2)^{-1}$ is the saturation intensity.

This expression displays the usual saturating gain curve, with no negative differential gain. It is clear then that this feature is intimately connected to the suppression of spontaneous emission, due to the large lifetime of the atoms as compared to the interaction time.

E. Production of sub-Poissonian atomic beams by micromasers

The micromaser field is not directly accessible to measurement. Indeed, introduction of a photodetector into a micromaser would spoil the Q factor of the cavity, and furthermore the field that leaks out of the cavity has an extremely small intensity. Measurement of the field is thus made by detection of atoms that have crossed the cavity. The atomic beam serves therefore a twofold purpose: it generates the micromaser field, and at the same time it is used to measure that field. In fact, if every atom that comes out of the cavity is detected, the evolution of the field may be markedly different from the case in which no atom is detected. The interaction between these two subsystems produces quantum-mechanical correlations between the atomic and field states, so that atomic detection may change the state of the field. However, if the detection efficiency is small, the fluctuations introduced by the detection process will be negligible, and the atomic distribution will then reflect the field statistics. In fact, it can be shown that if the field inside the cavity is sub-Poissonian, the distribution of atoms exiting the cavity in the ground state will also satisfy this condition. This was actually used by Rempe *et al.* (1990) to establish the sub-Poissonian character of the micromaser field.

This correlation between atomic and field statistics may be understood from the heuristic analysis presented in the last section. Indeed, rewriting Eq. (4.34) as

$$\sin^2(gt_{\text{int}}\sqrt{n_0}) = n_0/n_{\text{ex}}, \quad (4.36)$$

one can see that as the atomic flux n_{ex} increases, the slope of the loss curve decreases, implying a decrease in the probability of atomic transition to the lower level. This decrease compensates the flux increase, resulting in a sub-Poissonian distribution for the atoms that exit the cavity in the lower level.

This effect was treated in detail by Rempe and Walther (1990). Their result is expressed in terms of the Mandel parameter (Mandel, 1979), defined for the field as

$$Q_F = \frac{\langle \Delta n^2 \rangle}{\langle n \rangle} - 1, \quad (4.37)$$

a similar definition holding for the factor Q_g corresponding to the atoms in the ground state. For a sub-

Poissonian process, $Q_F < 0$. For a small detection efficiency η , the relation between these two factors is

$$Q_g = \eta P(\langle n \rangle) Q_F (2 + Q_F), \quad (4.38)$$

where $P(\langle n \rangle)$ is the probability that an excited atom suffers a transition to the ground state when the average number of photons in the cavity is $\langle n \rangle$.

This expression also shows that the micromaser can be used as a generator of sub-Poissonian atomic beams. The exiting atoms in state $|g\rangle$ could in principle be used as incoming atoms for another cavity.

A more detailed treatment of the photon statistics, beyond the above heuristic discussion, requires the full machinery of quantum mechanics. This will be given in the following section.

V. QUANTUM THEORY: THE GENERALIZED MASTER EQUATION

A. Derivation of the master equation

The quantum properties of the field may be described in terms of the reduced density matrix ρ . The probability of finding n photons in the field is given by $p(n) = \langle n | \rho | n \rangle$. The change in this operator produced by the passage of a single atom can be described in terms of a superoperator \mathcal{M} acting on ρ :

$$\rho(t + \Delta t) = \mathcal{M}\rho(t), \quad (5.1)$$

where Δt is larger than the interaction time t_{int} between the atom and the cavity field (for a laser, t_{int} coincides with the lifetime of the atom, while for a maser it should be taken as the transit time). In writing this equation, one assumes that dissipation due to cavity losses and transmission is negligible during the time Δt , and therefore during t_{int} , that is, $t_{\text{int}} \ll t_{\text{cav}}$. The superoperator \mathcal{M} depends on the atomic and field operators and on the initial conditions for each atom as it starts interacting with the cavity field. Thus, for instance, if the atoms are initially in the upper state, then taking the diagonal matrix elements of Eq. (5.1) in the Fock representation, one would get typically

$$\begin{aligned} p(n, t + \Delta t) &= [\mathcal{M}\rho(t)]_{nn} \\ &= -W_{n+1}p(n, t) + W_n p(n-1, t), \end{aligned} \quad (5.2)$$

where W_n is the atomic transition probability from the upper to the lower resonant state when there are n photons in the field. Calling Γ_a and Γ_b the decay rates of the upper level a and lower level b , respectively, we have for a laser (Sargent *et al.*, 1974)

$$W_n = \frac{\Gamma_b n / n_S}{2\Gamma_{ab}(1 + n/n_S)}, \quad (5.3)$$

where

$$\Gamma_{ab} = \frac{1}{2}(\Gamma_a + \Gamma_b), \quad (5.4)$$

and

$$n_S = \frac{\Gamma_a \Gamma_b}{4g^2} \quad (5.5)$$

is the saturation photon number, while g is the atom-field coupling constant. Note that W_n has precisely the behavior displayed in Fig. 9, attaining at saturation ($n \gg n_s$) the value $\Gamma_b/(\Gamma_a + \Gamma_b)$. Furthermore, for $\Gamma_a = \Gamma_b = 1/\tau$, Eq. (5.3) reduces to the gain function in Eq. (4.35), except of course for the pumping factor r in that expression, since here the contribution of only one atom is being considered.

If now k atoms cross the cavity during a time interval t , and if one assumes that they interact with the field independently (no cooperative effects), then the change in the density operator of the field can be described by the equation (still ignoring losses for the moment)

$$\rho(t) = \mathcal{M}^k \rho(0). \quad (5.6)$$

Since k is actually a random variable, one should describe the change in the field by taking a statistical average of Eq. (5.6). Assuming again a binomial distribution for the atoms, one finds

$$\begin{aligned} \bar{\rho}(t) &= \sum_{k=0}^K p^k (1-p)^{K-k} \mathcal{M}^k \rho(0) \\ &= [1 + p(\mathcal{M} - 1)]^K \rho(0), \end{aligned} \quad (5.7)$$

where $K = Rt$. From Eq. (5.7), one can now obtain a generalized master equation by differentiating both members of this equation with respect to time, and adding the usual loss contribution:

$$\frac{d}{dt} \bar{\rho}(t) = r \log[1 + p(\mathcal{M} - 1)] \bar{\rho}(t) + \mathcal{L} \bar{\rho}(t), \quad (5.8)$$

where \mathcal{L} is a superoperator that represents the dissipation process. This equation was obtained for the case $p=1$ by Golubev and Sokolov (1984), and later generalized by several authors (Bergou *et al.*, 1989a, 1989b; Haake *et al.*, 1989; Davidovich *et al.*, 1992; Bergou and Hillery, 1994). Detailed consideration of the steps leading to Eq. (5.8) was given in Davidovich *et al.* (1992). There are in fact two crucial approximations involved in the derivation of Eq. (5.8). The first is a coarse-graining approximation: one assumes $\Delta\rho/\Delta t \approx d\rho/dt$, where Δt is such that many excited atoms are injected into the cavity over this time, but the reduced density matrix of the field does not change appreciably. And second, one assumes that the loss and gain mechanisms act independently over the time interval p/r .

The first approximation is very good for normal lasers and masers, but may lead to wrong results when considering the time-dependent behavior of micromasers, especially when the number of photons in the cavity is very small. In any case, it is not relevant for the steady-state solution. The second approximation can be shown

to hold exactly for the Poissonian case. It may lead, however, to incorrect results for the steady state, when $p \neq 0$ (Davidovich *et al.*, 1992).

The superoperator \mathcal{L} can be constructed explicitly by considering a model Hamiltonian describing the interaction between the harmonic oscillator corresponding to the cavity mode, and a bath of harmonic oscillators associated with the modes of the field outside the cavity (Cohen-Tannoudji *et al.*, 1988; Gardiner, 1991; Walls and Milburn, 1994). One finds

$$\begin{aligned} \mathcal{L}\rho &= \frac{1}{2t_{\text{cav}}} (n_T + 1) (2\hat{a}\rho\hat{a}^\dagger - \hat{a}^\dagger\hat{a}\rho - \rho\hat{a}^\dagger\hat{a}) \\ &\quad + \frac{1}{2t_{\text{cav}}} n_T (2\hat{a}^\dagger\rho\hat{a} - \hat{a}\hat{a}^\dagger\rho - \rho\hat{a}\hat{a}^\dagger), \end{aligned} \quad (5.9)$$

where \hat{a}^\dagger (\hat{a}) is the creation (annihilation) operator for a photon corresponding to the resonant cavity mode, and n_T is the average number of thermal photons. The diagonal elements of Eq. (5.9), in the number representation and with $n_T=0$, yield the master equation (4.19).

B. Results for Poissonian and regular pumping

When $p \rightarrow 0$ one gets from Eq. (5.8) the usual Scully-Lamb master equation (Scully and Lamb, 1967),

$$\frac{d}{dt} \bar{\rho}(t) = r(\mathcal{M} - 1) \bar{\rho}(t) + \mathcal{L} \bar{\rho}(t). \quad (5.10)$$

which corresponds therefore to the Poissonian limit of the generalized master equation.

The same equation is obtained, for arbitrary pumping statistics, if the action of each atom on ρ is sufficiently small (this corresponds to a small probability P of deexcitation, in the heuristic argument developed in the last section).

In order to actually use Eq. (5.8) in a specific problem, one has to expand the logarithm. As shown by Bergou *et al.* (1989a, 1989b), the first two terms in the expansion are all one needs in order to calculate up to second-order correlation functions (in particular, diffusion coefficients), if the average number of photons is sufficiently large and the distribution sufficiently narrow. One finds then

$$\frac{d}{dt} \bar{\rho}(t) = r(\mathcal{M} - 1) \bar{\rho}(t) + \frac{1}{2} r p (\mathcal{M} - 1)^2 \bar{\rho}(t) + \mathcal{L} \bar{\rho}(t). \quad (5.11)$$

From this equation, one can derive equations of motion for the average number of photons and for the dispersion, taking matrix elements in the Fock representation and replacing the operator \mathcal{M} by its explicit expression. Using Eq. (5.2), one finds (taking $n_T=0$ for simplicity)

$$\begin{aligned} \dot{p}(n) &= r[-W_{n+1}p(n) + W_n p(n-1)] + \frac{rp}{2} [-W_{n+1}^2 p(n) + W_n(W_n + W_{n+1})p(n-1) - W_n W_{n-1} p(n-2)] \\ &\quad + \gamma[-np(n) + (n+1)p(n+1)]. \end{aligned} \quad (5.12)$$

and then

$$\langle \dot{n} \rangle = \sum_{n=0}^{\infty} n \dot{p}(n) = r \langle \alpha_n \rangle - \gamma \langle n \rangle, \quad (5.13)$$

where

$$\alpha_n = W_{n+1} \left[1 + \frac{p}{2} (W_{n+1} - W_{n+2}) \right]. \quad (5.14)$$

This equation should be compared with Eq. (4.22). Identifying W_{n+1} with $P(n)$, we see that the p -dependent terms in the above equation, which represent quantum corrections to the semiclassical result Eq. (4.22), do indeed represent very small contributions for large average photon numbers, and smooth contributions as well, since $W_{n+1} - W_{n+2} \approx -dW_n/dn \approx O(1/\langle n \rangle)$. Under these conditions, the quantum equation (5.13) coincides with the semiclassical one (4.22).

For the variance $v = \langle n^2 \rangle - \langle n \rangle^2$, one finds

$$\dot{v} = 2r \langle \alpha_n (n - \langle n \rangle) \rangle + r \langle \alpha_n - p W_{n+1} W_{n+2} \rangle - 2\gamma v + \gamma \langle n \rangle. \quad (5.15)$$

In the semiclassical limit (sharp distribution around $\langle n \rangle \gg 1$), we again retrieve Eq. (4.23), obtained in the heuristic treatment. It is clear then that the same result should hold for the steady-state variance, namely Eq. (4.31). In particular, one gets for a laser the result (4.32).

In spite of the fact that it yields reasonable results for the variance, the generalized master equation (5.8) may become highly pathological. In fact, it may even give rise to negative photon-number probabilities (Davidovich *et al.*, 1992).

The micromaser has been a good testing ground for the methods presented above. It allows a detailed discussion of the assumptions and approximations involved in getting Eqs. (5.8) and (5.11). We turn therefore to a discussion of the quantum theory of this device.

C. Application to the micromaser

For a one-photon micromaser, in which nondecaying atoms pass through the cavity during a time interval t_{int} , after being pumped to the excited state, the master equation is given by Eq. (5.12), with the transition probability now given by the Rabi oscillation factor:

$$W_n = \sin^2(g \sqrt{n} t_{\text{int}}), \quad (5.16)$$

where g is the electric dipole coupling constant.

Let us first review the results for Poissonian pumping.

1. Poissonian-pumped micromaser

In this case $p=0$, and the master equation for the diagonal matrix elements becomes

$$\begin{aligned} \dot{p}(n) = & r[-\sin^2(g \sqrt{n+1} t_{\text{int}}) p(n) + \sin^2(g \sqrt{n} t_{\text{int}}) p(n-1)] + \gamma(n_T+1)[(n+1)p(n+1) - np(n)] \\ & + \gamma n_T [np(n-1) - (n+1)p(n)]. \end{aligned} \quad (5.17)$$

At steady state the detailed-balance condition holds:

$$\begin{aligned} [r \sin^2(g \sqrt{n+1} t_{\text{int}}) + \gamma n_T (n+1)] p_0(n) \\ = \gamma (n_T+1) (n+1) p_0(n+1), \end{aligned} \quad (5.18)$$

where $p_0(n)$ is a steady-state solution of Eq. (5.17). This recursion relation leads to an explicit form of the steady-state solution, here expressed in terms of the constants n_{ex} and θ_{int} defined earlier (Filipowicz *et al.*, 1986a):

$$p_0(n) = p(0) \left(\frac{n_T}{n_T+1} \right)^n \prod_{k=1}^n \left[1 + \frac{n_{\text{ex}} \sin^2(\theta_{\text{int}} \sqrt{k/n_{\text{ex}}})}{n_T k} \right]. \quad (5.19)$$

The probability $p(0)$ is determined by the normalization condition $\sum_{n=0}^{\infty} p_0(n) = 1$. A typical plot of the steady-state distribution $p_0(n)$ is displayed in Fig. 11. The peaks correspond to the stable steady-state solutions of the semiclassical analysis (see Fig. 10). From Eq. (5.19) one may also get the variance at steady state as a function of the parameter θ_{int} . The result is displayed in Fig. 12, and is seen to corroborate our previous heuristic analysis. The sub-Poissonian behavior is associated with the negative differential gain displayed in Fig. 10, while the super-Poissonian peaks correspond to the appear-

ance of two or more local maxima of comparable magnitude in the photon distribution $P(n)$.

2. Trapping states

For $n_T=0$, Eq. (5.19) presents a very peculiar behavior. One has then

$$p_0(n) = p(0) (n_{\text{ex}})^n \prod_{k=1}^n [\sin^2(\theta_{\text{int}} \sqrt{k/n_{\text{ex}}})/k]. \quad (5.20)$$

If θ_{int} is such that for some $n=n_{\text{tr}}$ one has $\sin^2(\theta_{\text{int}} \sqrt{(n_{\text{tr}}+1)/n_{\text{ex}}}) = 0$, i.e., if

$$\theta_{\text{int}} \sqrt{(n_{\text{tr}}+1)/n_{\text{ex}}} = q\pi, \quad q = 1, 2, \dots, \quad (5.21)$$

then $p_0(n)$ will vanish for $n > n_{\text{tr}}$. These special values of n define the *trapping states* (Filipowicz *et al.*, 1986b; Meystre *et al.*, 1988). An especially interesting case corresponds to $n_{\text{tr}}=0$: the vacuum is then a trapping state, so that as the atoms cross the cavity the field remains in the vacuum state. The physical origin of this behavior is evident from Eq. (5.21): each excited atom suffers one or more complete Rabi turns as it crosses the cavity, exiting it in the same state, and therefore not leaving any excitation inside the cavity. Dissipation is harmless in

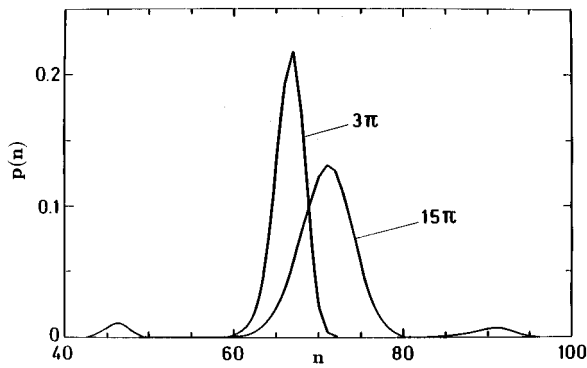


FIG. 11. Steady-state photon-number distribution for a micromaser, using values $n_{\text{ex}}=200$, $n_t=0.1$, and $\theta_{\text{int}}=3\pi$ and 15π . For $\theta_{\text{int}}=15\pi$, the distribution becomes three peaked. From Filipowicz *et al.* (1986a).

this case: the reservoir temperature being zero, no photon would come into the cavity, and there is no leaking out of the cavity, since there are no photons inside.

In the limit of zero dissipation, Fock states can be obtained with photon numbers different from zero. These are the remnants of the sub-Poissonian states discussed before, and correspond to the situation in which the loss curve in Fig. 10 coincides with the horizontal axis. Each pair of stable and unstable points merges together, yielding a marginally stable state (stable from the left but unstable from the right). From the semiclassical analysis it is clear that, in this limit, if one starts with a number of photons between two consecutive marginally stable states, this number evolves towards the rightmost one, and stops there, thus justifying the name “trapping states” for these points. Of course, any small perturbation will make it evolve further towards the next steady state to the right, and so on.

Quantum mechanically, one arrives at corresponding conclusions starting from Eq. (5.17), in the limit $n_T = \gamma = 0$ (Carvalho *et al.*, 1989). One gets

$$\dot{p}(n) = -rW_{n+1}p(n) + rW_n p(n-1), \quad (5.22)$$

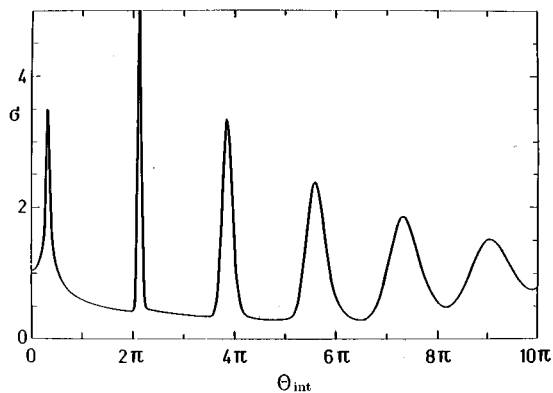


FIG. 12. Normalized standard deviation $\sigma = (\langle \Delta n^2 \rangle / \langle n \rangle)^{1/2}$ as a function of the parameter θ_{int} . Here $n_{\text{ex}}=200$ and $n_T=0.1$. A Poissonian distribution corresponds to $\sigma=1$. From Filipowicz *et al.* (1986a).

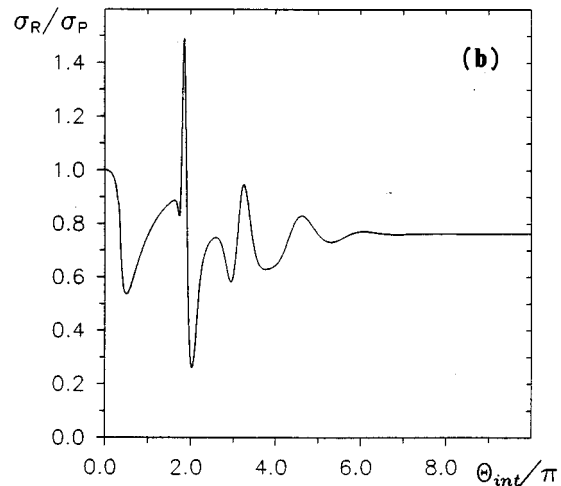
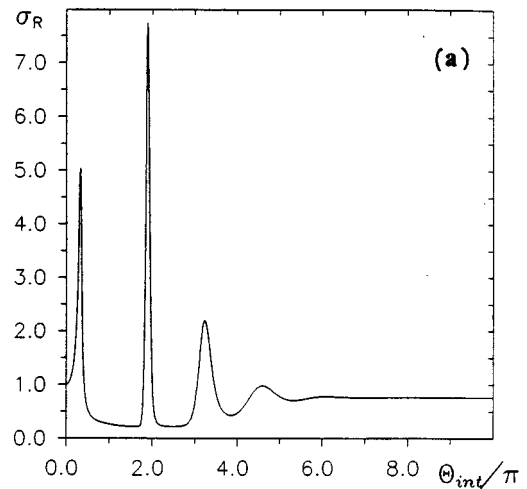


FIG. 13. Normalized standard deviation of the photon-number distribution for a micromaser, for regular (σ_R) and Poissonian (σ_P) pumping, as a function of θ_{int} . (a) σ_R ; (b) σ_R/σ_P . Here $n_{\text{ex}}=49$, $n_T=0$, and the atomic velocity dispersion is $\Delta v = 0.1\bar{v}$. From Guerra *et al.* (1991).

where W_n is given by Eq. (5.16). The steady-state distribution $p_0(n)$ must obey, therefore, the relations $W_{n+1}p_0(n) = W_n p_0(n-1) = \dots = W_1 p_0(0) = C$. Thus

$$\sum_{n=0}^{\infty} W_{n+1} p_0(n) = \sum_{n=0}^{\infty} C = \infty, \quad (5.23)$$

unless $C=0$. Since $W_n \leq 1$, one has

$$\sum_{n=0}^{\infty} W_{n+1} p_0(n) \leq \sum_{n=0}^{\infty} p_0(n); \quad (5.24)$$

therefore, for a normalizable $p_0(n)$, one must necessarily have $C=0$, which implies that $p_0(n)=0$, unless $W_{n+1}=0$. This means that the steady-state distribution is concentrated on values of n for which $W_{n+1}=0$, which corresponds precisely to the condition (5.21) for the trapping states. Furthermore, if one starts with a population distributed between two consecutive trapping

states, corresponding, say, to the populations n' and n'' (with $n'' > n' + 1$), so that $p(n) \neq 0$ only if $n' < n \leq n''$, it follows from Eq. (5.22) that $p(n' + 1)$ will decrease steadily to zero, since $p(n') = 0$, and therefore the same will happen with $p(n' + 2), \dots, p(n'' - 1)$. Since $p(n)$ remains normalized, this implies that $p(n'')$ approaches one, and thus the photon-number distribution gets concentrated at the rightmost trapping state, exactly as in the semiclassical analysis. Furthermore, since $p(n) = 0$ for all n except for $n = n''$, it follows that the field evolves towards a Fock state.

Trapping states provide therefore, in principle, a way to build up Fock states in cavities. One should note, however, that the above discussion is highly idealized, even in the case of the trapping vacuum state, which does not require the assumption of zero dissipation. The main point is that it is based on a one-atom Hamiltonian. Two-atom events inside the cavity may drastically change these results. In particular, a Poissonian distribution for the incoming atoms giving a probability as small as 1% that two atoms are found in the cavity already produces an important leaking of the trapped solutions (Orszag *et al.*, 1994; Wehner *et al.*, 1994).

3. Regularly pumped micromaser

For regular pumping, an alternative approach to Eq. (5.8) can be adopted, based on a step-by-step calculation (Guerra *et al.*, 1991), which computes the change in the reduced density matrix of the field after each atom crosses the cavity:

$$\rho(t + t_{\text{at}}) = e^{\mathcal{L}t_{\text{at}}} \mathcal{M}(t_{\text{int}}) \rho(t). \quad (5.25)$$

Here t_{at} is the (constant) time interval between two successive atoms. This equation also decouples gain and loss, but now only over the time t_{int} of the interaction between each atom and the cavity mode. The results of the numerical calculations based on Eq. (5.25) can then be compared with those resulting from the generalized master equation (5.8). The main conclusions of this analysis are the following (Davidovich *et al.*, 1992). Regularization of the pumping does not necessarily lead to noise decrease in micromasers. In fact, it is even possible to get an increase in photon-number variance by regularizing the atomic excitation (Guerra *et al.*, 1991). This is due to the fact that a variation of the statistical parameter p produces a change in the photon-number probability distribution. In particular, regularization of the pumping may cause two peaks in that distribution to assume the same height, leading thus to an increase in the variance. The generalized master equation (5.8) provides very good results when the photon-number probability distribution is sharp and the average number of photons is large, while the number of Rabi turns in the cavity is not very large: $\theta_{\text{int}} \ll n_{\text{ex}}$. It may lead, however, to incorrect results in situations corresponding to multi-peaked distributions with peaks of approximately equal height, or when θ_{int} becomes of the order of n_{ex} . For $\theta_{\text{int}} \ll n_{\text{ex}}$, adding up more terms in the expansion of the logarithm helps to improve the result, leading to a very

good approximation, so long as the number of terms is not comparable to the average number of photons. In this sense, the successive approximations in this region behave like an asymptotic expansion. When θ_{int} becomes of the same order as n_{ex} , one should not expect reliable results from Eq. (5.8), no matter how many terms are kept in the expansion of the logarithm. One should note, however, that this region has not been explored by the experiments to date. Figure 13 compares the variance of a micromaser for regular and Poissonian pumping, for several values of θ_{int} .

The above analysis, based on the master-equation approach, assumes that different time scales govern the decay of the field in the cavity and the interaction time between the atom and the cavity mode. For lasers, this means that $t_{\text{cav}} \gg \tau_a, \tau_b$, while for micromasers one must have $t_{\text{cav}} \gg t_{\text{int}}$. This precludes consideration of effects associated with atomic dynamics, which will be considered in the next section, using the Heisenberg-Langevin approach.

VI. LANGEVIN APPROACH AND ATOMIC DYNAMIC EFFECTS

Theoretical studies of the nonlinear-dynamic behavior of single-mode homogeneously broadened lasers deal frequently with simplified models which are characterized by three dynamic variables, namely, field amplitude, atomic polarization, and population inversion (see, for instance, Abraham *et al.*, 1988). The dynamic evolution of such models is governed by three relaxation rates: γ_{\parallel} for the population inversion, γ_{\perp} for the polarization, and κ for the field intensity in the cavity (frequently one has two different population decay rates, for the upper and the lower lasing levels). Corresponding to the different possible relations between these parameters, single-mode lasers are grouped into four main classes with different dynamic characteristics, as follows (Abraham *et al.*, 1988):

- (i) $\gamma_{\perp}, \gamma_{\parallel} \gg \kappa$; dye lasers are in this class.
- (ii) $\gamma_{\perp} \gg \kappa \sim \gamma_{\parallel}$; includes helium-neon (0.6 and 1.15 μm) and argon-ion lasers.
- (iii) $\gamma_{\perp} \gg \kappa \gg \gamma_{\parallel}$; includes ruby, neodymium yttrium aluminum garnet, carbon dioxide, and semiconductor lasers.
- (iv) $\kappa \gg \gamma_{\perp}, \gamma_{\parallel}$; near-infrared noble gas lasers and many far-infrared gas lasers (including He-Ne at 3.39 μm) are in this class.

The master-equation theory developed in the last section refers to the first of these classes (*good-cavity lasers*). This is a quite limiting feature, especially in view of the fact that lasers operating in the bad-cavity limit (i.e., having cavity damping time much shorter than the atomic damping time) have attracted considerable attention lately.

There are two reasons for this upsurge of interest. First, it has been shown that in many systems a careful consideration of polarization dynamics is essential when considering the fluctuation spectrum of the produced light. This is already true for single-atom resonance fluo-

rescence, and also holds for multiwave mixing in two-level atoms (Reid and Walls, 1986). For absorptive optical bistability, Carmichael (1986) showed, in a treatment that does not adiabatically eliminate the polarization, that a low- Q cavity may produce better squeezing than a high- Q cavity. The general case, also without adiabatic elimination of the polarization, was studied by several authors (Castelli *et al.*, 1988; Reid, 1988), confirming that the high- Q cavity was less favorable for squeezing. Squeezing enhancement in dispersive optical bistability, in the regime of low intensities and comparable atomic and cavity decay rates, was demonstrated experimentally by Raizen *et al.* (1987) and Orozco *et al.* (1987).

The second reason for the interest in bad-cavity lasers is the recent development of semiconductor microlasers. In these devices a substantial fraction of spontaneous emission couples to the lasing mode, so that an extremely low oscillation threshold can be attained, of the order of one photon (Björk *et al.*, 1993). A necessary condition for this to happen is that the spectral width of the gain curve (Γ_{\perp}) be smaller than the width of the cavity mode (γ), which implies a nonadiabatic regime for the atomic variables.

A theory of quantum fluctuations in a laser that accommodates the four different classes mentioned above has recently been developed by Kolobov *et al.* (1993). While completely analytic, the new theory fully includes the effects of polarization and population dynamics. In addition, it takes into account the possibility of non-Poissonian pumping.

The main results are: (i) a generalization of the regular-pumping results, to include all possible relative values between atomic and field decay constants; (ii) a non-Markovian phase evolution, resulting from the polarization dynamics, and implying a short-time reduction in spontaneous-emission noise, and an important reduction of the linewidth in the bad-cavity case (large cavity damping), that is, for lasers of the fourth class; and (iii) a reduction of up to 50% in noise in the spectrum of amplitude fluctuations for the field outside the cavity, for Poissonian pumping and lasers of the third class, around a frequency given by the geometric mean of the decay rates of the field and the lower-level population, when the decay of this population is much faster than that of the upper level.

The theoretical framework for this general treatment is based on the Heisenberg-Langevin equations (Lax, 1968b; Sargent *et al.*, 1974; see also Benkert, Scully, Bergou, Davidovich, Hillery, and Orszag, 1990). The method is quite general, and can be applied to other systems, such as lasers with injected signals and coupled lasers. This is the reason why it is reviewed with some detail in the following subsections. Even though the language used throughout the following sections is more appropriate for atomic lasers, similar equations can be applied to semiconductor lasers, with an adequate reinterpretation of the atomic variables, such that the atomic inversion becomes the carrier density (Kennedy and Walls, 1989).

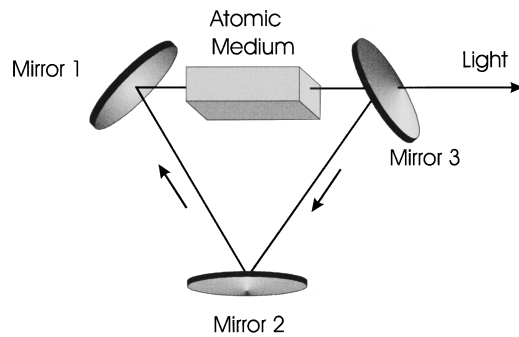


FIG. 14. Ring laser. Mirrors 1 and 2 completely reflect the light beam, while mirror 3 is partially transparent. The total length of the ring is L .

A. Heisenberg-Langevin equations

Let us consider a single-mode laser, with the active atoms inside a ring-shaped cavity of length L and volume V . This geometry (Fig. 14) implies a propagating field, which is approximated by a plane wave. The field is coupled to the outside world through a mirror with intensity-transmission coefficient equal to T . The active medium is composed of homogeneously broadened two-level atoms having transition frequency ω resonant with a cavity mode. The corresponding Hamiltonian is (for notational simplicity, hats over operators are dropped)

$$H = \hbar \omega a^\dagger a + \sum_j (E_a \sigma_a^j + E_b \sigma_b^j) + \hbar g \sum_j \Theta(t-t_j) (a^\dagger \sigma^j e^{-i\vec{k} \cdot \vec{r}_j} + \sigma^{j\dagger} a e^{i\vec{k} \cdot \vec{r}_j}). \quad (6.1)$$

The first line of this expression represents the sum of the unperturbed Hamiltonians for the field and the atoms, while the second line describes the electric dipole interaction between atoms and field in the rotating-wave approximation (Jaynes and Cummings, 1963). In Eq. (6.1), E_a and E_b are the energies of the upper and lower atomic levels, $\sigma_a^j = (|a\rangle\langle a|)^j$ and $\sigma_b^j = (|b\rangle\langle b|)^j$ are the projection operators corresponding to the resonant upper and lower atomic levels, and $\sigma^j(t) = (|b\rangle\langle a|)^j$ is the “spin-flip” operator which, applied to the upper state $|a\rangle^j$, produces the lower state $|b\rangle^j$, while its adjoint $\sigma^{j\dagger}(t) = (|a\rangle\langle b|)^j$, applied to the lower state, produces the upper state. The average of $\sigma^j(t)$ with respect to the atomic density operator ρ_{at}^j yields the off-diagonal matrix element of ρ_{at}^j between states a and b , and for this reason σ^j is associated with the atomic coherence. In a similar way, σ_b^j and σ_a^j are associated with the populations of levels a and b . Furthermore, if the parity of levels a and b is well defined, the electric dipole operator will have only off-diagonal matrix elements, and therefore will be proportional to σ^j , in the two-level subspace. Therefore, σ^j may be associated to the atomic polarization. The function $\Theta(t)$ is the Heaviside step function [$\Theta(t)=1$ for $t>0$, $\Theta(t)=1/2$ for $t=0$, and $\Theta(t)=0$ for $t<0$], which guarantees that the j th atom,

localized at \vec{r}_j , starts interacting with the cavity mode at time t_j . The coupling constant g is given by

$$g = \sqrt{\frac{\omega}{2\hbar\epsilon_0 V}}\mu, \quad (6.2)$$

where $\omega = (E_a - E_b)/\hbar$, and μ is the magnitude of the atomic dipole moment (assumed to be real).

From Eq. (6.1), one gets the Heisenberg equations of motion for the atomic and field operators:

$$\dot{a}(t) = -i\omega a(t) - ig \sum_j \Theta(t-t_j) \sigma_j(t) e^{-i\vec{k}\cdot\vec{r}_j}, \quad (6.3a)$$

$$\begin{aligned} \dot{\sigma}^j(t) = & -i\omega \sigma^j(t) + ig \Theta(t-t_j) [\sigma_a^j(t) \\ & - \sigma_b^j(t)] e^{i\vec{k}\cdot\vec{r}_j} a(t), \end{aligned} \quad (6.3b)$$

$$\begin{aligned} \dot{\sigma}_a^j(t) = & ig \Theta(t-t_j) [a^\dagger(t) \sigma^j(t) e^{-i\vec{k}\cdot\vec{r}_j} \\ & - \sigma^{j\dagger}(t) a(t) e^{i\vec{k}\cdot\vec{r}_j}], \end{aligned} \quad (6.3c)$$

$$\begin{aligned} \dot{\sigma}_b^j(t) = & -ig \Theta(t-t_j) [a^\dagger(t) \sigma^j(t) e^{-i\vec{k}\cdot\vec{r}_j} \\ & - \sigma^{j\dagger}(t) a(t) e^{i\vec{k}\cdot\vec{r}_j}]. \end{aligned} \quad (6.3d)$$

These equations are rather intuitive. The atomic polarization acts as a source for the field, while the atomic populations are affected by the electric dipole interaction between the polarization and the field.

It is convenient to define slowly varying field and spin-flip operators, subtracting the time-dependence involving the frequency ω :

$$\tilde{a}(t) = e^{i\omega t} a(t), \quad \tilde{\sigma}^j(t) = e^{i\omega t} \sigma^j(t).$$

It is easy to see that the resulting Heisenberg equations differ from Eq. (6.3) only in the absence of the terms proportional to ω .

One must now add to the above Heisenberg equations the atomic and field decay, which result from the coupling between these systems and their respective reservoirs. The reservoir for the cavity mode corresponds to the modes of the field external to the cavity, which are coupled to the internal field through the semitransparent mirror, while the atomic reservoirs correspond to lower atomic levels, to which levels a and b are coupled through collisions or spontaneous emission. The field can also be damped by absorption at the cavity walls. These couplings result not only in decay terms, but also in fluctuation forces (Langevin forces). The diffusion coefficients associated with these forces can be obtained through specific reservoir models (see, for instance, Cohen-Tannoudji *et al.*, 1988), or, in the case of atomic forces, by using generalizations of the Einstein relation (4.16).

One gets then the following Heisenberg-Langevin equations (the tilde on the operators is dropped in the following, since from now on all the operators will be slowly varying ones):

$$\dot{a}(t) = -ig \sum_j \Theta(t-t_j) \sigma_j(t) e^{-i\vec{k}\cdot\vec{r}_j} - \frac{\gamma}{2} a(t) + F_\gamma(t), \quad (6.4a)$$

$$\dot{\sigma}_j(t) = +ig \Theta(t-t_j) [\sigma_a^j(t) - \sigma_b^j(t)] e^{i\vec{k}\cdot\vec{r}_j} a(t) - \Gamma \sigma_j(t) + f_\sigma^j(t), \quad (6.4b)$$

$$\dot{\sigma}_a^j(t) = ig \Theta(t-t_j) [a^\dagger(t) \sigma^j(t) e^{-i\vec{k}\cdot\vec{r}_j} - \sigma^{j\dagger}(t) a(t) e^{i\vec{k}\cdot\vec{r}_j}] - (\Gamma_a + \Gamma'_a) \sigma_a^j(t) + f_a^j(t), \quad (6.4c)$$

$$\dot{\sigma}_b^j(t) = -ig \Theta(t-t_j) [a^\dagger(t) \sigma^j(t) e^{-i\vec{k}\cdot\vec{r}_j} - \sigma^{j\dagger}(t) a(t) e^{i\vec{k}\cdot\vec{r}_j}] - \Gamma_b \sigma_b^j(t) + \Gamma'_a \sigma_a^j(t) + f_b^j(t). \quad (6.4d)$$

For purely radiative decay, the polarization decay rate Γ is related to the population decay rates Γ_a , Γ'_a , and Γ_b . Indeed, if $\psi_a(t)$ and $\psi_b(t)$ are the probability amplitudes for finding an atom in states a and b , the corresponding decays are described by the equations $d\psi_a(t)/dt = -[(\Gamma_a + \Gamma'_a)/2]\psi_a(t)$ and $d\psi_b(t)/dt = (-\Gamma_b/2)\psi_b(t)$ (the feeding of b by a is not considered here, since one is interested only in the decay contributions). This implies that

$$\begin{aligned} \frac{d}{dt} [\langle \psi(t) | b \rangle \langle a | \psi(t) \rangle] &= \left[\frac{d}{dt} \psi_b^*(t) \right] \psi_a(t) + \psi_b^*(t) \left[\frac{d}{dt} \psi_a(t) \right] \\ &= -[(\Gamma_a + \Gamma'_a + \Gamma_b)/2] \psi_b^*(t) \psi_a(t) \\ &= -\Gamma \psi_b^*(t) \psi_a(t), \end{aligned}$$

and therefore in this case one has $2\Gamma = \Gamma_a + \Gamma'_a + \Gamma_b$. Collision processes may, however, affect the relative phase between states a and b , without affecting their

populations, implying a faster average decay of the coherence, and leading to the inequality

$$2\Gamma \geq \Gamma_a + \Gamma'_a + \Gamma_b. \quad (6.5)$$

One should note that, in this model, the step functions turn on the interaction between each atom and the cavity mode, the turning off being accomplished by the atomic decay to lower (nonresonant) levels. On the other hand, the fact that one deals here with just one mode imposes a restriction on the field decay rate: the width of the cavity mode, given by $\gamma/2$, should be much smaller than the mode separation $2\pi c/L$.

1. Langevin forces for the field

The Langevin forces are defined by their first- and second-order moments (Lax, 1966b; Sargent *et al.*, 1974; Cohen-Tannoudji *et al.*, 1988). For the field Langevin force $F_\gamma(t)$ one gets

$$\langle F_\gamma(t) \rangle = 0, \quad (6.6)$$

and

$$\langle F_\gamma^\dagger(t) F_\gamma(t') \rangle = \gamma n_T \delta(t-t'), \quad (6.7a)$$

$$\langle F_\gamma(t) F_\gamma^\dagger(t') \rangle = \gamma(n_T + 1) \delta(t-t'), \quad (6.7b)$$

$$\langle F_\gamma(t) F_\gamma(t') \rangle = 0, \quad (6.7c)$$

$$\langle F_\gamma^\dagger(t) F_\gamma^\dagger(t') \rangle = 0, \quad (6.7d)$$

where as before n_T is the average number of thermal photons in the laser cavity, at temperature T , in the mode with frequency ω . It will be assumed here that $T=0$, for simplicity. These moments are sufficient for complete determination of the fluctuation forces only if the corresponding statistical process is Gaussian [see, for instance, Gardiner (1991)].

2. Atomic Langevin forces

The diffusion coefficients for the atomic Langevin forces may be obtained from the *generalized Einstein relations*. Let a system be described by N operators \mathcal{A}_i , $i=1, \dots, N$, satisfying the Heisenberg-Langevin equations

$$\frac{d}{dt} \mathcal{A}_i(t) = \mathcal{D}_i[\mathcal{A}_1(t), \dots, \mathcal{A}_N(t)] + F_i(t), \quad (6.8)$$

where the forces F_i satisfy the equations

$$\langle F_i(t) \rangle = 0, \quad (6.9)$$

and

$$\langle F_i^\dagger(t) F_j(t') \rangle = 2D_{ij}^{(\mathcal{N})} \delta(t-t'), \quad (6.10)$$

the index \mathcal{N} corresponding to the normal order of F_i^\dagger , F_j . Similar relations hold for antinormal ordering.

One shows then the relation

$$\langle F_i^\dagger(t) \mathcal{A}_j(t) + \mathcal{A}_i^\dagger(t) F_j(t) \rangle = 2D_{ij}^{(\mathcal{N})}, \quad (6.11)$$

and also the *generalized Einstein relation* (Cohen-Tannoudji *et al.*, 1988)

$$2D_{ij}^{(\mathcal{N})} = \langle \mathcal{D}(\mathcal{A}_i^\dagger \mathcal{A}_j) \rangle - \mathcal{D}_i^\dagger \mathcal{A}_j - \mathcal{A}_i^\dagger \mathcal{D}_j, \quad (6.12)$$

where $\mathcal{D}(\mathcal{A}_i^\dagger \mathcal{A}_j)$ is the drift coefficient corresponding to the equation

$$\frac{d}{dt} \langle \mathcal{A}_i^\dagger(t) \mathcal{A}_j(t) \rangle = \langle \mathcal{D}(\mathcal{A}_i^\dagger \mathcal{A}_j) \rangle. \quad (6.13)$$

This relation is very useful for finding the atomic diffusion coefficients, due to the fact that the atomic operators obey a closed algebra, namely,

$$\begin{aligned} (\sigma_a^j)^2 = \sigma_a^j, \quad (\sigma_b^j)^2 = \sigma_b^j, \quad (\sigma^j)^2 = 0, \\ \sigma^j \sigma^{j\dagger} = \sigma_b^j, \quad \sigma^{j\dagger} \sigma^j = \sigma_a^j, \quad \sigma^j \sigma_a^j = \sigma^j, \quad \sigma^{j\dagger} \sigma_b^j = \sigma^{j\dagger}. \end{aligned} \quad (6.14)$$

For example, the diffusion coefficient corresponding to the fluctuation force f_a^j ,

$$\langle f_a^j(t) f_a^j(t') \rangle = 2D_{aa} \delta(t-t'), \quad (6.15)$$

can be obtained from Eqs. (6.12) and (6.4c):

$$\begin{aligned} 2D_{aa} &= \left\langle \frac{d}{dt} (\sigma_a^j)^2 - \left(\frac{d}{dt} \sigma_a^j \right) \sigma_a^j - \sigma_a^j \left(\frac{d}{dt} \sigma_a^j \right) \right\rangle \\ &= (-\Gamma_a - \Gamma'_a + \Gamma_a + \Gamma'_a + \Gamma_a + \Gamma'_a) \langle \sigma_a^j \rangle \\ &= (\Gamma_a + \Gamma'_a) \langle \sigma_a^j \rangle. \end{aligned} \quad (6.16)$$

Applying the same procedure to all possible products of correlation forces, one gets for the normal-ordered non-vanishing correlations

$$\langle f_\sigma^{ij}(t) f_\sigma^j(t') \rangle = (2\Gamma - \Gamma_a - \Gamma'_a) \langle \sigma_a^j(t) \rangle \delta(t-t'), \quad (6.17a)$$

$$\langle f_\sigma^j(t) f_\sigma^{ij}(t') \rangle = [(2\Gamma - \Gamma_b) \langle \sigma_b^j(t) \rangle + \Gamma'_a \langle \sigma_a^j(t) \rangle] \delta(t-t'), \quad (6.17b)$$

$$\langle f_\sigma^j(t) f_\sigma^j(t') \rangle = (\Gamma_a + \Gamma'_a) \langle \sigma^j(t) \rangle \delta(t-t'), \quad (6.17c)$$

$$\langle f_\sigma^j(t) f_b^j(t') \rangle = -\Gamma'_a \langle \sigma^j(t) \rangle \delta(t-t'), \quad (6.17d)$$

$$\langle f_\sigma^{ij}(t) f_b^j(t') \rangle = \Gamma_b \langle \sigma_i^\dagger(t) \rangle \delta(t-t'), \quad (6.17e)$$

$$\langle f_a^j(t) f_a^j(t') \rangle = (\Gamma_a + \Gamma'_a) \langle \sigma_a^j(t) \rangle \delta(t-t'), \quad (6.17f)$$

$$\langle f_a^j(t) f_b^j(t') \rangle = -\Gamma'_a \langle \sigma_a^j(t) \rangle \delta(t-t'), \quad (6.17g)$$

$$\langle f_b^j(t) f_b^j(t') \rangle = [\Gamma_b \langle \sigma_b^j(t) \rangle + \Gamma'_a \langle \sigma_a^j(t) \rangle] \delta(t-t'). \quad (6.17h)$$

The correlations between forces associated with different atoms vanish, as do the correlations involving atom and field operators, since the corresponding reservoirs are independent.

3. Macroscopic operators

One is usually interested in the behavior of macroscopic observables. The above equations will therefore be reexpressed in terms of the macroscopic operators, defined by

$$M(t) = -i \sum_j \Theta(t-t_j) \sigma^j(t) e^{-i\vec{k} \cdot \vec{r}_j}, \quad (6.18a)$$

$$N_a(t) = \sum_j \Theta(t-t_j) \sigma_a^j(t), \quad (6.18b)$$

$$N_b(t) = \sum_j \Theta(t-t_j) \sigma_b^j(t). \quad (6.18c)$$

The additional factor $(-i)$ in Eq. (6.18a) is introduced for mathematical convenience. The operator $M(t)$ represents the macroscopic atomic polarization for the atoms that started their interaction with the cavity mode before t . The operators $N_a(t)$ and $N_b(t)$ stand for the macroscopic populations of the upper and lower level, respectively. The introduction of macroscopic operators leads in a subtle way to the problem of pumping statistics. Indeed, one should note that, in order to calculate the average values or correlation functions of the macroscopic operators (6.18), two averages must be implemented, namely, the quantum average and the classical average over the excitation (or arrival) times t_j of the atoms in the cavity. This last average introduces the pumping statistics.

With the above definitions of macroscopic atomic operators, Eq. (6.4a) for the electromagnetic field becomes simpler:

$$\dot{a}(t) = -\gamma/2a(t) + gM(t) + F_\gamma(t). \quad (6.19)$$

On the other hand, the Langevin equations for the macroscopic atomic operators are found by differentiating Eq. (6.18) and replacing in the resulting expression Eqs. (6.4b)–(6.4d) for the individual atomic operators. For instance, for the operator $N_a(t)$ one finds

$$\begin{aligned} \dot{N}_a(t) &= \sum_j [\delta(t-t_j)\sigma_a^j(t) + \Theta(t-t_j)\dot{\sigma}_a^j(t)] \\ &= \sum_j \delta(t-t_j)\sigma_a^j(t_j) - (\Gamma_a + \Gamma'_a)N_a(t) \\ &\quad - g[a^\dagger(t)M(t) + M^\dagger(t)a(t)] + \sum_j \Theta(t-t_j)f_a^j(t). \end{aligned} \quad (6.20)$$

The first term on the right-hand side of Eq. (6.20) corresponds to the pumping of atoms into the upper lasing level. Indeed, the average value of this term is

$$\begin{aligned} \left\langle \sum_j \delta(t-t_j)\sigma_a^j(t_j) \right\rangle &= \left\langle \sum_j \delta(t-t_j)\langle \sigma_a^j(t_j) \rangle \right\rangle_S \\ &= \left\langle \sum_j \delta(t-t_j) \right\rangle_S, \end{aligned} \quad (6.21)$$

since $\langle \sigma_a^j(t_j) \rangle = 1$, due to the fact that the atoms are injected in the upper state. The index S stands for the classical statistical average, which must still be carried out. It yields the average pumping rate into the upper lasing level:

$$\left\langle \sum_j \delta(t-t_j) \right\rangle_S = R \int_{-\infty}^{+\infty} dt_j \delta(t-t_j) = R. \quad (6.22)$$

In view of this result, the first term on the right-hand side of Eq. (6.20) may be written in the form

$$\sum_j \delta(t-t_j)\sigma_a^j(t_j) = R + \left[\sum_j \delta(t-t_j)\sigma_a^j(t_j) - R \right], \quad (6.23)$$

which clearly displays a constant drift contribution, given by R , and a fluctuation force with zero average, associated with the remaining contribution on the right-hand side of the above equation. Inserting this result into (6.20), one finds

$$\begin{aligned} \dot{N}_a(t) &= R - (\Gamma_a + \Gamma'_a)N_a(t) - g[a^\dagger(t)M(t) \\ &\quad + M^\dagger(t)a(t)] + F_a(t), \end{aligned} \quad (6.24)$$

with

$$F_a(t) = \sum_j \Theta(t-t_j)f_a^j(t) + \sum_j \delta(t-t_j)\sigma_a^j(t_j) - R. \quad (6.25)$$

The new Langevin operator $F_a(t)$ is the total-noise operator for the macroscopic atomic population $N_a(t)$. It

incorporates the fluctuations in the population of the upper level due to radiative decay and to pump fluctuations.

The equations for the macroscopic population of the lower resonant level and for the macroscopic atomic polarization are derived in a similar way:

$$\begin{aligned} \dot{N}_b(t) &= -\Gamma_b N_b(t) + \Gamma'_a N_a(t) + g[a^\dagger(t)M(t) \\ &\quad + M^\dagger(t)a(t)] + F_b(t), \end{aligned} \quad (6.26)$$

$$\dot{M}(t) = -\Gamma M(t) + g[N_a(t) - N_b(t)]a(t) + F_M(t), \quad (6.27)$$

with

$$F_b(t) = \sum_j \Theta(t-t_j)f_b^j(t) + \sum_j \delta(t-t_j)\sigma_b^j(t_j), \quad (6.28)$$

$$F_M(t) = -i \left[\sum_j \Theta(t-t_j)f_a^j(t) + \sum_j \delta(t-t_j)\sigma^j(t_j) \right]. \quad (6.29)$$

The correlation functions of the macroscopic Langevin forces may be calculated by using the results already obtained for the microscopic forces, and considering also the statistics of injection times. Thus, for instance,

$$\begin{aligned} \langle F_a(t)F_a(t') \rangle &= \sum_j \sum_k \Theta(t-t_j)\Theta(t'-t_k) \\ &\quad \times \langle f_a^j(t)f_a^k(t') \rangle + I(t,t') - R^2, \end{aligned} \quad (6.30)$$

where

$$I(t,t') = \left\langle \sum_{j,k} \delta(t-t_j)\delta(t'-t_k) \right\rangle_S. \quad (6.31)$$

In deriving these expressions, one uses the fact that $f_a^j(t)$ and $\sigma_a^j(t_j)$ are uncorrelated, since $t_j < t$. The first term on the right-hand side of Eq. (6.30) may be obtained from Eqs. (6.15) and (6.16), so that

$$\begin{aligned} \langle F_a(t)F_a(t') \rangle &= (\Gamma_a + \Gamma'_a)\langle N_a(t) \rangle \delta(t-t') + I(t,t') \\ &\quad - R^2. \end{aligned} \quad (6.32)$$

The function $I(t,t')$ can be calculated easily in two extreme cases. For regular pumping, one may set $t_j = t_0 + j\tau$, where τ is the constant time interval between two successive atoms, and t_0 is an arbitrary time origin. Since in this case there are no pumping fluctuations, there is no correlation between the two delta functions in the products in Eq. (6.31), so that

$$\left\langle \sum_{j,k} \delta(t-t_j)\delta(t'-t_k) \right\rangle_S = R^2. \quad (6.33)$$

On the other hand, for Poissonian pumping, t_j is not correlated with t_k , unless $j=k$. Separating these two types of contributions, one has

$$\begin{aligned} \left\langle \sum_{j,k} \delta(t-t_j) \delta(t'-t_k) \right\rangle_S &= \left\langle \sum_j \delta(t-t_j) \delta(t'-t_j) \right\rangle_S \\ &+ \left\langle \sum_{j \neq k} \delta(t-t_j) \delta(t'-t_k) \right\rangle_S. \end{aligned} \quad (6.34)$$

One finds for the first contribution

$$\begin{aligned} \left\langle \sum_j \delta(t-t_j) \delta(t'-t_j) \right\rangle_S &= \left\langle \delta(t-t') \sum_j \delta(t-t_j) \right\rangle_S \\ &= R \delta(t-t'). \end{aligned} \quad (6.35)$$

and for the second one may write

$$\begin{aligned} \left\langle \sum_{j \neq k} \delta(t-t_j) \delta(t'-t_k) \right\rangle_S \\ = \sum_j \langle \delta(t-t_j) \rangle_S \left\langle \sum_{k \neq j} \delta(t-t_k) \right\rangle_S = R^2, \end{aligned} \quad (6.36)$$

since the second sum misses just one atom (atom j), which gives an irrelevant contribution to the average of the sum (which is equal to R). We get therefore

$$\left\langle \sum_{j,k} \delta(t-t_j) \delta(t'-t_k) \right\rangle_S = R \delta(t-t') + R^2. \quad (6.37)$$

A detailed treatment, including the intermediate case between Poissonian and regular pumping, was given by Benkert, Scully, Bergou, Davidovich, Hillery, and Orszag (1990). As in the master-equation discussion, the results depend on a parameter p , which is equal to 1 if the excitation is regular, and equal to 0 for Poissonian pumping. Values of p between 0 and 1 correspond to intermediate statistical distributions. The result for the function $I(t, t')$ is then simply

$$I(t, t') = (1-p)R \delta(t-t') + R^2. \quad (6.38)$$

For the correlation functions of the Langevin forces corresponding to the macroscopic operators one finds then

$$\begin{aligned} \langle F_a(t) F_a(t') \rangle &= [(\Gamma_a + \Gamma'_a) \langle N_a(t) \rangle + R(1-p)] \\ &\times \delta(t-t'), \end{aligned} \quad (6.39a)$$

$$\begin{aligned} \langle F_M^\dagger(t) F_M(t') \rangle &= [(2\Gamma - \Gamma_a - \Gamma'_a) \langle N_a(t) \rangle + R] \\ &\times \delta(t-t'), \end{aligned} \quad (6.39b)$$

$$\langle F_b(t) F_b(t') \rangle = [\Gamma_b \langle N_b(t) \rangle + \Gamma'_a \langle N_a(t) \rangle] \delta(t-t'), \quad (6.39c)$$

$$\langle F_b(t) F_M(t') \rangle = \Gamma_b \langle M(t) \rangle \delta(t-t'), \quad (6.39d)$$

$$\langle F_a(t) F_b(t') \rangle = -\Gamma'_a \langle N_a(t) \rangle \delta(t-t'), \quad (6.39e)$$

$$\langle F_M(t) F_a(t') \rangle = (\Gamma_a + \Gamma'_a) \langle M(t) \rangle \delta(t-t'), \quad (6.39f)$$

$$\langle F_M(t) F_b(t') \rangle = -\Gamma'_a \langle M(t) \rangle \delta(t-t'), \quad (6.39g)$$

$$\begin{aligned} \langle F_M(t) F_M^\dagger(t') \rangle &= [(2\Gamma - \Gamma_b) \langle N_b(t) \rangle + \Gamma'_a \langle N_a(t) \rangle] \\ &\times \delta(t-t'). \end{aligned} \quad (6.39h)$$

Equations (6.19), (6.24), (6.26), and (6.27), together with the correlation functions (6.7) and (6.39), completely describe the dynamics of the laser and of its quantum fluctuations, for arbitrary pumping statistics, if the Langevin forces are assumed to be Gaussian.

4. Equivalent c -number equations

The operator equations

$$\dot{a}(t) = gM(t) - \frac{\gamma}{2}a(t) + F_\gamma(t), \quad (6.40a)$$

$$\dot{M}(t) = g[N_a(t) - N_b(t)]a(t) - \Gamma M(t) + F_M(t), \quad (6.40b)$$

$$\begin{aligned} \dot{N}_a(t) &= R - g[a^\dagger(t)M(t) + M^\dagger(t)a(t)] \\ &- (\Gamma_a + \Gamma'_a)N_a(t) + F_a(t), \end{aligned} \quad (6.40c)$$

$$\begin{aligned} \dot{N}_b(t) &= g[a^\dagger(t)M(t) + M^\dagger(t)a(t)] - \Gamma_b N_b(t) \\ &+ \Gamma'_a N_a(t) + F_b(t), \end{aligned} \quad (6.40d)$$

cannot be directly solved. However, they may be replaced by completely equivalent c -number equations, as long as one is interested in at most second-order correlation functions of the operators (which is consistent with the definition of the Langevin forces). The c -number equations are obtained through the following steps. One first replaces the operators in the above equations by c numbers, getting

$$\dot{\mathcal{A}}(t) = g\mathcal{M}(t) - \frac{\gamma}{2}\mathcal{A}(t) + \mathcal{F}_\gamma(t), \quad (6.41a)$$

$$\dot{\mathcal{M}}(t) = g[\mathcal{N}_a(t) - \mathcal{N}_b(t)]\mathcal{A}(t) - \Gamma\mathcal{M}(t) + \mathcal{F}_M(t), \quad (6.41b)$$

$$\begin{aligned} \dot{\mathcal{N}}_a(t) &= R - g[\mathcal{A}^*(t)\mathcal{M}(t) + \mathcal{M}^*(t)\mathcal{A}(t)] \\ &- (\Gamma_a + \Gamma'_a)\mathcal{N}_a(t) + \mathcal{F}_a(t), \end{aligned} \quad (6.41c)$$

$$\begin{aligned} \dot{\mathcal{N}}_b(t) &= g[\mathcal{A}^*(t)\mathcal{M}(t) + \mathcal{M}^*(t)\mathcal{A}(t)] - \Gamma_b\mathcal{N}_b(t) \\ &+ \Gamma'_a\mathcal{N}_a(t) + \mathcal{F}_b(t), \end{aligned} \quad (6.41d)$$

where $\mathcal{F}_k(t)$ are Langevin noise forces with the following properties:

$$\langle \mathcal{F}_k(t) \rangle = 0, \quad (6.42a)$$

$$\langle \mathcal{F}_k(t) \mathcal{F}_l(t') \rangle = 2\mathcal{D}_{kl} \delta(t-t'). \quad (6.42b)$$

The replacement of operators by c numbers does not lead in general to unique results, since the equation to be transformed may contain products of operators that do not commute with each other. Thus, for instance, the product $a^\dagger a = aa^\dagger + 1$ would be transformed by this procedure into either $|\mathcal{A}|^2$ or $|\mathcal{A}|^2 + 1$, depending on the operator form used as a starting point. In this case, in order to define this operation uniquely, it is necessary to specify the ordering in the initial expression. Equations

(6.40) do not present this problem, since they contain on the right-hand side products of commuting operators. On the other hand, the calculation of correlation functions from (6.40) leads necessarily to ordering problems. Thus, from (6.40b), one may write

$$\begin{aligned} \frac{d}{dt}\langle M^\dagger(t)M(t)\rangle &= \langle \dot{M}^\dagger(t)M(t)\rangle + \langle M^\dagger(t)\dot{M}(t)\rangle \\ &= g\langle a^\dagger(N_a - N_b)M\rangle \\ &\quad + g\langle M^\dagger(N_a - N_b)a\rangle \\ &\quad - 2\Gamma\langle M^\dagger M\rangle + 2D_{M^\dagger M}, \end{aligned} \quad (6.43)$$

where it has been used that, from Eq. (6.11),

$$\langle F_M^\dagger M\rangle + \langle M^\dagger F_M\rangle = 2D_{M^\dagger M}. \quad (6.44)$$

Equation (6.43) contains products of the polarization operator with population operators. Since M does not commute with N_a or N_b , one has here an ordering problem. On the other hand, from Eqs. (6.41b) and (6.42), one finds

$$\begin{aligned} \frac{d}{dt}\langle \mathcal{M}^*(t)\mathcal{M}(t)\rangle &= \langle \dot{\mathcal{M}}^*(t)\mathcal{M}(t)\rangle + \langle \mathcal{M}^*(t)\dot{\mathcal{M}}(t)\rangle, \\ &= g\langle \mathcal{A}^*(\mathcal{N}_a - \mathcal{N}_b)\mathcal{M}\rangle \\ &\quad + g\langle \mathcal{M}^*(\mathcal{N}_a - \mathcal{N}_b)\mathcal{A}\rangle \\ &\quad - 2\Gamma\langle \mathcal{M}^*\mathcal{M}\rangle + 2\mathcal{D}_{\mathcal{M}^*\mathcal{M}}. \end{aligned} \quad (6.45)$$

From Eq. (6.39b), one can see that Eqs. (6.43) and (6.45) coincide if

$$2\mathcal{D}_{\mathcal{M}^*\mathcal{M}} = (2\Gamma - \Gamma_a - \Gamma'_a)\langle \mathcal{N}_a(t)\rangle + R$$

and if the replacement of operators by c numbers in (6.43) keeps the order in which these operators are found in that equation. This motivates the definition of a “normal order” for field and atomic operators, by the sequence $a^\dagger, M^\dagger, N_a, N_b, M, a$. Note that Eqs. (6.40) are already in normal order. This is a generalization of the concept used previously for field operators alone. In fact, it is also possible to define a phase-space representation for field and atomic variables, given a certain ordering (Louisell, 1973). For the purposes of the present discussion, however, the explicit form of this distribution is not needed.

One should still examine what happens with the other equations. It will become clear that, keeping to the ordering defined above, the equivalence of the c -number and operator equations will require a redefinition of the diffusion coefficients.

Thus, for instance, from Eq. (6.41b), one gets

$$\begin{aligned} \frac{d}{dt}\langle M(t)M(t)\rangle &= \langle \dot{M}(t)M(t)\rangle + \langle M(t)\dot{M}(t)\rangle \\ &= g\langle (N_a - N_b)aM\rangle + g\langle M(N_a - N_b)a\rangle \\ &\quad - 2\Gamma\langle MM\rangle + \langle F_M M\rangle + \langle M F_M\rangle. \end{aligned} \quad (6.46)$$

The first two terms on the right-hand side are not in the previously defined normal order, so they must be reor-

dered, using the corresponding commutation relations. While atomic and field operators commute, one has $[M, N_a - N_b] = 2M$. This implies

$$\begin{aligned} \frac{d}{dt}\langle M(t)M(t)\rangle &= 2g\langle (N_a - N_b)Ma\rangle + 2g\langle Ma\rangle \\ &\quad - 2\Gamma\langle MM\rangle, \end{aligned} \quad (6.47)$$

since $2D_{MM} = 0$. The corresponding equation for c numbers is

$$\begin{aligned} \frac{d}{dt}\langle \mathcal{M}(t)\mathcal{M}(t)\rangle &= 2g\langle (\mathcal{N}_a - \mathcal{N}_b)\mathcal{M}\mathcal{A}\rangle - 2\Gamma\langle \mathcal{M}\mathcal{M}\rangle \\ &\quad + 2\mathcal{D}_{\mathcal{M}\mathcal{M}}. \end{aligned} \quad (6.48)$$

Comparing the right-hand sides of both equations, one concludes that they are equivalent as long as

$$2\mathcal{D}_{\mathcal{M}\mathcal{M}} = 2g\langle \mathcal{M}(t)\mathcal{A}(t)\rangle.$$

All the other diffusion coefficients for the c -number equations are obtained in analogous ways. The nonvanishing coefficients are the following:

$$2\mathcal{D}_{\mathcal{M}^*\mathcal{M}} = (2\Gamma - \Gamma_a - \Gamma'_a)\langle \mathcal{N}_a(t)\rangle + R, \quad (6.49a)$$

$$2\mathcal{D}_{\mathcal{M}\mathcal{M}} = 2g\langle \mathcal{M}(t)\mathcal{A}(t)\rangle, \quad (6.49b)$$

$$2\mathcal{D}_{\mathcal{M}\mathcal{M}^*} = \Gamma_b\langle \mathcal{M}(t)\rangle, \quad (6.49c)$$

$$\begin{aligned} 2\mathcal{D}_{aa} &= (\Gamma_a + \Gamma'_a)\langle \mathcal{N}_a(t)\rangle + R(1-p) \\ &\quad - g[\langle \mathcal{A}^*(t)\mathcal{M}(t) + \mathcal{M}^*(t)\mathcal{A}(t)\rangle], \end{aligned} \quad (6.49d)$$

$$\begin{aligned} 2\mathcal{D}_{bb} &= \Gamma_b\langle \mathcal{N}_b(t)\rangle + \Gamma'_a\langle \mathcal{N}_a(t)\rangle - g[\langle \mathcal{A}^*(t)\mathcal{M}(t) \\ &\quad + \mathcal{M}^*(t)\mathcal{A}(t)\rangle], \end{aligned} \quad (6.49e)$$

$$\begin{aligned} 2\mathcal{D}_{ab} &= -\Gamma'_a\langle \mathcal{N}_a(t)\rangle + g[\langle \mathcal{A}^*(t)\mathcal{M}(t) \\ &\quad + \mathcal{M}^*(t)\mathcal{A}(t)\rangle]. \end{aligned} \quad (6.49f)$$

One should note in particular that for zero temperature, the diffusion coefficients of the normal-ordered field fluctuation forces are all equal to zero. This implies that the fluctuation force $\mathcal{F}_\gamma(t)$ in Eq. (6.41a) may be set equal to zero, a simplifying feature of the normal-ordered representation.

Equations (6.41) and (6.49) are c -number Langevin equations completely equivalent to (6.40) with respect to the calculation of correlation functions up to second order. They are, however, easier to deal than the operator equations.

The above equations also allow one to state precisely in what sense the fluctuation forces are small. The macroscopic atomic variables scale as the number of atoms in the system. On the other hand, it follows from Eq. (6.2) that the coupling constant g scales as the square root of the inverse of this number (assuming that the volume V of the cavity is of the same order as the volume of the sample; in general, V is larger than the volume of the sample, and one should say more precisely that the coupling constant has an upper bound that scales as the number of atoms). This, together with Eq. (6.41a), implies that the field amplitude scales as the

square root of the number of atoms (so that the intensity scales as the number of atoms). From Eq. (6.49) one sees then that the mean squares of the fluctuation forces also scale as the number of atoms, and so the atomic fluctuation forces scale as the square root of this number, and indeed become small compared with the deterministic terms when this number is very large, as is the case in lasers.

If the fluctuation forces are neglected, one gets a semiclassical laser theory, which yields the steady-state solution.

B. Semiclassical theory

One should note first that, in the absence of the fluctuation forces, the field and polarization variables remain real, if real initially. In this case, the semiclassical equations of motion become

$$\dot{\mathcal{A}}(t) = g\mathcal{M}(t) - \frac{\gamma}{2}\mathcal{A}(t), \quad (6.50a)$$

$$\dot{\mathcal{M}}(t) = g[\mathcal{N}_a(t) - \mathcal{N}_b(t)]\mathcal{A}(t) - \Gamma\mathcal{M}(t), \quad (6.50b)$$

$$\dot{\mathcal{N}}_a(t) = R - 2g\mathcal{M}(t)\mathcal{A}(t) - (\Gamma_a + \Gamma'_a)\mathcal{N}_a(t), \quad (6.50c)$$

$$\dot{\mathcal{N}}_b(t) = 2g\mathcal{M}(t)\mathcal{A}(t) - \Gamma_b\mathcal{N}_b(t) + \Gamma'_a\mathcal{N}_a(t). \quad (6.50d)$$

1. Adiabatic elimination and rate equations

The above system of equations is frequently simplified, when distinct time scales occur for the decays of different subsets of variables. Thus, for instance, in He-Ne lasers at 0.6 and 1.15 μm , the polarization relaxation constant is much larger than those of the populations or the field ($\Gamma \gg \Gamma_a, \Gamma_b, \gamma$). Furthermore, Γ is also much larger than the Rabi frequency associated with the coupling between the polarization and the field in Eqs. (6.50c) and (6.50d). Taking this case as an example of the usual procedure, let us consider the formal solution of Eq. (6.50b):

$$\mathcal{M}(t) = g \int_{-\infty}^t dt' e^{-\Gamma(t-t')} [\mathcal{N}_a(t') - \mathcal{N}_b(t')] \mathcal{A}(t'), \quad (6.51)$$

where the initial value of the polarization has been taken as zero, since the atoms are injected in the excited state. If Γ is much larger than the typical rates of variation of the populations and the field, the terms depending on the atomic and field variables can be taken out of the above integral, leading to

$$\mathcal{M}(t) = \frac{g}{\Gamma} [\mathcal{N}_a(t) - \mathcal{N}_b(t)] \mathcal{A}(t), \quad (6.52)$$

which could also be obtained by equating the time derivative in (6.50b) to zero.

Equation (6.52) shows that, under the above conditions, the polarization follows the other variables in time ("adiabatic following"). Therefore, the dimension of the system is reduced, and one says that the polarization is

adiabatically eliminated. Inserting Eq. (6.52) in Eqs. (6.50a), (6.50c), and (6.50d), the following equations are obtained:

$$\dot{\mathcal{A}}(t) = -\frac{\gamma}{2}\mathcal{A}(t) + \frac{g^2}{\Gamma} [\mathcal{N}_a(t) - \mathcal{N}_b(t)] \mathcal{A}(t), \quad (6.53a)$$

$$\dot{\mathcal{N}}_a(t) = R - (\Gamma_a + \Gamma'_a)\mathcal{N}_a(t) - \frac{2g^2}{\Gamma} [\mathcal{N}_a(t) - \mathcal{N}_b(t)] \mathcal{A}^2(t), \quad (6.53b)$$

$$\dot{\mathcal{N}}_b(t) = -\Gamma_b\mathcal{N}_b(t) + \Gamma'_a\mathcal{N}_a(t) + \frac{2g^2}{\Gamma} [\mathcal{N}_a(t) - \mathcal{N}_b(t)] \mathcal{A}^2(t). \quad (6.53c)$$

Multiplying Eq. (6.53a) by $\mathcal{A}(t)$, and defining $I \equiv \mathcal{A}^2$ as the intensity of the classical field (normalized to the number of photons in the cavity), one finds

$$\dot{I}(t) = -\gamma I(t) + \frac{2g^2}{\Gamma} [\mathcal{N}_a(t) - \mathcal{N}_b(t)] I(t), \quad (6.54a)$$

$$\dot{\mathcal{N}}_a(t) = R - (\Gamma_a + \Gamma'_a)\mathcal{N}_a(t) - \frac{2g^2}{\Gamma} [\mathcal{N}_a(t) - \mathcal{N}_b(t)] I(t), \quad (6.54b)$$

$$\dot{\mathcal{N}}_b(t) = -\Gamma_b\mathcal{N}_b(t) + \Gamma'_a\mathcal{N}_a(t) + \frac{2g^2}{\Gamma} [\mathcal{N}_a(t) - \mathcal{N}_b(t)] I(t). \quad (6.54c)$$

These equations show that, in the limit in which the polarization can be adiabatically eliminated, the laser is described by rate equations for the atomic and photon populations. If in addition the atomic relaxation constants are much larger than γ and the Rabi frequency, then the atomic populations may also be adiabatically eliminated, and one gets then a single equation for the number of photons.

2. Steady state

The steady-state solutions of Eq. (6.50) are obtained by setting the time derivatives equal to zero. One then finds for the steady-state intensity $I_0 (\equiv \mathcal{A}_0^2)$:

$$I_0 = I_S (R/R_T - 1), \quad (6.55)$$

where I_S is the saturation intensity, given by

$$I_S = \frac{\Gamma\Gamma_b}{2g^2} \frac{\Gamma_a + \Gamma'_a}{\Gamma_a + \Gamma_b}, \quad (6.56)$$

and R_T is the threshold pumping rate,

$$R_T = \frac{\gamma\Gamma\Gamma_b}{2g^2} \frac{\Gamma_a + \Gamma'_a}{\Gamma_b - \Gamma'_a}. \quad (6.57)$$

The expression (6.56) for I_S generalizes Eq. (5.5), reducing to it when $\Gamma'_a = 0$ and $\Gamma = (\Gamma_a + \Gamma_b)/2$ (the purely radiative case).

From Eq. (6.57) one can see that a necessary condition for laser oscillation is that $\Gamma_b > \Gamma'_a$, that is, level b

must be emptied through decay to lower levels faster than it is fed by the decay of level a . This is quite intuitive—otherwise, the population inversion necessary for laser oscillation could not be maintained. For the populations, one finds

$$\mathcal{N}_{a_0} = \frac{R - \gamma I_0}{\Gamma_a + \Gamma'_a}, \quad (6.58a)$$

$$\mathcal{N}_{b_0} = \frac{\Gamma'_a R + \gamma \Gamma_a I_0}{\Gamma_b (\Gamma_a + \Gamma'_a)}. \quad (6.58b)$$

Using (6.55) and (6.56), these equations may be expressed in terms of the steady-state intensity I_0 and the saturation intensity I_S :

$$\mathcal{N}_{a_0} = \frac{\gamma}{\Gamma_b - \Gamma'_a} \left(I_0 + \frac{\Gamma_a + \Gamma_b}{\Gamma_a + \Gamma'_a} I_S \right), \quad (6.59a)$$

$$\mathcal{N}_{b_0} = \frac{\gamma}{\Gamma_b - \Gamma'_a} \left(I_0 + \frac{\Gamma'_a}{\Gamma_b} \frac{\Gamma_a + \Gamma_b}{\Gamma_a + \Gamma'_a} I_S \right). \quad (6.59b)$$

On the other hand, using Eq. (6.50a) one may express the steady-state atomic polarization in terms of the steady-state intensity:

$$\mathcal{M}_0 = \frac{\gamma}{2g} \mathcal{A}_0, \quad (6.60)$$

the proportionality coefficient being the value at resonance of the atomic susceptibility. Note that if \mathcal{A}_0 is real, the same will be true for the steady-state polarization.

The stability of the above solutions can be checked by studying the behavior of small fluctuations of the atomic

and field variables around the steady state. The general analysis may become quite complex (Abraham *et al.*, 1986; Milonni *et al.*, 1987). Indeed, for $\Gamma'_a = 0$ and $\Gamma_a = \Gamma_b = \Gamma_{\parallel}$, Eqs. (6.50) become equivalent to the Lorenz equations (Lorenz, 1963), as shown by Haken (1975), leading to chaotic behavior. In any case, in order to calculate the spectra of fluctuations around steady state, one should identify the regions of stable behavior, to make sure that those fluctuations do not diverge with time.

In the next section, the fluctuation forces are again taken into account, and the dynamics of the fluctuations around these steady-state solutions is considered. The measured spectra of field fluctuations will be directly related to these quantities.

C. Dynamics of fluctuations

The dynamic variables are now expressed as a sum of the steady-state values plus small fluctuations. It is assumed that the laser is operating sufficiently above threshold so that the fluctuations of the dynamic variables are much smaller than their steady-state values (it will be shown that the fluctuations scale as the square root of the number of atoms, so that since the dynamic variables scale as the number of atoms, it will not be necessary to be very far above threshold). It is also assumed that the linearization is made in a region of parameters that renders the steady state stable. Neglecting terms of second order and higher in the fluctuations, one gets from Eq. (6.41), setting $\mathcal{F}_{\gamma}(t) = 0$, as discussed before,

$$\delta \dot{\mathcal{N}}_a(t) = -(\Gamma_a + \Gamma'_a) \delta \mathcal{N}_a(t) - g \mathcal{A}_0 [\delta \mathcal{M}(t) + \delta \mathcal{M}^*(t)] - g \mathcal{M}_0 [\delta \mathcal{A}(t) + \delta \mathcal{A}^*(t)] + \mathcal{F}_a(t), \quad (6.61a)$$

$$\delta \dot{\mathcal{N}}_b(t) = -\Gamma_b \delta \mathcal{N}_b(t) + \Gamma'_a \delta \mathcal{N}_a(t) + g \mathcal{A}_0 [\delta \mathcal{M}(t) + \delta \mathcal{M}^*(t)] + g \mathcal{M}_0 [\delta \mathcal{A}(t) + \delta \mathcal{A}^*(t)] + \mathcal{F}_b(t), \quad (6.61b)$$

$$\delta \dot{\mathcal{M}}(t) = -\Gamma \delta \mathcal{M}(t) + g (\mathcal{N}_{a_0} - \mathcal{N}_{b_0}) \delta \mathcal{A}(t) + g \mathcal{A}_0 [\delta \mathcal{N}_a(t) - \delta \mathcal{N}_b(t)] + \mathcal{F}_{\mathcal{M}}(t), \quad (6.61c)$$

$$\delta \dot{\mathcal{A}}(t) = -\gamma/2 \delta \mathcal{A}(t) + g \delta \mathcal{M}(t), \quad (6.61d)$$

in which the reality of \mathcal{A}_0 and \mathcal{M}_0 has been used. These equations can now be solved exactly, by reexpressing them in terms of the Fourier transforms of the atomic and field variables:

$$\delta \mathcal{N}_a(\Omega) = (2\pi)^{-1/2} \int_{-\infty}^{+\infty} dt e^{i\Omega t} \delta \mathcal{N}_a(t), \quad (6.62)$$

and analogously for the other dynamic variables. To simplify the notation, the same symbol is used for both members of the Fourier transform pair, which will be distinguished therefore through their arguments (time or frequency). One gets then

$$\begin{aligned} -i\Omega \delta \mathcal{N}_a(\Omega) = & -(\Gamma_a + \Gamma'_a) \delta \mathcal{N}_a(\Omega) - g \mathcal{A}_0 [\delta \mathcal{M}(\Omega) \\ & + \delta \mathcal{M}^*(-\Omega)] - g \mathcal{M}_0 [\delta \mathcal{A}(\Omega) + \delta \mathcal{A}^* \\ & (-\Omega)] + \mathcal{F}_a(\Omega), \end{aligned} \quad (6.63a)$$

$$\begin{aligned} -i\Omega \delta \mathcal{N}_b(\Omega) = & -\Gamma_b \delta \mathcal{N}_b(\Omega) + \Gamma'_a \delta \mathcal{N}_a(\Omega) \\ & + g \mathcal{A}_0 [\delta \mathcal{M}(\Omega) + \delta \mathcal{M}^*(-\Omega)] \\ & + g \mathcal{M}_0 [\delta \mathcal{A}(\Omega) + \delta \mathcal{A}^*(-\Omega)] + \mathcal{F}_b(\Omega), \end{aligned} \quad (6.63b)$$

$$\begin{aligned}
-i\Omega \delta \mathcal{M}(\Omega) &= -\Gamma \delta \mathcal{M}(\Omega) + g(\mathcal{N}_{a_0} - \mathcal{N}_{b_0}) \delta \mathcal{M}(\Omega) \\
&\quad + g \mathcal{A}_0 [\delta \mathcal{N}_a(\Omega) - \delta \mathcal{N}_b(\Omega)] + \mathcal{F}_{\mathcal{M}}(\Omega),
\end{aligned} \tag{6.63c}$$

$$-i\Omega \delta \mathcal{A}(\Omega) = -\gamma/2 \delta \mathcal{A}(\Omega) + g \delta \mathcal{M}(\Omega), \tag{6.63d}$$

where the Ω -dependent fluctuation forces obey the equations [which follow immediately from the definition (6.62) and Eq. (6.42)]

$$\langle \mathcal{F}_k(\Omega) \mathcal{F}_l(\Omega') \rangle = 2 \mathcal{D}_{kl} \delta(\Omega + \Omega'). \tag{6.64}$$

Note that, since $\mathcal{F}_{\mathcal{M}^*}(t) = \mathcal{F}_{\mathcal{M}}^*(t)$, it follows that $\mathcal{F}_{\mathcal{M}^*}(\Omega) = \mathcal{F}_{\mathcal{M}}^*(-\Omega)$. Furthermore, since $\mathcal{F}_a(t)$ and $\mathcal{F}_b(t)$ are real, one should have $\mathcal{F}_i(\Omega) = \mathcal{F}_i^*(-\Omega)$, for $i = a, b$.

The solution of this linear system is easily obtained. The interesting quantities are the amplitude and phase quadrature components, which for the choice of phase made for the steady-state solution (real field) are defined by

$$\delta X(t) = \frac{1}{2} [\delta \mathcal{A}(t) + \delta \mathcal{A}^*(t)], \tag{6.65a}$$

$$\delta Y(t) = \frac{1}{2i} [\delta \mathcal{A}(t) - \delta \mathcal{A}^*(t)]. \tag{6.65b}$$

These definitions correspond to the vectors sketched in Fig. 15. The amplitude and phase fluctuations are parallel and perpendicular to the field, respectively. It will be shown that while the amplitude fluctuations remain bounded, the dispersion of the phase fluctuations grows

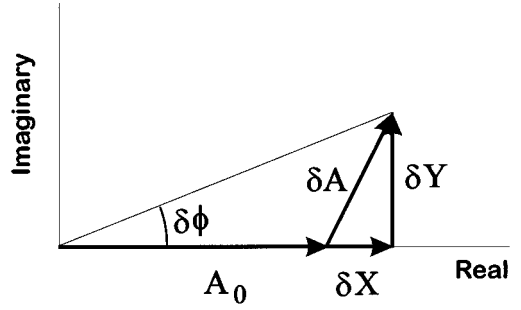


FIG. 15. Phase (δY) and amplitude (δX) quadratures corresponding to a field fluctuation $\delta \mathcal{A}$ around the steady-state value \mathcal{A}_0 . The steady-state phase is chosen so that \mathcal{A}_0 is oriented along the real axis. The phase fluctuation is given by $\delta \phi \approx \delta Y / |\mathcal{A}_0|$, as long as $\delta Y / |\mathcal{A}_0| \ll 1$.

with time. This implies that the picture sketched in Fig. 15 has a limited validity in time: due to random fluctuations, the tip of the field vector diffuses around the origin, while its amplitude is kept approximately constant.

Using (6.62), one gets, from (6.65):

$$\delta X(\Omega) = \frac{1}{2} [\delta \mathcal{A}(\Omega) + \delta \mathcal{A}^*(-\Omega)], \tag{6.66a}$$

$$\delta Y(\Omega) = \frac{1}{2i} [\delta \mathcal{A}(\Omega) - \delta \mathcal{A}^*(-\Omega)]. \tag{6.66b}$$

Note that $\delta X^*(\Omega) = \delta X(-\Omega)$, $\delta Y^*(\Omega) = \delta Y(-\Omega)$, which result from the fact that $\delta X(t)$ and $\delta Y(t)$ are real. Solving the system (6.63), one finds

$$\begin{aligned}
\delta X(\Omega) &= \frac{\Gamma_a + \Gamma'_a - i\Omega}{g(\Gamma_a + \Gamma_b - 2i\Omega)(\gamma - i\Omega)[C(\Omega) + 2\mathcal{A}_0^2]} \left\{ \frac{1}{2} [\mathcal{F}_{\mathcal{M}}(\Omega) + \mathcal{F}_{\mathcal{M}}^*(-\Omega)] (\Gamma_b - i\Omega) + g \mathcal{A}_0 \frac{\Gamma_b - \Gamma'_a - i\Omega}{\Gamma_a + \Gamma'_a - i\Omega} \mathcal{F}_a(\Omega) \right. \\
&\quad \left. - g \mathcal{A}_0 \mathcal{F}_b(\Omega) \right\},
\end{aligned} \tag{6.67a}$$

$$\delta Y(\Omega) = \frac{g}{2\Omega(\gamma/2 + \Gamma - i\Omega)} [\mathcal{F}_{\mathcal{M}}(\Omega) - \mathcal{F}_{\mathcal{M}}^*(-\Omega)], \tag{6.67b}$$

where

$$C(\Omega) = \frac{-i\Omega(\gamma/2 + \Gamma - i\Omega)(\Gamma_b - i\Omega)(\Gamma_a + \Gamma'_a - i\Omega)}{g^2(\Gamma_a + \Gamma_b - 2i\Omega)(\gamma - i\Omega)}. \tag{6.68}$$

Both $\delta X(\Omega)$ and $\delta Y(\Omega)$ are proportional to atomic fluctuation forces, which scale as the square root of the number of atoms. Therefore, if this number is very large, as in typical lasers, these fluctuations will indeed be much smaller than the steady-state values of the corresponding quadratures (which scale as the number of atoms), even without going far above threshold. Furthermore, $\delta X(\Omega) \rightarrow 0$ when $\mathcal{A}_0^2 \rightarrow \infty$ (since the atomic fluctuation forces depend only on the atomic variables

and remain finite in this limit), i.e., the amplitude fluctuations decrease as the intensity increases. This justifies the common approximation of neglecting the amplitude fluctuations for a laser operating well above threshold. The analogous result does not hold for $\delta Y(\Omega)$, however—even when the laser operates well above threshold, phase fluctuations remain important. The singularity of $\delta Y(\Omega)$ near the origin might lead one to suspect this result, since it was derived under the linearization assumption. One should note, however, that, since $\delta Y(\Omega)$ scales as the square root of the number of atoms, it is possible to approach the origin arbitrarily closely, as long as the number of atoms in the system is sufficiently large.

Equation (6.67b) displays yet another interesting feature: the fluctuation in the phase quadrature depends only on the polarization fluctuation force. This implies that this fluctuation is associated with the spontaneous-emission process. This result is dependent, however, on the ordering adopted on going from the operator to the c -number equations. For normal ordering, as noted above, the field fluctuation forces vanish, and this is the

reason why they do not contribute to Eq. (6.67b).

From Eqs. (6.64) and (6.67), one finds

$$\langle \delta X(\Omega) \delta X(\Omega') \rangle = (\delta X^2)_\Omega \delta(\Omega + \Omega'), \quad (6.69a)$$

$$\langle \delta Y(\Omega) \delta Y(\Omega') \rangle = (\delta Y^2)_\Omega \delta(\Omega + \Omega'), \quad (6.69b)$$

where

$$\begin{aligned} (\delta X^2)_\Omega = & \frac{(\Gamma_a + \Gamma'_a)^2 + \Omega^2}{g^2[(\Gamma_a + \Gamma_b)^2 + 4\Omega^2](\gamma^2 + \Omega^2)} \left\{ C(\Omega) + 2\mathcal{A}_0^2 \right\} \left\{ (\Gamma_b^2 + \Omega^2)[(\Gamma - \Gamma_a - \Gamma'_a)\mathcal{N}_{a_0} + R] \right. \\ & + g^2 \mathcal{A}_0^2 \frac{(\Gamma_b - \Gamma'_a)^2 + \Omega^2}{(\Gamma_a + \Gamma'_a)^2 + \Omega^2} [2(\Gamma_a + \Gamma'_a)\mathcal{N}_{a_0} - pR] + 2g^2 \mathcal{A}_0^2 \Gamma'_a \mathcal{N}_{a_0} \\ & \left. - 2g^2 \mathcal{A}_0^2 \frac{(\Gamma_a + \Gamma'_a)(\Gamma_b - \Gamma'_a) + \Omega^2}{(\Gamma_a + \Gamma'_a)^2 + \Omega^2} (\Gamma_b \mathcal{N}_{b_0} - 2\Gamma'_a \mathcal{N}_{a_0}) - \gamma \mathcal{A}_0^2 \Gamma_b^2 \right\}, \end{aligned} \quad (6.70a)$$

$$(\delta Y^2)_\Omega = \frac{g^2 \Gamma_a \mathcal{N}_{a_0}}{\Omega^2[(\gamma/2 + \Gamma)^2 + \Omega^2]}. \quad (6.70b)$$

Note that $(\delta X^2)_\Omega$ and $(\delta Y^2)_\Omega$ are real and symmetrical with respect to Ω , since $C(-\Omega) = C^*(\Omega)$. While $(\delta X^2)_\Omega$ is always bounded (and actually goes to zero as the intensity increases), this is not the case for $(\delta Y^2)_\Omega$, which has a singularity at $\Omega = 0$. This singularity will be shown to correspond to phase diffusion. It plays another important role as well, in view of the Heisenberg inequalities: it opens the way to the possibility of squeezing at zero frequency of the amplitude quadrature fluctuations.

The linearization procedure adopted in this section is closely related to the one used in linear stability analysis. Here one transformed (6.61) into (6.63) by setting, for a variable \mathcal{Y} representing an atomic population or the field amplitude, $\delta \mathcal{Y}(t) = \exp(-i\Omega t) \delta \mathcal{Y}(\Omega)$, $\delta \mathcal{Y}^*(t) = \exp(-i\Omega t) \delta \mathcal{Y}^*(-\Omega)$; similarly, the stability analysis sets $\delta \mathcal{Y}(t) = \exp(-st) \delta \mathcal{Y}(0)$. This implies that the characteristic polynomial of the linear stability analysis is proportional to the denominator of Eq. (6.67a), with Ω replaced by $-is$. In particular, as one gets closer to a region of laser instability, one of the roots s_0 of the characteristic polynomial approaches the imaginary axis, implying that the corresponding root Ω_0 of $C(\Omega) + 2\mathcal{A}_0^2$, with $C(\Omega)$ given by Eq. (6.68), has a small imaginary part. This may result in large fluctuations around the frequency given by the real part of Ω_0 . Some features of the spectrum can therefore be explained by proximity to regions of laser instability.

It will be shown now that the photon-number dispersion and the time evolution of the phase dispersion may also be obtained directly from Eq. (6.70).

D. Photon-number variance

As seen in Eq. (2.28), the photon-number variance may be written as

$$\langle \Delta n^2 \rangle = \langle n \rangle + \langle (|\mathcal{A}|^2 - \langle |\mathcal{A}|^2 \rangle)^2 \rangle = \langle n \rangle + \langle \Delta I^2 \rangle, \quad (6.71)$$

where $\langle \Delta I^2 \rangle$ is the c -number intensity dispersion, in the normal-ordered representation, and $\langle n \rangle$ is the average number of photons in the state (shot noise). Sufficiently far above threshold, since the amplitude fluctuations go to zero, one may use Eq. (2.35) to relate the c -number intensity dispersion to the amplitude quadrature fluctuation:

$$\langle \Delta n^2 \rangle = \langle n \rangle + 4\mathcal{A}_0^2 \langle [\delta X(t)]^2 \rangle. \quad (6.72)$$

On the other hand, from Eq. (6.69a), one finds

$$\langle [\delta X(t)]^2 \rangle = \frac{1}{2\pi} \int_{-\infty}^{+\infty} d\Omega (\delta X^2)_\Omega. \quad (6.73)$$

One may therefore write

$$\langle \Delta n^2 \rangle = \langle n \rangle + \frac{2}{\pi} \mathcal{A}_0^2 \int_{-\infty}^{+\infty} d\Omega (\delta X^2)_\Omega. \quad (6.74)$$

Taking for simplicity $\Gamma'_a = 0$, $\Gamma_a, \Gamma_b \gg \gamma$ (first-class lasers), one gets

$$\langle (\Delta n)^2 \rangle = \langle n \rangle \left\{ 1 + \left[\frac{1}{r-1} - \frac{p\Gamma_b}{2(\Gamma_a + \Gamma_b)} \right] \right\}, \quad (6.75)$$

where $r = R/R_T$. Far above threshold ($r \gg 1$),

$$\langle \Delta n^2 \rangle = \langle n \rangle \left[1 - \frac{p\Gamma_b}{2(\Gamma_a + \Gamma_b)} \right]. \quad (6.76)$$

For $\Gamma_b \gg \Gamma_a$, this yields

$$\langle \Delta n^2 \rangle = \langle n \rangle \left(1 - \frac{p}{2} \right). \quad (6.77)$$

For Poissonian pumping $p = 0$, so that

$$\langle \Delta n^2 \rangle = \langle n \rangle, \quad (6.78)$$

which is typical of a Poisson distribution for the field. On the other hand, if $p = 1$ (regular pumping), one may ob-

tain a reduction of up to 50% in the photon-number dispersion. Note that Eq. (6.76) precisely coincides with Eq. (4.32).

E. Phase diffusion

For a small phase fluctuation, the spectrum of phase fluctuations can be easily related to the spectrum of the phase quadrature fluctuations. Indeed, from Fig. 15 one is led to

$$\langle \delta\varphi^2 \rangle_\Omega = \frac{1}{I_0} \langle \delta Y^2 \rangle_\Omega. \quad (6.79)$$

From Eq. (6.70b), one finds

$$\langle \delta\varphi^2 \rangle_\Omega = \frac{D_{ST}}{\Omega^2} \frac{(\gamma/2 + \Gamma)^2}{(\gamma/2 + \Gamma)^2 + \Omega^2} \left(\frac{\Gamma}{\gamma/2 + \Gamma} \right)^2, \quad (6.80)$$

where D_{ST} is the Schawlow-Townes diffusion coefficient (Schawlow and Townes, 1958), given by

$$D_{ST} = \frac{g^2 \mathcal{N}_{a_0}}{I_0 \Gamma}. \quad (6.81)$$

Replacing \mathcal{N}_{a_0} in the above expression by Eq. (6.59a), and using Eq. (6.56), one finds

$$D_{ST} = \frac{g^2 \gamma}{\Gamma \Gamma_b} + \frac{\gamma}{2I_0}. \quad (6.82)$$

In the limit $\Gamma \gg \gamma$, Ω (when the polarization may be eliminated adiabatically), Eq. (6.80) reduces to

$$\langle \delta\varphi^2 \rangle_\Omega = \frac{D_{ST}}{\Omega^2}, \quad (6.83)$$

an expression frequently found in the literature.

From Eq. (6.80) one may directly calculate the correlation function of the time derivative of the phase fluctuation:

$$\begin{aligned} \langle \delta\dot{\varphi}(t) \delta\dot{\varphi}(t') \rangle &= \frac{1}{2\pi} \int_{-\infty}^{+\infty} d\Omega e^{-i\Omega(t-t')} \Omega^2 \langle \delta\varphi^2 \rangle_\Omega \\ &= \frac{D}{2\pi} \int_{-\infty}^{+\infty} d\Omega e^{-i\Omega(t-t')} \frac{(\gamma/2 + \Gamma)^2}{(\gamma/2 + \Gamma)^2 + \Omega^2} \\ &= (D/2) (\gamma/2 + \Gamma) \exp\{-(\gamma/2 + \Gamma)|t-t'|\}, \end{aligned} \quad (6.84)$$

where

$$D = D_{ST} \left(\frac{\Gamma}{\gamma/2 + \Gamma} \right)^2. \quad (6.85)$$

When Γ becomes much larger than all the other relevant frequencies, this expression becomes

$$\langle \delta\dot{\varphi}(t) \delta\dot{\varphi}(t') \rangle = D \delta(t-t'), \quad (6.86)$$

which corresponds to a Markovian time evolution for the phase, $\delta\dot{\varphi}(t) = F(t)$, the random force $F(t)$ being without memory [i.e., $\langle F(t)F(t') \rangle = D \delta(t-t')$]. For a finite polarization relaxation time, one does not get Markovian behavior for the phase (Scully, Süssman, and

Benkert, 1988; Scully, Zubairy, and Wódkiewicz, 1988; Benkert, Scully, Rangwala, and Schleich, 1990; Benkert, Scully, and Süssman, 1990): the random force $F(t)$ then acquires a memory, with a characteristic time $\tau = (\gamma/2 + \Gamma)^{-1}$. This is the time it takes for a photon to be spontaneously emitted in the coupled atom-field system. A time interval $t < \tau$ is too short to conclude a spontaneous-emission event—this is the root of the non-Markovian behavior.

Integrating Eq. (6.84) twice in time, gives

$$\begin{aligned} \langle \delta\varphi^2(t) \rangle &= \int_0^t dt' \int_0^{t'} dt'' \langle \delta\dot{\varphi}(t') \delta\dot{\varphi}(t'') \rangle \\ &= D \left[|t| + \frac{e^{-(\gamma/2 + \Gamma)|t|} - 1}{\gamma/2 + \Gamma} \right]. \end{aligned} \quad (6.87)$$

For times large compared to the memory time τ , dispersion grows linearly with time, characterizing a diffusion process, with diffusion coefficient D . On the other hand, if $t > 0$ is small compared to the memory time, one may expand the exponential in Eq. (6.87), finding then a quadratic dependence on time:

$$\langle \delta\varphi^2(t) \rangle \approx Dt \left(\frac{1}{2} \frac{t}{\tau} \right) \ll Dt. \quad (6.88)$$

Therefore for short times, phase noise is reduced by a factor $t/2\tau \ll 1$ with respect to the usual expression; the phase diffusion is limited by the fact that there is too little time to conclude a spontaneous-emission process (Scully, Süssman, and Benkert, 1988).

F. Laser linewidth

The power spectrum of the field inside the cavity is again given by the Wiener-Khinchine theorem (Lax, 1968b; Louisell, 1973):

$$\langle \mathcal{A}^2 \rangle_\Omega = \int_{-\infty}^{+\infty} dt e^{i\Omega t} \langle \mathcal{A}^*(t) \mathcal{A}(0) \rangle. \quad (6.89)$$

Well above threshold, one may neglect the amplitude fluctuations, and write (restoring free evolution of the field for the sake of clarity)

$$\mathcal{A}(t) \approx \mathcal{A}_0 e^{-i\omega t} e^{i(\varphi_0 + \delta\varphi)}, \quad (6.90)$$

where φ_0 is the steady-state value of the field phase, so that the power spectrum may be written as

$$\langle \mathcal{A}^2 \rangle_\Omega \approx I_0 \int_{-\infty}^{+\infty} dt e^{i(\Omega - \omega)t} \langle e^{-i[\delta\varphi(t) - \delta\varphi(0)]} \rangle. \quad (6.91)$$

Since the phase fluctuations are proportional to δY , the statistical distribution for $\delta\phi$ has the same nature as the one for δY . On the other hand δY , together with δX and the atomic fluctuations, depends linearly on the fluctuation forces. Thus, if these forces are assumed to be Gaussian (which is consistent with the fact that they are the sum of a large number of microscopic fluctuation forces), the same should be true for the field and atomic fluctuations, since linear combinations of Gaussian variables are also Gaussian (Risken, 1984). Therefore one

may assume that the phase fluctuations follow a Gaussian process, so that the corresponding statistical distribution is completely determined by its second-order moments. It follows in particular that

$$\langle e^{i[\delta\varphi(t) - \delta\varphi(0)]} \rangle = e^{-1/2\langle \delta\varphi^2(t) \rangle}. \quad (6.92)$$

Inserting this relation into Eq. (6.91), and using Eq. (6.87), one arrives at

$$(\mathcal{A}^2)_\Omega = 2I_0 \exp\left[\frac{D}{2(\gamma/2 + \Gamma)}\right] \sum_{m=0}^{\infty} \frac{1}{m!} \left[-\frac{D}{2(\gamma/2 + \Gamma)}\right]^m \times \frac{D/2 + (\gamma/2 + \Gamma)m}{(\omega - \Omega)^2 + [D/2 + (\gamma/2 + \Gamma)m]^2}. \quad (6.93)$$

The usual expression, due to Schawlow and Townes (Schawlow and Townes, 1958), is recovered when $\Gamma \rightarrow \infty$. In this case the only surviving term in the above sum is the one corresponding to $m=0$, and one has

$$(\mathcal{A}^2)_\Omega = 2I_0 \frac{D_{ST}/2}{(\omega - \Omega)^2 + (D_{ST}/2)^2}. \quad (6.94)$$

Therefore, when the polarization follows the field adiabatically, the power spectrum of the intracavity field is Lorentzian, with width given by the Schawlow-Townes diffusion coefficient. From Eqs. (6.82) and (6.94), one sees that the linewidth decreases as the steady-state intensity increases, which is a consequence of the dominance of stimulated processes over spontaneous ones, as the laser operates farther and farther above threshold.

The spectrum in the general case is shown in Fig. 16, where it is plotted as a function of the dimensionless frequency $(\omega - \Omega)/(D_{ST}/2)$. It depends on two dimensionless parameters, D_{ST}/γ and $2\Gamma/\gamma$. Since the first parameter is usually very small, the sum converges very quickly, and may be approximated by the first term with $m=0$ and diffusion coefficient D . Figure 16 displays the reduction of the linewidth as the polarization lifetime increases. This effect, which has been known for quite a long time (Lax, 1966b; Haken, 1970), has only recently been subjected to experimental test (Kuppens *et al.*, 1994).

G. Spectra of the output field

The above results refer to the intracavity field. Usually, one is interested in the output field. The relation between the fields inside and outside the cavity was first discussed by Collett and Gardiner (1984). Based on this analysis, useful expressions have been obtained for the spectra of the output fields (Caves and Schumaker, 1985; Collett and Walls, 1985; Gardiner and Collett, 1985; Schumaker and Caves, 1985; Gardiner, 1991; Walls and Milburn, 1994).

The main results may be summarized as follows. As shown in Fig. 17, the output field results from two contributions: the internal field, transmitted through the coupling mirror, and the vacuum field incident on the same mirror. Assuming that losses in the laser are negligible, so that the only source of field decay is transmission through the mirror (assumed to be very small), the output field may be expressed in the following way (Gardiner and Collett, 1985):

$$\hat{b}_{\text{out}}(t) = \hat{b}_{\text{in}}(t) + \sqrt{\gamma} \hat{a}(t), \quad (6.95)$$

where $\hat{b}_{\text{out}}(t)$, $\hat{b}_{\text{in}}(t)$, and $\hat{a}(t)$ are the annihilation operators corresponding to the output field, input vacuum, and intracavity field, respectively (all of them expressed in the Heisenberg picture). Note that the relative sign between the transmitted and reflected field on the right-hand side of Eq. (6.95) agrees with the choice made in Eq. (2.50b). Equation (6.95), which can be derived from a reservoir theory with the cavity mode coupled to a continuum of external modes (Gardiner, 1991), corresponds to the Lehmann-Symanzik-Zimmermann formulation of quantum field theory (Lehmann *et al.*, 1955), the “out” and “in” fields being asymptotic noninteracting Heisenberg fields.

From Eq. (6.95) one is able to relate the second-order correlation functions of the fields inside and outside the cavity; indeed,

$$\langle \hat{b}_{\text{out}}^\dagger(t) \hat{b}_{\text{out}}(t') \rangle = \langle [\sqrt{\gamma} \hat{a}^\dagger(t) + \hat{b}_{\text{in}}^\dagger(t)] \times [\sqrt{\gamma} \hat{a}(t') + \hat{b}_{\text{in}}(t')] \rangle. \quad (6.96)$$

If the initial state of the field is the vacuum, then all terms in the above equation that have an operator \hat{b}_{in} to the right or an operator $\hat{b}_{\text{in}}^\dagger$ to the left give zero contribution, so that

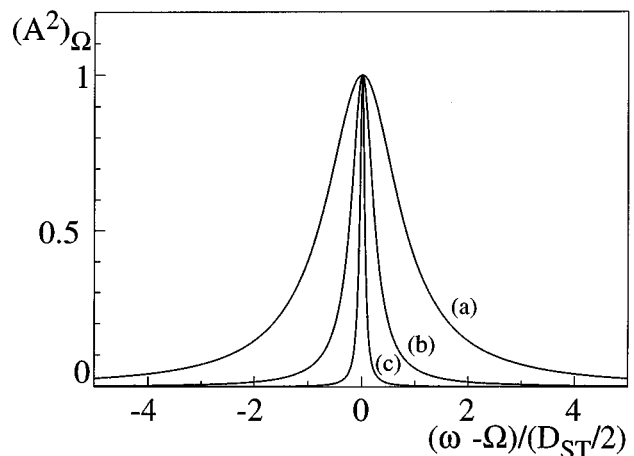


FIG. 16. Normalized power spectrum for a laser. For the three curves one has $D_{ST}/\gamma = 10^{-10}$. (a) $2\Gamma/\gamma = 10$, the Schawlow-Townes limit; (b) $2\Gamma/\gamma = 1$; and (c) $2\Gamma/\gamma = 0.3$ (long-lived atomic polarization). From Kolobov *et al.* (1993).

$$\langle \hat{b}_{\text{out}}^\dagger(t) \hat{b}_{\text{out}}(t') \rangle = \gamma \langle \hat{a}^\dagger(t) \hat{a}(t') \rangle. \quad (6.97)$$

The above argument does not, however, allow the calculation of $\langle \hat{b}_{\text{out}}(t) \hat{b}_{\text{out}}(t') \rangle$, since the analogous procedure for this quantity will leave an operator \hat{b}_{in} to the left. One needs a further ingredient, derived from a causality condition: the operator $\hat{a}(t')$ is independent of $\hat{b}_{\text{in}}(t)$ for $t > t'$. Therefore one can write

$$[\hat{a}(t'), \hat{b}_{\text{in}}(t)] = 0, \quad t > t'. \quad (6.98)$$

Assuming that $t > t'$, one has

$$\begin{aligned} \langle \hat{b}_{\text{out}}(t) \hat{b}_{\text{out}}(t') \rangle &= \langle [\sqrt{\gamma} \hat{a}(t) + \hat{b}_{\text{in}}(t)] [\sqrt{\gamma} \hat{a}(t') + \hat{b}_{\text{in}}(t')] \rangle \\ &= \gamma \langle \hat{a}(t) \hat{a}(t') \rangle. \end{aligned} \quad (6.99)$$

On the other hand, for $t < t'$ one can use the commutation relation $[\hat{b}_{\text{out}}(t), \hat{b}_{\text{out}}(t')] = 0$, which derives from the fact that \hat{b}_{out} can be expressed in terms of the free-field operators corresponding to the modes of the field outside the cavity (for details, see Gardiner, 1991), to put the product of out operators in time-ordered form, getting

$$\langle \hat{b}_{\text{out}}(t) \hat{b}_{\text{out}}(t') \rangle = \gamma \langle T[\hat{a}(t) \hat{a}(t')] \rangle, \quad (6.100)$$

where T is the time-ordering operator

$$T[O(t_1)O(t_2)] = O(t_>)O(t_<), \quad (6.101)$$

and $t_>(t_<)$ is the largest (smallest) time.

These arguments can be generalized to an arbitrary normal-ordered product of field operators (Gardiner and Collett, 1985):

$$\begin{aligned} \langle b_{\text{out}}^\dagger(t_1) \dots b_{\text{out}}^\dagger(t_n) b_{\text{out}}(t_{n+1}) \dots b_{\text{out}}(t_m) \rangle \\ = \gamma^{m/2} \langle \tilde{T}[a^\dagger(t_1) \dots a^\dagger(t_n)] T[a(t_{n+1}) \dots a(t_m)] \rangle, \end{aligned} \quad (6.102)$$

where \tilde{T} is the time-antiordering operator.

If $\hat{b}_{\text{out}}^\dagger$ and \hat{b}_{out} are not in normal order, one should first reorder them, using the commutation relations

$$[\hat{b}_{\text{out}}(t), \hat{b}_{\text{out}}^\dagger(t')] = \delta(t - t'). \quad (6.103)$$

These results will now be used to derive the spectra of quadrature fluctuations.

1. Quadrature spectra

The spectrum of fluctuations corresponding to the quadrature

$$X_\theta = \hat{b}_{\text{out}}(t) e^{-i\theta} + \hat{b}_{\text{out}}^\dagger(t) e^{i\theta} \quad (6.104)$$

is again given by the Wiener-Khinchine theorem

$$\begin{aligned} V(\theta, \Omega) &= \int_{-\infty}^{+\infty} d\tau e^{i\Omega\tau} \langle [X_\theta(t+\tau) - \langle X_\theta(t+\tau) \rangle] \\ &\quad \times [X_\theta(t) - \langle X_\theta(t) \rangle] \rangle \\ &= \int_{-\infty}^{+\infty} d\tau e^{i\Omega\tau} \langle X_\theta(t+\tau), X_\theta(t) \rangle, \end{aligned} \quad (6.105)$$

where $\langle X, Y \rangle = \langle XY \rangle - \langle X \rangle \langle Y \rangle$.

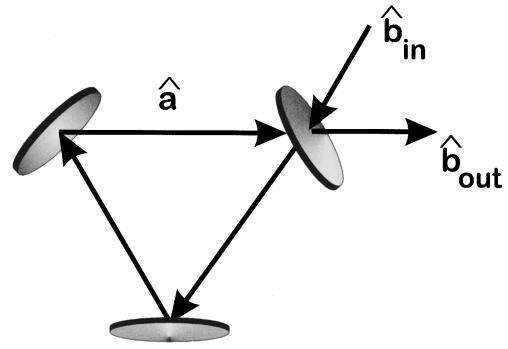


FIG. 17. Input, internal, and output fields.

There is an important conceptual difference between this spectrum and the one previously defined in terms of field amplitudes: they refer to different measurement procedures. The quadrature spectrum corresponds to a homodyne detection, while the spectrum (6.89) refers to a direct photodetection measurement of the field (Glauber, 1963a, 1965).

Note that (6.104) differs from the definitions (2.3) by a factor 1/2, which is suppressed here for convenience (this factor is absorbed by the normalization of the spectrum). Inserting (6.104) into (6.105), one finds

$$\begin{aligned} V(\theta, \Omega) &= \int_{-\infty}^{\infty} d\tau e^{i\Omega\tau} \langle [\hat{b}_{\text{out}}(t+\tau), \hat{b}_{\text{out}}^\dagger(t)] \\ &\quad + \langle \hat{b}_{\text{out}}^\dagger(t+\tau), \hat{b}_{\text{out}}(t) \rangle + \langle \hat{b}_{\text{out}}(t+\tau), \hat{b}_{\text{out}}(t) \rangle \\ &\quad \times e^{-2i\theta} + \langle \hat{b}_{\text{out}}^\dagger(t+\tau), \hat{b}_{\text{out}}^\dagger(t) \rangle e^{2i\theta}]. \end{aligned} \quad (6.106)$$

For a stationary field this quantity is independent of time, so that one may replace for instance $\langle \hat{b}_{\text{out}}(t+\tau), \hat{b}_{\text{out}}(t) \rangle$ by $\langle \hat{b}_{\text{out}}(\tau), \hat{b}_{\text{out}}(0) \rangle$.

Using Eq. (6.103), one may rewrite the first term on the right-hand side of Eq. (6.106) in normal order:

$$\begin{aligned} V(\theta, \Omega) &= 1 + \int_{-\infty}^{\infty} d\tau e^{i\Omega\tau} \langle [\hat{b}_{\text{out}}^\dagger(0), \hat{b}_{\text{out}}(\tau)] \\ &\quad + \langle \hat{b}_{\text{out}}^\dagger(\tau), \hat{b}_{\text{out}}(0) \rangle \\ &\quad + \langle \hat{b}_{\text{out}}(\tau), \hat{b}_{\text{out}}(0) \rangle e^{-2i\theta} \\ &\quad + \langle \hat{b}_{\text{out}}^\dagger(\tau), \hat{b}_{\text{out}}^\dagger(0) \rangle e^{2i\theta}]. \end{aligned} \quad (6.107)$$

The first term on the right-hand side of the above expression comes from the commutator between the bosonic operators of the output field. It gives rise to a constant contribution to the spectrum, analogous to the one found in Eq. (6.71), and corresponding therefore to shot noise. One can now apply to Eq. (6.107) the results of the previous section, rewriting the correlation functions of the output field in terms of those of the intracavity field. Furthermore, since these correlation functions are normal-ordered, they may be replaced by averages of the c numbers corresponding to the operators, so that

$$\begin{aligned}
V(\theta, \Omega) &= 1 + \gamma \int_{-\infty}^{\infty} d\tau e^{i\Omega\tau} [\langle \mathcal{A}^*(0), \mathcal{A}(\tau) \rangle + \langle \mathcal{A}^*(\tau), \mathcal{A}(0) \rangle + \langle \mathcal{A}(\tau), \mathcal{A}(0) \rangle e^{-2i\theta} + \langle \mathcal{A}^*(\tau), \mathcal{A}^*(0) \rangle e^{2i\theta}] \\
&= 1 + \gamma \int_{-\infty}^{\infty} d\tau e^{i\Omega\tau} [\langle \delta \mathcal{A}^*(0) \delta \mathcal{A}(\tau) \rangle + \langle \delta \mathcal{A}^*(\tau) \delta \mathcal{A}(0) \rangle + \langle \delta \mathcal{A}(\tau) \delta \mathcal{A}(0) \rangle e^{-2i\theta} + \langle \delta \mathcal{A}^*(\tau) \delta \mathcal{A}^*(0) \rangle e^{2i\theta}].
\end{aligned} \tag{6.108}$$

One should note that, for a coherent state, the fluctuations $\delta \mathcal{A}$ and $\delta \mathcal{A}^*$ vanish, since coherent states are eigenstates of the annihilation operator. We have then $V(\theta, \Omega) = 1$. The spectrum corresponding to a coherent state reduces to the shot-noise term. Therefore, $V(\theta, \Omega) < 1$ characterizes the situation in which one has squeezing, that is, quantum-noise reduction in the quadrature θ relative to the value for a coherent state. Complete noise reduction at some frequency Ω occurs when $V(\theta, \Omega) = 0$.

The above spectrum may be reexpressed in terms of the phase and amplitude quadratures, defined by Eq. (6.65):

$$\begin{aligned}
V(\theta, \Omega) &= 1 + 4\gamma \int_{-\infty}^{\infty} d\tau e^{i\Omega\tau} \{ \langle \delta X(\tau) \delta X(0) \rangle \cos^2 \theta \\
&\quad + \langle \delta Y(\tau) \delta Y(0) \rangle \sin^2 \theta + [\langle \delta X(\tau) \delta Y(0) \rangle \\
&\quad + \langle \delta Y(\tau) \delta X(0) \rangle] \cos \theta \sin \theta \}.
\end{aligned} \tag{6.109}$$

It may also be reexpressed, using (6.69), in terms of the Fourier components of $\delta X(t)$ and $\delta Y(t)$ given by (6.62):

$$\begin{aligned}
V(\theta, \Omega) &= 1 + 4\gamma [(\delta X^2)_{\Omega} \cos^2 \theta + (\delta Y^2)_{\Omega} \sin^2 \theta \\
&\quad - 2(\delta X \delta Y)_{\Omega} \cos \theta \sin \theta],
\end{aligned} \tag{6.110}$$

where $(\delta X \delta Y)_{\Omega}$ is defined by $\langle \delta X(\Omega) \delta Y(\Omega') \rangle = (\delta X \delta Y)_{\Omega} \delta(\Omega + \Omega')$.

The spectrum of amplitude fluctuations is obtained from the above equation by setting $\theta = 0$, and $\theta = \pi/2$ gives the spectrum of phase fluctuations. For θ between these two angles, Eq. (6.110) corresponds to the spectrum of fluctuations of an arbitrary quadrature. It is easy to show that the greatest quantum-noise reduction corresponds to

$$\cos 2\theta = -\frac{\text{Re}S(\Omega)}{|S(\Omega)|}, \quad \sin 2\theta = -\frac{\text{Im}S(\Omega)}{|S(\Omega)|},$$

where $S(\Omega) = (\delta X^2)_{\Omega} - (\delta Y^2)_{\Omega} + 2i(\delta X \delta Y)_{\Omega}$. Since $(\delta X \delta Y)_{\Omega}$ is zero (due to the resonance condition, and not in general), the greatest quantum-noise reduction occurs when $\theta = 0$, that is, for the amplitude quadrature, for which

$$V(\Omega) \equiv V_A(\Omega) = 1 + 4\gamma (\delta X^2)_{\Omega}. \tag{6.111}$$

This expression, combined with Eq. (6.70a), yields the spectrum of amplitude fluctuations for any relative magnitude of the atomic and field relaxation constants. Re-

sults obtained from this expression for different types of laser families are discussed in the next section.

2. Quantum-noise compression

A detailed study of Eq. (6.111) was made by Kolobov *et al.* (1993). In this review only the more interesting cases, from the point of view of noise reduction, are discussed. In the following we set $\Gamma'_a = 0$, and define the dimensionless parameters

$$\begin{aligned}
a &\equiv \Gamma_a / \gamma, & b &\equiv \Gamma_b / \gamma, \\
c &\equiv \Gamma / \gamma, & r &\equiv R / R_T.
\end{aligned} \tag{6.112}$$

Figure 18 displays the normalized spectrum of the field for a laser belonging to the first family ($a, b, c \gg 1$), for $p = 1$ (regular pumping), and for several values of the normalized pumping parameter r , with $a \ll b$. One should note the pronounced noise reduction for zero frequency (that is, at resonance). This is the counterpart, in the frequency spectrum, of the reduction in photon-number noise found before. Indeed, the photon-number dispersion and the output-amplitude fluctuation spectrum can be related through Eqs. (6.74) and (6.111), so that

$$\langle \Delta n^2 \rangle = \langle n \rangle + \frac{1}{2\pi} \mathcal{A}_0^2 \int_{-\infty}^{+\infty} d\Omega \frac{1}{\gamma} [V_A(\Omega) - 1]. \tag{6.113}$$

From this equation, it is clear that $\langle \Delta n^2 \rangle < \langle n \rangle$ only if $V_A(\Omega) < 1$ in some frequency region.

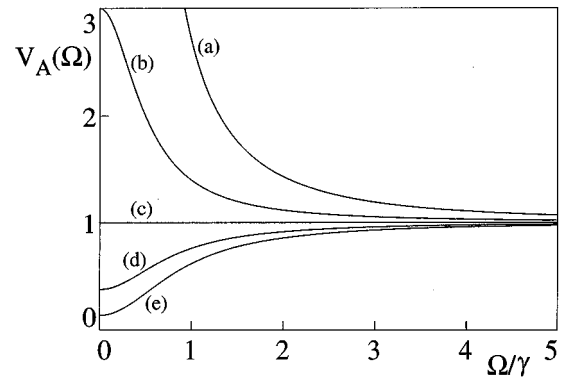


FIG. 18. Normalized spectrum of amplitude fluctuations for a laser of the first class, for several values of the pumping parameter r . (a) $r = 1$; (b) $r = 2$; (c) $r = 3$; (d) $r = 5$; and (e) $r = 10$. In all cases $p = 1$, corresponding to regular pumping, and $\Gamma_a \ll \Gamma_b$. From Kolobov *et al.* (1993).

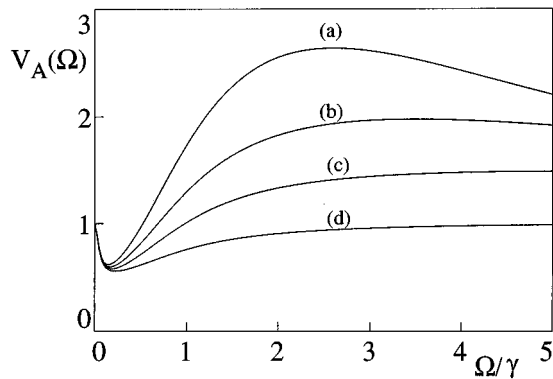


FIG. 19. Normalized spectrum of amplitude fluctuations for a laser of the third class, with Poissonian pumping, for several values of the pumping parameter r . (a) $r=3 \times 10^3$; (b) $r=5 \times 10^3$; (c) $r=10^4$; (d) $r=10^6$. In all cases $\Gamma_a/\gamma=0.001$, $\Gamma_b/\gamma=0.1$. From Kolobov *et al.* (1993).

For a laser working well above threshold, $r \gg 1$, it is possible to eliminate completely the noise at zero frequency. The same behavior is verified for other laser families (Kolobov *et al.*, 1993): pumping regularization can completely eliminate noise at zero frequency.

Interesting results are also obtained for Poissonian pumping. In this case, one also gets amplitude squeezing for sufficiently intense pumping. This is displayed in Fig. 19, which refers to the third class of lasers defined at the beginning of this section ($c \gg 1 \gg a, b$). One should note however that the range of pumping required for meaningful squeezing is extremely high, and nonrealistic. The injection of an external signal from another laser may, however, reduce these values considerably (Fontenelle and Davidovich, 1995).

VII. GENERATION OF FOCK STATES THROUGH QUANTUM NONDEMOLITION MEASUREMENTS

The utilization of a QND method to produce Fock states in cavities was discussed by Brune *et al.* (1990, 1992). The proposed experimental scheme is sketched in Fig. 20. It consists of a high- Q superconducting cavity containing the electromagnetic field to be reduced, and

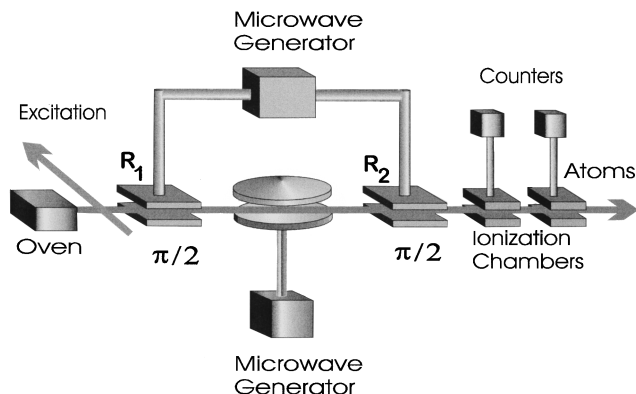


FIG. 20. Quantum nondemolition measurement in cavity quantum electrodynamics.

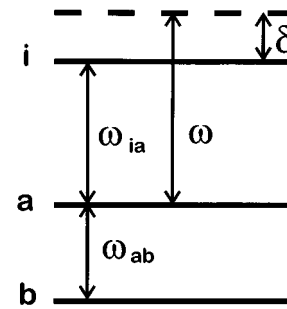


FIG. 21. Relevant atomic levels for the QND measurement.

placed between two other cavities R_1 and R_2 . A beam of excited atoms interacts resonantly with the field in R_1 and R_2 , and dispersively with the field in the superconducting cavity. Before crossing the first cavity R_1 , the atoms are prepared in a circular Rydberg state, that is, a state with high principal quantum number and maximum angular momentum, so as to increase its decay time and increase the atom-field coupling (Hulet and Kleppner, 1983; Nussenzveig *et al.*, 1991). This state will be denoted by $|a\rangle$ in the following. The relevant atomic levels are shown in Fig. 21. Levels i and b have the same parity, opposite to that of level a . The cavity mode, with angular frequency ω , is slightly detuned from the $a \rightarrow i$ transition, which corresponds to the angular frequency ω_{ia} . The field in R_1 induces resonant transitions between $|a\rangle$ and the lower-lying Rydberg state $|b\rangle$. One may assume that the interaction time and the intensity of the field in R_1 (which is essentially classical, as is the field in R_2) are such that the state of the atom, after it leaves R_1 , is $(|a\rangle + |b\rangle)/\sqrt{2}$ (one says then that the atom suffers a $\pi/2$ pulse). The atom then enters the superconducting cavity, where due to the dispersive coupling between the field and the transition $a \rightarrow i$, the state $|a\rangle$ suffers a second-order Stark level shift, given by $-\hbar\Omega^2 n/\delta$, if the field is in a Fock state $|n\rangle$, where Ω is the vacuum Rabi coupling between the atomic dipole on the $a \rightarrow i$ transition and the cavity mode, and $\delta = \omega - |\omega_{ab}|$ is the frequency mismatch (it is assumed here for simplicity that the Rabi coupling is constant throughout the cavity). It is assumed that δ is sufficiently large that $\Omega^2 n/\delta^2 \ll 1$, and at the same time small compared to the difference in frequency between the $a \rightarrow i$ transition and all the other transitions in the Rydberg-atom spectrum (especially the $a \rightarrow b$ one). In this case, only levels a and i are appreciably affected by the non-resonant atom-field coupling, which leaves the level b unperturbed.

If the field in the high- Q cavity is initially in the state $|\psi_0\rangle = \sum_n c_n |n\rangle$, then the state of the atom-field system right after the atom exits that cavity is

$$|\Psi_1\rangle = \frac{1}{\sqrt{2}} \left(|a\rangle \sum_n c_n e^{-in\epsilon} |n\rangle + |b\rangle \sum_n c_n |n\rangle \right), \quad (7.1)$$

where $\epsilon = (\Omega^2/\delta)t_{\text{int}}$ is the one-photon phase shift that originates from the Stark energy shift. The atom then crosses the cavity R_2 , where it interacts with another

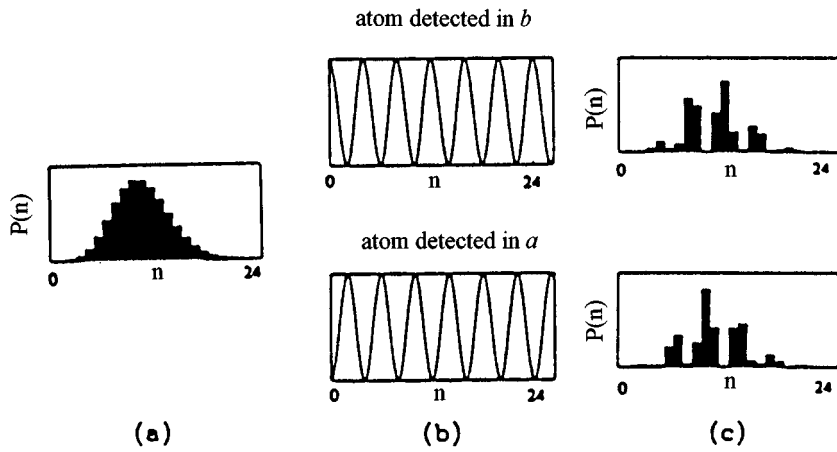


FIG. 22. Modulation of the original photon-number distribution after detection of the first atom. The initial distribution, displayed in (a), is Poissonian with $\bar{n}=10$. It is multiplied by the oscillating fringe function $\sin^2(n\epsilon/2)$, if the atom is detected in the state a , or $\cos^2(n\epsilon/2)$, if in state b . These functions are represented as a function of n in (b). In the resulting distributions (c), photon numbers closest to the “dark fringes” have been greatly reduced. From Brune *et al.* (1992).

$\pi/2$ pulse taking takes $|a\rangle$ again into $(|a\rangle+|b\rangle)/\sqrt{2}$, and $|b\rangle$ into $(-|a\rangle+|b\rangle)/\sqrt{2}$. The correlated atom-field state becomes

$$|\Psi_2\rangle = \frac{1}{2} \left[|a\rangle \sum_n (e^{-in\epsilon} - 1) c_n |n\rangle + |b\rangle \sum_n (e^{in\epsilon} + 1) c_n |n\rangle \right]. \quad (7.2)$$

After crossing R_2 , the atom is detected by letting it go through a set of ionization plates, the first one containing an electric field that ionizes the atom if it is in state $|a\rangle$, while the second, with a stronger electric field, ionizes the atom if it is in state $|b\rangle$. If the atom is found in the state $|a\rangle$, then the atom-field system is described by the state

$$|\Psi_a\rangle = \frac{\sum_n \sin(n\epsilon/2) e^{-in\epsilon/2} c_n |n\rangle}{[\sum_n |c_n|^2 \sin^2(n\epsilon/2)]^{1/2}} |a\rangle. \quad (7.3)$$

A similar expression applies if the atom is detected in state $|b\rangle$. Equation (7.3) shows that detection of the atom changes the field populations, even though the atom has not exchanged photons with the field (since the interaction is dispersive). The photon-number probability distribution previous to the passage of the atom is multiplied, after the detection, by a modulation factor that oscillates with n :

$$P_1^{(a)}(n) = \frac{\sin^2(n\epsilon/2)}{\sum_n P_0(n) \sin^2(n\epsilon/2)} P_0(n). \quad (7.4)$$

This modulation is displayed in Fig. 22. Depending on the choice of ϵ , detection of the first atom may deplete several populations. For instance, for $\epsilon=\pi$, one has $P_1^{(a)}(n)=0$ for all even values of n .

Detection of successive atoms, with changing velocities and therefore different values of ϵ , will deplete other populations, until one is left finally with a single Fock state, which is stable under the transformation (7.4). Figure 23 illustrates a typical QND sequence.

VIII. TWIN-PHOTON PROCESSES

As discussed in Sec. III.A, twin-photon beams have led to striking results for quantum-noise reduction. In

parametric downconversion, the essential physical feature for getting noise reduction in the difference of intensities is simultaneous twin-photon generation. One would thus expect the result to be valid for any oscillator sustained by a genuine nondegenerate two-photon process (as opposed to cascade transitions, in which an intermediate state gets populated, and there is a delay in the emission of the second photon).

In fact, with only the assumption that the intensity difference operator $I_1 - I_2$ is conserved by the parametric interaction, i.e.,

$$[H, I_1 - I_2] = 0, \quad (8.1)$$

Reynaud (1987) derived the noise spectrum for the difference in the transmitted intensities for the Optical Parametric Oscillator, in the case where the output mirror is the only source of the decay rates of signal and idler beams, assumed to be equal (“balanced single-

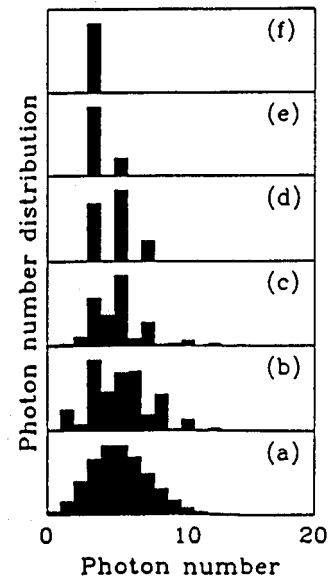


FIG. 23. Typical QND sequence. The initial state is coherent with $\bar{n}=5$, and its photon-number distribution is displayed in (a). Plots (b)–(f) correspond to the detection of 1, 3, 6, 10, and 15 atoms, respectively. In this realization, the field collapses, after detection of 15 atoms, into the $n=3$ Fock state. From Brune *et al.* (1992).

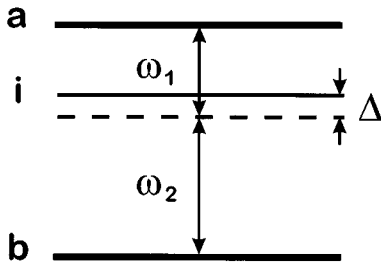


FIG. 24. Relevant level scheme for a two-photon laser.

ported" case). Using the same single property, Graham (1984) obtained general (and exact) identities for the steady-state intracavity field fluctuations generated in a parametric process.

A. Twin-beam effects in two-photon oscillators

Parametric downconversion is but one of the processes that lead to twin beams. Twin photons can also be generated by two-photon masers or lasers. Although proposed a long time ago (Sorokin and Braslau, 1964; Prokhorov, 1965), experimental demonstration of these devices has occurred only recently (Brune *et al.*, 1987; Gauthier *et al.*, 1992). The main difficulties in the realization of these systems are the exceedingly small gain on two-photon transitions, and the existence of very strong competing nonlinear processes, like multiple-wave mixing and the stimulated Raman effect. However, for two-photon lasers, Eq. (8.1) does not hold anymore, due to the presence of a relay level which mediates the transition between the excited and final atomic states. The relevant level scheme is shown in Fig. 24. The intermediate level is detuned so as to avoid a two-photon cascade process, whereas the upper and lower levels are resonantly coupled to the cavity. The corresponding Hamiltonian is given by

$$H = H_{at} + H_F + (\hbar \Omega_{ai} a_1 |a\rangle \langle i| + \hbar \Omega_{ib} a_2 |i\rangle \langle b| + \text{H.c.}), \quad (8.2)$$

where H_{at} , H_F are the Hamiltonians for the three-level atom and for the signal and idler modes, and Ω_{ai} , Ω_{ib} are the $a \rightarrow i$ and $i \rightarrow b$ atom-field couplings, in units of frequency. In this equation, we have neglected the couplings between the upper mode (of frequency ω_1) and the $i \rightarrow b$ transition, and between the lower mode (of frequency ω_2) and the $a \rightarrow i$ transition, corresponding to the limit $|\omega_2 - \omega_1| \gg \Delta$, where $\Delta = |\omega_{ib} - \omega|$ is the detuning.

The Hamiltonian (8.2) does not commute with $n_1 - n_2$ even in the large-detuning limit. In fact, the twin-photon effect appears here as the result of the association of the large- Δ atom-field interaction *and* the atomic excitation scheme, which must not provide atoms in the intermediate state $|i\rangle$.

A generalization of Eq. (8.1) was suggested by Maia Neto and Davidovich (1992), who derived expressions for the noise reduction in the intensity difference, for two-photon lasers. The main assumption is that the fluctuation in the difference between signal and idler pho-

ton numbers, $n_1 - n_2$, satisfies the equation

$$\frac{d}{dt} \langle (n_2 - n_1)^k \rangle |_{\text{gain}=0} = 0, \quad k=1,2, \quad (8.3)$$

that is, the gain process is exclusively based on simultaneous generation of pairs of signal and idler photons. Even though (8.3) may be trivially derived from (8.1), it applies nevertheless to systems for which (8.1) is not valid. One example is the two-photon laser with a relay level, described by the above Hamiltonian.

The field master equation for the two-photon laser cannot be obtained directly from the atom-field Hamiltonian, Eq. (8.2). Instead, one needs to consider a Hamiltonian describing the complete dynamics involved in the problem, including the excitation. Alternatively, one may calculate the change in the reduced density matrix of the field due to one atom, and then write down the master equation by summing up the contributions of the successive excited atoms introduced into the laser cavity, as done in Sec. V. In this case, it is easily seen that Eq. (8.3) holds if and only if the gain part of the master equation has the form

$$\begin{aligned} \frac{dP_{n_1 n_2}}{dt} |_{\text{gain}} = & -A(n_1 n_2) P_{n_1 n_2} \\ & + A(n_1 - 1, n_2 - 1) P_{n_1 - 1, n_2 - 1}, \end{aligned} \quad (8.4)$$

where $A(n_1 n_2)$ is any function. For a two-photon oscillator, it can be shown that this is equivalent to the condition that the intermediate-level detuning is much larger than the power-broadened linewidth of the atomic transitions (Maia Neto and Davidovich, 1992).

If Eq. (8.3) holds, then the following result can be shown. Let $P_{n_1 n_2} = \langle n_1 n_2 | \rho(t) | n_1 n_2 \rangle$ be the probability of finding n_1 and n_2 photons in modes 1 and 2, respectively. Here $\rho(t)$ is, as before, the reduced density operator for the field. Taking dissipation into account in the usual way, this probability distribution satisfies the equation

$$\begin{aligned} \frac{dP_{n_1 n_2}(t)}{dt} = & \frac{dP_{n_1 n_2}}{dt} |_{\text{gain}} - (\gamma_1 n_1 + \gamma_2 n_2) P_{n_1 n_2} \\ & + \gamma_1 (n_1 + 1) P_{n_1 + 1, n_2} + \gamma_2 (n_2 + 1) P_{n_1, n_2 + 1}. \end{aligned} \quad (8.5)$$

From Eqs. (8.3) and (8.5), one finds

$$\frac{d}{dt} \langle n_2 - n_1 \rangle = -\gamma_2 \langle n_2 \rangle + \gamma_1 \langle n_1 \rangle, \quad (8.6a)$$

$$\begin{aligned} \frac{d}{dt} \langle (n_2 - n_1)^2 \rangle = & \gamma_1 \langle n_1 \rangle + \gamma_2 \langle n_2 \rangle + 2\gamma_1 \langle n_1 (n_2 - n_1) \rangle \\ & - 2\gamma_2 \langle n_2 (n_2 - n_1) \rangle. \end{aligned} \quad (8.6b)$$

In the case of equal cavity decay rates (balanced case), the dynamics of the average difference between photon numbers is independent of the sum (and thus of the gain process), as may be seen directly from (8.6). The intracavity steady-state moments are, in this case, given by

$$\langle n_1 \rangle = \langle n_2 \rangle, \quad (8.7)$$

$$\langle (n_2 - n_1)^2 \rangle = \frac{\langle n_1 + n_2 \rangle}{2}. \quad (8.8)$$

On the other hand, for a classical-field distribution, one must have

$$\langle (n_2 - n_1)^2 \rangle - \langle n_2 - n_1 \rangle^2 \geq \langle n_1 + n_2 \rangle. \quad (8.9)$$

One gets then a squeezing factor of 50% for the intracavity field in the balanced case, either above or below the threshold of oscillation.

B. Noise spectrum of the output field

The noise spectrum $S(\omega)$ of the output signal-idler intensity difference may also be obtained on quite general grounds from the condition (8.3), by applying the input-output theory of Gardiner and Collett (1985), similarly to what was done in Sec. VI.G. The discussion here is restricted to the balanced case (cavity damping times identical for both modes).

The intracavity Heisenberg boson operators $a_k(t)$ ($k=1,2$) obey the usual commutation rules

$$[a_k(t), a_{k'}(t)] = 0, \quad (8.10a)$$

$$[a_k(t), a_{k'}^\dagger(t)] = \delta_{k,k'}, \quad (8.10b)$$

but the commutators between the operators at different times involve the dynamics of the field interaction with the active medium.

The output signal and idler operators are $b_k(t)$, $k=1,2$. We choose the normalization such that the intensity operators for the transmitted signal and idler beams, given by

$$I_k = b_k^\dagger b_k, \quad (8.11)$$

yield the number of transmitted photons per unit time. As seen in Sec. VI.G, these operators obey the commutation relations

$$[b_k(t), b_{k'}(t')] = 0, \quad (8.12a)$$

$$[b_k(t), b_{k'}^\dagger(t')] = \delta_{k,k'} \delta(t-t'). \quad (8.12b)$$

The spectrum $S(\omega)$ of fluctuations in the intensity difference of the signal and idler beams is given by

$$S(\omega) = \int_{-\infty}^{+\infty} e^{i\omega t} [\langle (I_1 - I_2)(t)(I_1 - I_2)(0) \rangle - \langle I_1 - I_2 \rangle^2] dt, \quad (8.13)$$

where the average is taken over the steady-state distribution.

In order to calculate $S(\omega)$ as a function of the intracavity field, using the method developed in Sec. VI.G, one writes Eq. (8.13) in normal ordering. From Eqs. (8.12) and (8.13), one finds

$$S(\omega) = \langle I_1 + I_2 \rangle + \int_{-\infty}^{+\infty} e^{i\omega t} [\langle : (I_1 - I_2)(t)(I_1 - I_2)(0) : \rangle - \langle I_1 - I_2 \rangle^2] dt. \quad (8.14)$$

The signal and idler cavity decay rates associated with transmission through the output mirror M are here assumed to be equal, and given by γ_M , while γ is the total field decay rate ($\gamma \geq \gamma_M$), corresponding to losses from transmission through the mirrors, as well as from intracavity and mirror absorption.

From Eqs. (8.14) and (6.102), $S(\omega)$ can be expressed as a function of the intracavity field moments:

$$S(\omega) = \gamma_M (\langle n_1 \rangle + \langle n_2 \rangle) + 2 \int_0^\infty dt \cos \omega t G(t), \quad (8.15)$$

where $G(t)$ is the normally time-ordered autocorrelation function at steady state:

$$\begin{aligned} G(t) &= \gamma_M^2 \langle : [n_2(t) - n_1(t)][n_2(0) - n_1(0)] : \rangle \\ &= \gamma_M^2 \sum_{k=1,2} (-)^k \langle a_k^\dagger(0)[n_2(t) - n_1(t)]a_k(0) \rangle. \end{aligned} \quad (8.16)$$

This expression was obtained using the condition (8.7), valid in the balanced case.

The first two terms on the right-hand side of Eq. (8.15) correspond to the shot-noise contribution. It is clear that the noise spectrum will be below shot-noise level whenever the Fourier transform of $G(t)$ becomes negative.

This expression is now explicitly calculated by using the Quantum Regression Theorem (Lax, 1968a), which may be summarized in the following way. Let us consider a set of operators A_i satisfying the Langevin equations

$$\frac{dA_i(t)}{dt} = \sum_j C_{ij} A_j(t) + \lambda_i + F_i(t), \quad (8.17)$$

where the fluctuation forces $F_i(t)$ are assumed to be delta correlated, corresponding to a Markovian evolution for the operators:

$$\langle F_i(t) F_j(t') \rangle = 2D_{ij} \delta(t-t'). \quad (8.18)$$

Multiplying (8.17) by $A_k(0)$, and taking the quantum average of the resulting equations, one gets

$$\begin{aligned} \frac{d}{dt} \langle A_i(t) A_k(0) \rangle &= \sum_j C_{ij} \langle A_j(t) A_k(0) \rangle + \lambda_i \langle A_k(0) \rangle \\ &\quad + \langle F_i(t) A_k(0) \rangle. \end{aligned} \quad (8.19)$$

Now if t is positive and much larger than the correlation time of the fluctuation forces [which in (8.18) is assumed to be zero], the last term on the right-hand side of (8.19) should vanish, since the operator $A_k(0)$ should be uncorrelated with fluctuation forces at later times [in fact, formal integration of Eq. (8.17) shows that the operators $A_i(t)$ depend only on fluctuation forces in the past]. This is confirmed by a more rigorous analysis, which takes into account the finite correlation time of the Langevin forces (Cohen-Tannoudji *et al.*, 1988). The final conclusion is that the two-time correlation functions obey the equations

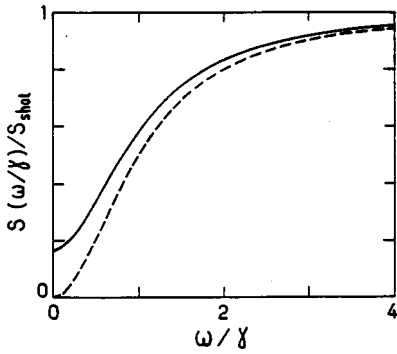


FIG. 25. Normalized spectrum of fluctuations of the intensity difference for a two-photon laser, in the balanced case. Full line: $\gamma/\gamma_M=1.2$; dashed line: $\gamma/\gamma_M=1$. From Maia Neto and Davidovich (1992).

$$\frac{d}{dt}\langle A_i(t)A_k(0)\rangle = \sum_j C_{ij}\langle A_j(t)A_k(0)\rangle + \lambda_i\langle A_k(0)\rangle, \quad (8.20)$$

which have the same structure as the equations describing the time evolution of the average values $\langle A_i(t)\rangle$:

$$\frac{d}{dt}\langle A_i(t)\rangle = \sum_j C_{ij}\langle A_j(t)\rangle + \lambda_i. \quad (8.21)$$

This result is easily generalized to products of three operators. Thus, for instance,

$$\begin{aligned} \frac{d}{dt}\langle B(t)\rangle &= \langle b(t)\rangle \Rightarrow \frac{d}{dt}\langle A(0)B(t)C(0)\rangle \\ &= \langle A(0)b(t)C(0)\rangle, \quad (t>0), \end{aligned} \quad (8.22)$$

where A , B , b , and C are operators undergoing Markovian time evolutions. It follows then from Eqs. (8.6a), (8.16), and (8.22) that

$$\frac{d}{dt}G(t) = -\gamma G(t), \quad (8.23)$$

so that

$$G(t) = G(0)e^{-\gamma t}. \quad (8.24)$$

Therefore, using the commutation relations (8.10a), one has

$$G(t) = \gamma_M^2 e^{-\gamma t} [\langle (n_2 - n_1)^2 \rangle - \langle n_1 + n_2 \rangle]. \quad (8.25)$$

From Eqs. (8.8), (8.15), (8.16), and (8.25), one finally obtains the noise spectrum:

$$S(\omega) = \gamma_M \langle n_1 + n_2 \rangle \frac{\omega^2 + \gamma^2 - \gamma\gamma_M}{\omega^2 + \gamma^2}. \quad (8.26)$$

In Fig. 25, the spectrum $S(\omega)$ is shown for $\gamma/\gamma_M=1.2$ and $\gamma/\gamma_M=1$. One should notice that $S(\omega)$ approaches the shot-noise level

$$S_{\text{shot}} = \gamma_M \langle n_1 + n_2 \rangle \quad (8.27)$$

when $\omega \gg \gamma, \gamma_M$.

There is a dip in the spectrum for $\omega < \gamma, \gamma_M$, representing the nonclassical noise reduction discussed ear-

lier. This noise reduction is degraded by any loss not caused by the output mirror M_1 . In particular, the maximum noise-reduction factor (which occurs at $\omega=0$), given by

$$\frac{S_{\text{shot}} - S(0)}{S_{\text{shot}}} = \frac{\gamma_M}{\gamma}, \quad (8.28)$$

decreases from 1 down to 0 when γ/γ_M is increased. This can be understood simply following the reasoning outlined in Sec. III.F. After a long counting time, many twin-photon pairs leave the cavity, but a fraction of them (equal to γ_M/γ in the case of ideal detectors) are not detected. Therefore, at $\omega=0$, extra losses introduce noise exactly as does a detector of quantum efficiency $\eta = \gamma_M/\gamma$.

One can see therefore that when the cavity damping times are equal, the dynamics of the intensity difference in two-photon oscillators becomes completely independent of the gain mechanism, which allows one to derive its noise spectrum in a general and exact way. This implies that such different systems as the two-photon laser and the nondegenerate optical parametric oscillator may generate output fields with identical intensity-difference noise spectra. Furthermore, the twin-photon effect in two-photon lasers is not degraded by the population of the upper resonant level and its incoherent decay. This is usually a strong source of noise, which spoils squeezing in resonant devices.

IX. CONCLUSIONS AND OUTLOOK

In this review, I have tried to show that the idea of reducing the quantum noise in light is a unifying concept, which spans several different areas of research in optics, from nonlinear optics to laser physics and cavity quantum electrodynamics. It has led to interesting refinements in the understanding of quantum noise, and to new insights into laser theory. Furthermore, it has touched fundamental questions in quantum measurement theory. What has happened since the invention of the laser amounts to a conceptual revolution. Its touchstone has been the increasing ability to master photon beams, molding them so as to produce nonclassical states of the field. Even though abiding by the Heisenberg inequalities, these states may exhibit variances smaller than those of a coherent state, either in a quadrature, in the photon number, or in the phase of the field.

Nonclassical properties of light have been observed in many different situations. Most of the observations refer to parametric processes, in which the atomic medium intervenes through a nonlinear index of refraction. In many instances, however, atomic dynamics plays an essential role, leading to the generation of sub-Poissonian light in resonant processes like atomic fluorescence, and in lasers and masers.

The richness of this subject is due not only to the variety of processes involved, but also to the strong interplay of basic and applied research. Applications of sub-Poissonian beams and quadrature-squeezed light

have been envisaged in communications, in precise interferometric measurements, and in the detection of gravitational waves. At the present moment, there remain two obstacles to the practical implementation of the results obtained in basic research. The first one is the narrow bandwidth and still-small amount of noise reduction (reduction of more than 90% is necessary for applications). The second is the complexity of the techniques involved, which require very careful control of the experimental conditions. The rapid succession of major achievements in this field does, however, inspire optimism for the actual realization of practical devices.

ACKNOWLEDGMENTS

My understanding of the subjects covered by this paper benefited a great deal from the interaction I have had with many colleagues and students. It is thus a pleasure to acknowledge the collaboration with C. Benkert, J. Bergou, C. R. Carvalho, S. M. Dutra, C. Fabre, M. T. Fontenelle, E. Giacobino, P. Goy, E. S. Guerra, M. Hillery, R. J. Horowicz, A. Z. Houry, M. I. Kolobov, P. A. Maia Neto, H. M. Nussenzveig, P. A. Nussenzveig, M. Orszag, S. Reynaud, M. O. Scully, C. Su, S.-Y. Zhu, and M. S. Zubairy. I wish to thank especially, for a long-lived and fruitful collaboration, M. Brune, S. Haroche, and J. M. Raimond, from the École Normale Supérieure, in Paris, and N. Zagury, from the Universidade Federal do Rio de Janeiro.

This research was partially supported by the Brazilian agency CNPq (Conselho Nacional de Desenvolvimento Científico e Tecnológico).

REFERENCES

- Abraham, N. A., P. Mandel, and L. M. Narducci, 1988, in *Dynamic Instabilities and Pulsations in Lasers*, edited by E. Wolf, Progress in Optics XXV (Elsevier, Amsterdam).
- Agarwal, G. S., J. A. Bergou, C. Benkert, and M. O. Scully, 1991, Phys. Rev. A **43**, 6451.
- An, K., J. J. Childs, R. R. Dasari, and M. S. Feld, 1994, Phys. Rev. Lett. **73**, 3375.
- Arecchi, F. T., 1965, Phys. Rev. Lett. **15**, 912.
- Barnett, S. M., and D. T. Pegg, 1989, J. Mod. Optics **36**, 7.
- Benkert, C., M. O. Scully, J. Bergou, L. Davidovich, M. Hillery, and M. Orszag, 1990, Phys. Rev. A **41**, 2756.
- Benkert, C., M. O. Scully, and M. Orszag, 1990, Phys. Rev. A **42**, 1487.
- Benkert, C., M. O. Scully, A. A. Rangwala, and W. Schleich, 1990, Phys. Rev. A **42**, 1503.
- Benkert, C., M. O. Scully, and G. Süssmann, 1990, Phys. Rev. A **41**, 6119.
- Bergou, J., C. Benkert, L. Davidovich, M. O. Scully, S.-Y. Zhu, and M. S. Zubairy, 1990, Phys. Rev. A **42**, 5544.
- Bergou, J., L. Davidovich, M. Orszag, C. Benkert, M. Hillery, and M. O. Scully, 1989a, Opt. Commun. **72**, 82.
- Bergou, J., L. Davidovich, M. Orszag, C. Benkert, M. Hillery, and M. O. Scully, 1989b, Phys. Rev. A **40**, 5073.
- Bergou, J., and M. Hillery, 1994, Phys. Rev. A **49**, 1214.
- Björk, G., H. Heitmann, and Y. Yamamoto, 1993, Phys. Rev. A **47**, 4451.
- Björk, G., and Y. Yamamoto, 1988, Phys. Rev. A **37**, 125.
- Bohr, N., 1928, Nature **121**, 580.
- Bondurant, R. S., and J. H. Shapiro, 1984, Phys. Rev. D **30**, 2548.
- Braginsky, V. B., and Yu. I. Vorontsov, 1974, Usp. Fiz. Nauk **114**, 41 [Sov. Phys. Usp. **12**, 644 (1975)].
- Braginsky, V. B., Yu. I. Vorontsov, and F. Ya. Khalili, 1977, Zh. Eksp. Teor. Fiz. **73**, 1340 [Sov. Phys. JETP **46**, 705 (1977)].
- Brune, M., S. Haroche, V. Lefèvre, J. M. Raimond, and N. Zagury, 1990, Phys. Rev. Lett. **65**, 976.
- Brune, M., S. Haroche, J. M. Raimond, L. Davidovich, and N. Zagury, 1992, Phys. Rev. A **45**, 5193.
- Brune, M., J. M. Raimond, P. Goy, L. Davidovich, and S. Haroche, 1987, Phys. Rev. Lett. **59**, 1899.
- Burnham, D. C., and D. L. Weinberg, 1970, Phys. Rev. Lett. **58**, 2539.
- Carmichael, H. J., 1986, Phys. Rev. A **33**, 3262.
- Carmichael, H. J., and D. Walls, 1976a, J. Phys. B **9**, L43.
- Carmichael, H. J., and D. Walls, 1976b, J. Phys. B **9**, 1199.
- Carvalho, C. R., L. Davidovich, and N. Zagury, 1989, Opt. Commun. **72**, 306.
- Castelli, F., L. A. Lugiato, and M. Vadicchino, 1988, Nuovo Cimento **10**, 183.
- Caves, C. M., 1980, Phys. Rev. Lett. **45**, 75.
- Caves, C. M., 1981, Phys. Rev. D **23**, 1693.
- Caves, C. M., 1987, Opt. Lett. **12**, 971.
- Caves, C. M., and B. L. Schumaker, 1985, Phys. Rev. A **31**, 3068.
- Caves, C. M., K. S. Thorne, R. W. D. Drever, V. D. Sandberg, and M. Zimmermann, 1980, Rev. Mod. Phys. **52**, 431.
- Chow, W. W., J. Gea-Banacloche, L. M. Pedrotti, V. E. Sanders, W. Schleich, and M. O. Scully, 1985, Rev. Mod. Phys. **57**, 61.
- Cohen-Tannoudji, C., 1977, in *Frontiers in Laser Spectroscopy*, Les Houches, Session XXVII (1975), edited by R. Balian, S. Haroche, and S. Liberman (North-Holland, Amsterdam), p. 4.
- Cohen-Tannoudji, C., J. Dupont-Roc, and G. Grynberg, 1988, *Processus d'Interaction entre Photons et Atomes* (InterEditions/Éditions du CNRS, Paris) [*Atom-Photon Interactions: Basic Processes and Applications*, Wiley, New York, 1992].
- Collett, M. J., and C. W. Gardiner, 1984, Phys. Rev. A **30**, 1386.
- Collett, M. J., and D. F. Walls, 1985, Phys. Rev. A **32**, 2887.
- Compton, A. H., 1923, Phys. Rev. **21**, 483 (1923).
- Dagenais, M., and L. Mandel, 1978, Phys. Rev. A **18**, 2217.
- Davidovich, L., J. M. Raimond, M. Brune, and S. Haroche, 1987, Phys. Rev. A **36**, 3771.
- Davidovich, L., S.-Y. Zhu, A. Z. Houry, and C. Su, 1992, Phys. Rev. A **46**, 1630.
- Debuisschert, T., S. Reynaud, A. Heidmann, E. Giacobino, and C. Fabre, 1989, Quantum Opt. **1**, 3.
- Diedrich, F., and H. Walther, 1987, Phys. Rev. Lett. **58**, 203.
- Dirac, P. A. M., 1927, Proc. Roy. Soc. A **114**, 243.
- Dorschner, T. A., H. A. Haus, M. Holz, I. W. Smith, and H. Statz, 1980, IEEE J. Quantum Electron. **16**, 1376.
- Drummond, P. D., and C. W. Gardiner, 1980, J. Phys. A **13**, 2353.
- Dutra, S. M., and L. Davidovich, 1994, Phys. Rev. A **49**, 2986.
- Einstein, A., 1905, Ann. Phys. **17**, 132.
- Einstein, A., 1906, Ann. Phys. **20**, 199.

- Einstein, A., 1909a, Phys. Z. **10**, 185.
- Einstein, A., 1909b, Phys. Z. **10**, 817.
- Einstein, A., 1917, Phys. Z. **18**, 121.
- Ezekiel, S., J. A. Cole, J. Harrison, and G. Sanders, 1978, in *Laser Inertial Rotation Sensors*, edited by S. Ezekiel and G. E. Knausenberger (*Society of Photo-Optical Instrumentation Engineers*, Bellingham, Washington), p. 68.
- Fabre, C., 1992, Phys. Rep. **219**, 215.
- Fabre, C., E. Giacobino, A. Heidmann, and S. Reynaud, 1989, J. Phys. (Paris) **50**, 1209.
- Filipowicz, P., J. Javanainen, and P. Meystre, 1986a, Phys. Rev. A **34**, 3077.
- Filipowicz, P., J. Javanainen, and P. Meystre, 1986b, J. Opt. Soc. Am. B **14**, 906.
- Fontenelle, Márcia T., and L. Davidovich, 1995, Phys. Rev. A **51**, 2560.
- Freeman, M. J., H. Wang, D. G. Steel, R. Craig, and D. R. Scifres, 1993, Opt. Lett. **18**, 379.
- Friberg, S., C. K. Hong, and L. Mandel, 1984, Phys. Rev. Lett. **54**, 2011.
- Gardiner, C. W., 1986, Phys. Rev. Lett. **56**, 1917.
- Gardiner, C. W., 1991, *Quantum Noise* (Springer, Berlin).
- Gardiner, C. W., and M. J. Collett, 1985, Phys. Rev. A **31**, 3761.
- Gardiner, C. W., A. S. Parkins, and M. J. Collett, 1987, J. Opt. Soc. Am. B **4**, 1683.
- Gauthier, D. J., Q. Wu, S. E. Morin, and T. W. Mossberg, 1992, Phys. Rev. Lett. **68**, 464.
- Glauber, R. J., 1963a, Phys. Rev. **130**, 2529.
- Glauber, R. J., 1963b, Phys. Rev. **131**, 2766.
- Glauber, R. J., 1963c, Phys. Rev. Lett. **10**, 84.
- Glauber, R. J., 1965, in *Quantum Optics and Electronics*, edited by C. de Witt, A. Blandin, and C. Cohen-Tannoudji (Gordon and Breach, New York).
- Golubev, Yu. M., and I. V. Sokolov, 1984, Zh. Eksp. Teor. Fiz. **87**, 408 [Sov. Phys. JETP **60**, 234 (1984)].
- Gordon, J. P., 1967, Phys. Rev. **161**, 367.
- Graham, R., 1984, Phys. Rev. Lett. **52**, 117.
- Grangier, P., R. E. Slusher, B. Yurke, and A. La Porta, 1987, Phys. Rev. Lett. **59**, 2153.
- Guerra, E. S., A. Z. Khoury, L. Davidovich, and N. Zagury, 1991, Phys. Rev. A **44**, 7785.
- Haake, F., S. M. Tan, and D. F. Walls, 1989, Phys. Rev. A **40**, 7121.
- Haake, F., S. M. Tan, and D. F. Walls, 1990, Phys. Rev. A **41**, 2808.
- Haken, H., 1970, in *Handbuch der Physik*, Vol. XXV/2C, edited by L. Genzel (Springer, Berlin); reproduced in *Laser Theory*, by H. Haken (Springer, Berlin, 1984).
- Haken, H., 1975, Phys. Lett. A **53**, 77.
- Hanbury-Brown, R., and R. W. Twiss, 1956, Nature **177**, 27.
- Haroche, S., 1992, in *Fundamental Systems in Quantum Optics*, Lectures delivered at the Les Houches Summer School, Session LIII, 1990, edited by J. Dalibard, J. M. Raimond, and J. Zinn-Justin (North-Holland, New York), p. 767.
- Haus, H. A., and Y. Yamamoto, 1986, Phys. Rev. A **34**, 270.
- Heidmann, A., R. J. Horowicz, S. Reynaud, E. Giacobino, C. Fabre, and C. Camy, 1987, Phys. Rev. Lett. **59**, 2555.
- Hillery, M., R. F. O'Connell, M. O. Scully, and E. P. Wigner, 1984, Phys. Rep. **106**, 121.
- Hulet, R. G., and D. Kleppner, 1983, Phys. Rev. Lett. **51**, 1430.
- Imoto, N., H. A. Haus, and Y. Yamamoto, 1985, Phys. Rev. A **32**, 2287.
- Inoue, S., S. Machida, Y. Yamamoto, and H. Ohzu, 1993, Phys. Rev. A **48**, 2230.
- Jaekel, M. T., and S. Reynaud, 1990, Europhys. Lett. **13**, 301.
- Jakeman, E. T., and J. H. Jefferson, 1986, Opt. Acta **33**, 557.
- Jaynes, E. T., and F. W. Cummings, 1963, Proc. IEEE **51**, 89.
- Katanaev, I. I., and A. S. Troshin, 1987, Zh. Eksp. Teor. Fiz. **92**, 475 [Sov. Phys. JETP **65**, 268 (1987)].
- Kennedy, T. A. B., and D. F. Walls, 1989, Phys. Rev. A **40**, 6366.
- Kim, C., and P. Kumar, 1991, Opt. Lett. **16**, 755.
- Kim, C., and P. Kumar, 1992, J. Opt. Soc. Am. B **9**, 1379.
- Kim, C., and P. Kumar, 1994, Phys. Rev. Lett. **73**, 1605.
- Kimble, H. J., 1992, in *Fundamental Systems in Quantum Optics*, edited by J. Dalibard, J. M. Raimond, and J. Zinn-Justin (Elsevier, Amsterdam).
- Kimble, H. J., M. Dagenais, and L. Mandel, 1977, Phys. Rev. Lett. **39**, 691.
- Kimble, H. J., M. Dagenais, and L. Mandel, 1978, Phys. Rev. A **18**, 201.
- Kimble, H. J., and L. Mandel, 1976, Phys. Rev. A **13**, 2123.
- Kitching, J., R. Boyd, A. Yariv, and Y. Shevy, 1994, Opt. Lett. **19**, 1331.
- Klauder, J. R., J. McKenna, and D. G. Currie, 1965, J. Math. Phys. **6**, 733.
- Klauder, J. R., and B. S. Skagerstam, 1987, *Coherent States: Applications in Physics and Mathematical Physics* (World Scientific, Singapore).
- Kolobov, M. I., L. Davidovich, E. Giacobino, and C. Fabre, 1993, Phys. Rev. A **46**, 1630.
- Kolobov, M. I., and I. V. Sokolov, 1986, Zh. Eksp. Teor. Fiz. **90**, 1889 [Sov. Phys. JETP **63**, 1105 (1986)].
- Krause, J., M. O. Scully, and H. Walther, 1987, Phys. Rev. A **36**, 4547.
- Kuppens, S. J. M., M. P. van Exter, and J. P. Woerdman, 1994, Phys. Rev. Lett. **72**, 3815.
- Lai, Y., H. Haus, and Y. Yamamoto, 1991, Opt. Lett. **19**, 1517.
- Lane, A. S., M. D. Reid, and D. F. Walls, 1988, Phys. Rev. A **38**, 788.
- LaPorta, A., R. E. Slusher, and B. Yurke, 1989, Phys. Rev. Lett. **62**, 28.
- Lax, M., 1966a, Phys. Rev. **145**, 110.
- Lax, M., 1966b, in *Physics of Quantum Electronics*, edited by P. L. Kelley, B. Lax, and P. E. Tannenwald (McGraw-Hill, New York), p. 735.
- Lax, M., 1967, Phys. Rev. **157**, 213.
- Lax, M., 1968a, Phys. Rev. **172**, 350.
- Lax, M., 1968b, in *Statistical Physics, Phase Transitions and Superconductivity*, edited by M. Chrétien, E. P. Gross, and S. Dreser (Gordon and Breach, New York), Vol. 2, p. 425.
- Lax, M., and W. H. Louisell, 1969, Phys. Rev. **185**, 568.
- Lehman, H., K. Symanzik, and W. Zimmerman, 1955, Nuovo Cimento **1**, 1425.
- Levenson, M. B., R. M. Shelby, M. Reid, and D. F. Walls, 1986, Phys. Rev. Lett. **57**, 2473.
- Levine, D. F., and C. G. Bethea, 1984, Appl. Phys. Lett. **44**, 649.
- Lorenz, E. N., 1963, J. Atmos. Sci. **20**, 130.
- Loudon, R., 1980, Rep. Prog. Phys. **43**, 913.
- Loudon, R., 1983, *The Quantum Theory of Light*, 2nd ed. (Clarendon Press, London).
- Loudon, R., and P. Knight, 1987, J. Mod. Opt. **34**, 709.
- Louisell, W. H., 1973, *Quantum Statistical Properties of Radiation* (Wiley, New York).

- Lugiato, L. A., 1984, in *Progress in Optics*, Vol. 21, edited by E. Wolf (North-Holland, Amsterdam), p. 69.
- Lugiato, L. A., and G. Strini, 1982, *Opt. Commun.* **41**, 447.
- Machida, S., and Y. Yamamoto, 1986, *Opt. Commun.* **57**, 290.
- Machida, S., and Y. Yamamoto, 1988, *Phys. Rev. Lett.* **60**, 792.
- Machida, S., and Y. Yamamoto, 1989, *Opt. Lett.* **60**, 1045.
- Machida, S., Y. Yamamoto, and Y. Itaya, 1987, *Phys. Rev. Lett.* **58**, 1000.
- Maeda, M. W., P. Kumar, and J. H. Shapiro, 1986, *Opt. Lett.* **12**, 161.
- Maia Neto, P. A., and L. Davidovich, 1992, *Phys. Rev. A* **45**, 3139.
- Maiman, T. H., 1960, *Nature* **187**, 493.
- Mandel, L., 1979, *Opt. Lett.* **4**, 205.
- Mandel, L., 1982, *Phys. Rev. Lett.* **49**, 136.
- Mandel, L., 1986, *Phys. Scr. T* **12**, 34.
- Mandel, L., and E. Wolf, 1965, *Rev. Mod. Phys.* **37**, 231.
- Marte, M. and P. Zoller, 1990, *Quantum Opt.* **2**, 229.
- Mehta, C. L., and E. C. G. Sudarshan, 1965, *Phys. Rev.* **138**, B274.
- Mertz, J., T. Debuisschert, A. Heidmann, C. Fabre, and E. Giacobino, 1991, *Opt. Lett.* **16**, 1234.
- Mertz, J., A. Heidmann, C. Fabre, E. Giacobino, and S. Reynaud, 1990, *Phys. Rev. Lett.* **64**, 2897.
- Meschede, D., H. Walther, and G. Mueller, 1985, *Phys. Rev. Lett.* **54**, 551.
- Meystre, P., G. Rempe, and H. Walther, 1988, *Opt. Lett. B* **13**, 1078.
- Milonni, P., M.-L. Shi, and J. R. Ackerhalt, 1987, *Chaos in Laser-Matter Interactions* (World Scientific, Singapore).
- Nabors, C. D., and R. M. Shelby, 1990, *Phys. Rev. A* **42**, 556.
- Nussenzveig, A., J. Hare, A. M. Steinberg, L. Moi, M. Gross, and S. Haroche, 1991, *Europhys. Lett.* **14**, 755.
- Nussenzveig, H. M., 1974, *Introduction to Quantum Optics* (Gordon and Breach, New York).
- Orozco, L. A., M. G. Raizen, M. Xiao, R. J. Brecha, and H. J. Kimble, 1987, *J. Opt. Soc. Am. B* **4**, 1490.
- Orszag, M., R. Ramirez, J. C. Retamal, and C. Saavedra, 1994, *Phys. Rev. A* **49**, 2933.
- Pace, A. F., M. J. Collett, and D. F. Walls, 1993, *Phys. Rev. A* **47**, 3173.
- Pais, A., 1982, *Subtle is the Lord... The Science and the Life of Albert Einstein* (Oxford University, New York).
- Parkins, A. S., and C. W. Gardiner, 1988, *Phys. Rev. A* **37**, 3867.
- Pegg, D. T., and S. M. Barnett, 1988, *Europhys. Lett.* **6**, 483.
- Pegg, D. T., and S. M. Barnett, 1989, *Phys. Rev. A* **39**, 1665.
- Pereira, S. F., M. Xiao, H. J. Kimble, and J. L. Hall, 1989, *Phys. Rev. A* **38**, 4931.
- Planck, M., 1900a, *Verh. Deutsch. Phys. Ges.* **2**, 202.
- Planck, M., 1900b, *Verh. Deutsch. Phys. Ges.* **2**, 237.
- Polzik, E. S., J. Carri, and H. J. Kimble, 1992, *Phys. Rev. Lett.* **68**, 3020.
- Prokhorov, A. M., 1965, *Science* **149**, 828.
- Quang, T., 1992, *Phys. Rev. A* **46**, 682.
- Raizen, M. G., L. A. Orozco, M. Xiao, T. L. Boyd, and H. J. Kimble, 1987, *Phys. Rev. Lett.* **29**, 198.
- Ralph, T. C., and C. M. Savage, 1991, *Opt. Lett.* **16**, 1113.
- Rarity, J. G., P. R. Tapster, and E. Jakeman, 1987, *Opt. Commun.* **62**, 201.
- Reid, M. D., 1988, *Phys. Rev. A* **37**, 4792.
- Reid, M. D., and D. Walls, 1983, *Phys. Rev. A* **28**, 332.
- Reid, M. D., and D. Walls, 1986, *Phys. Rev. A* **34**, 4929.
- Rempe, G., F. Schmidt-Kaler, and H. Walther, 1990, *Phys. Rev. Lett.* **64**, 2783.
- Rempe, G., and H. Walther, 1990, *Phys. Rev. A* **42**, 1650.
- Rempe, G., H. Walther, and N. Klein, 1987, *Phys. Rev. Lett.* **58**, 353.
- Reynaud, S., 1987, *Europhys. Lett.* **4**, 427.
- Reynaud, S., 1990, *Ann. Phys. (Paris)* **15**, 63 (1990).
- Reynaud, S., C. Fabre, and E. Giacobino, 1987, *J. Opt. Soc. Am. B* **4**, 1520.
- Reynaud, S., A. Heidmann, E. Giacobino, and C. Fabre, 1992, in *Progress in Optics*, Vol. 30, edited by E. Wolf (Elsevier, Amsterdam).
- Richardson, W. H., S. Machida, and Y. Yamamoto, 1991, *Phys. Rev. Lett.* **66**, 2867.
- Richardson, W. H., and R. E. Shelby, 1990, *Phys. Rev. Lett.* **64**, 400.
- Risken, H., 1984, *The Fokker-Planck Equation* (Springer, Berlin).
- Ritsch, H., M. Marte, and P. Zoller, 1992, *Europhys. Lett.* **19**, 7.
- Ritsch, H., P. Zoller, C. W. Gardiner, and D. F. Walls, 1991, *Phys. Rev. A* **44**, 3361.
- Sargent, M., III, M. O. Scully, and W. E. Lamb, Jr., 1974, *Laser Physics* (Addison-Wesley, Reading, MA).
- Schawlow, A. L., and C. H. Townes, 1958, *Phys. Rev.* **112**, 1940.
- Schleich, W., and M. O. Scully, 1988, *Phys. Rev. A* **37**, 1261.
- Schumaker, B. L., 1984, *Opt. Lett.* **9**, 189.
- Schumaker, B. L., and C. M. Caves, 1985, *Phys. Rev. A* **31**, 3093.
- Scully, M. O., 1985, *Phys. Rev. Lett.* **55**, 2802.
- Scully, M. O., and W. E. Lamb, Jr., 1967, *Phys. Rev.* **159**, 208.
- Scully, M. O., G. Süssman, and C. Benkert, 1988, *Phys. Rev. Lett.* **60**, 1014.
- Scully, M. O., K. Wódkiewicz, M. S. Zubairy, J. Bergou, N. Lu, and J. Meyer ter Vehn, 1988, *Phys. Rev. Lett.* **60**, 1832.
- Scully, M. O., and M. S. Zubairy, 1987, *Phys. Rev. A* **35**, 752.
- Scully, M. O., M. S. Zubairy, and K. Wódkiewicz, 1988, *Opt. Commun.* **65**, 440.
- Shapiro, J. H., G. Saplakoglu, S. T. Ho, P. Kumar, B. E. A. Saleh, and M. C. Teich, 1987, *J. Opt. Soc. Am. B* **4**, 1604.
- Shelby, R. M., M. D. Levenson, and P. W. Byer, 1985, *Phys. Rev. Lett.* **54**, 939.
- Shelby, R. M., M. D. Levenson, S. H. Perlmutter, R. G. DeVoe, and D. F. Walls, 1986, *Phys. Rev. Lett.* **57**, 691.
- Short, R., and L. Mandel, 1983, *Phys. Rev. Lett.* **51**, 384.
- Sizman, A., R. J. Horowicz, G. Wagner, and G. Leuchs, 1990, *Opt. Commun.* **80**, 138.
- Slusher, R. E., L. W. Hollberg, B. Yurke, J. C. Mertz, and J. F. Valley, 1985, *Phys. Rev. Lett.* **55**, 2409.
- Snyder, J. J., E. Giacobino, C. Fabre, A. Heidmann, and M. Ducloy, 1990, *J. Opt. Soc. Am. B* **7**, 2132.
- Sorokin, P. P., and N. Braslau, 1964, *IBM J. Res. Dev.* **8**, 177.
- Stoler, D., 1970, *Phys. Rev. D* **1**, 3217.
- Stoler, D., 1971, *Phys. Rev. D* **4**, 1925.
- Stoler, D., and Yurke, B., 1986, *Phys. Rev. A* **34**, 3143.
- Sudarshan, E. C. G., 1963, *Phys. Rev. Lett.* **10**, 277.
- Susskind, L., and J. Glogower, 1964, *Physics* **1**, 49.
- Takahashi, H., 1965, in *Advances in Communication Systems*, Vol. 1, edited by A. V. Balakrishnan (Academic, New York).
- Tapster, P. R., J. G. Rarity, and J. S. Satchell, 1987, *Europhys. Lett.* **4**, 293.
- Tapster, P. R., S. F. Seward, and J. G. Rarity, 1991, *Phys. Rev. A* **44**, 3266.

- Teich, M. C., and B. E. A. Saleh, 1985, *J. Opt. Soc. Am. B* **2**, 275.
- Teich, M. C., and B. E. A. Saleh, 1988, in *Progress in Optics*, Vol. 26, edited by E. Wolf (North-Holland, Amsterdam), p. 104.
- Teich, M. C., and B. E. A. Saleh, 1989, *Quantum Opt.* **1**, 153.
- Unruh, W. G., 1978, *Phys. Rev. D* **18**, 1764.
- Unruh, W. G., 1983, in *Quantum Optics, Experimental Gravity, and Measurement Theory*, edited by P. Meystre and M. O. Scully (Plenum, New York), p. 647.
- Van Kampen, N. G., 1981, *Stochastic Processes in Physics and Chemistry* (Elsevier, Amsterdam).
- Walker, J. G., and E. Jakeman, 1985, *Opt. Acta* **32**, 1303.
- Walls, D. F., 1983, *Nature* **306**, 141.
- Walls, D. F., and G. J. Milburn, 1994, *Quantum Optics* (Springer, Berlin).
- Wang, H., M. Freeman, D. G. Steel, 1993, *Phys. Rev. Lett.* **71**, 3951.
- Wehner, E., R. Seno, N. Sterpi, B.-G. Englert, and H. Walther, 1994, *Opt. Commun.* **110**, 655.
- Wigner, E. P., 1932, *Phys. Rev.* **40**, 769.
- Winters, M., J. Hall, and P. Toschek, 1990, *Phys. Rev. Lett.* **65**, 3116.
- Wu, L.-A., H. J. Kimble, J. L. Hall, and H. Wu, 1986, *Phys. Rev. Lett.* **57**, 2520.
- Wu, L.-A., M. Xiao, and H. J. Kimble, 1988, *J. Opt. Soc. Am. B* **4**, 1465.
- Xiao, M., L.A. Wu, and H. J. Kimble, 1987, *Phys. Rev. Lett.* **59**, 278.
- Yamamoto, Y., N. Imoto, and S. Machida, 1986, *Phys. Rev. A* **33**, 3243.
- Yamamoto, Y., and S. Machida, 1987, *Phys. Rev. A* **35**, 5114.
- Yamamoto, Y., S. Machida, N. Imoto, M. Kitagawa, and G. Björk, 1987, *J. Opt. Soc. Am. B* **4**, 1645.
- Yamamoto, Y., S. Machida, and O. Nilsson, 1986, *Phys. Rev. A* **34**, 4025.
- Yamamoto, Y., S. Machida, S. Saito, N. Imoto, T. Yanagawa, M. Kitagawa, and G. Bjork, 1990, in *Progress in Optics*, Vol. 28, edited E. Wolf (North-Holland, Amsterdam), p. 89.
- Yuen, H. P., 1975, *Phys. Lett. A* **51**, 1.
- Yuen, H. P., 1976, *Phys. Rev. A* **13**, 2226.
- Yuen, H. P., 1986, *Phys. Rev. Lett.* **56**, 2176.
- Yuen, H. P., and V. W. S. Chan, 1983, *Opt. Lett.* **8**, 177.
- Yuen, H. P., and J. H. Shapiro, 1980, *IEEE Trans. Inf. Theory* **26**, 78.
- Yurke, B., 1984, *Phys. Rev. A* **29**, 408.
- Zhu, S.-Y., C. Su, and L. Z. Wang, 1991, *Opt. Commun.* **85**, 350.
- Zhu, S.-Y., M. S. Zubairy, C. Su, and J. Bergou, 1992, *Phys. Rev. A* **45**, 499.
- Zou, X. T., and L. Mandel, 1990, *Phys. Rev. A* **41**, 475.